DESIGN AND IMPLEMENTATION

OF

DC MOTOR DRIVE

Major Project Report

Submitted in Partial Fulfillment of the Requirements for the degree of

MASTER OF TECHNOLOGY

IN

ELECTRICAL ENGINEERING

(Power Apparatus & Systems)

By

Kaushalkumar J. Patel
(05Mee010)

Department of Electrical Engineering
INSTITUTE OF TECHNOLOGY
NIRMA UNIVERSITY OF SCIENCE AND TECHNOLOGY,
AHMEDABAD 382 481

MAY 2007

CERTIFICATE

This is to certify that the Major Project Report entitled "**DESIGN AND IMPLEMENTATION OF DC MOTOR DRIVE USING TMS320F2811**"submitted by Mr. **Kaushalkumar J. Patel (05MEE010)** towards the partial fulfillment of the requirements for the award of degree in Master of Technology (Electrical Engineering) in the field of Power Apparatus & Systems of Nirma University of Science and Technology is the record of work carried out by him under our supervision and guidance. The work submitted has in our opinion reached a level required for being accepted for examination. The results embodied in this major project work to the best of our knowledge have not been submitted to any other University or Institution for award of any degree or diploma.

Date:

Industry - Guide

Mr. Vinod Patel
Manager
R&D Department
Amtech Electronics (I) Ltd.
Gandhinagar.

Institute - Guide

Dr. P. N. Tekwani
Professor
Department of Electrical Engineering
Institute of Technology
Nirma University

Head of Department

Department of Electrical Engineering
Institute of Technology
Nirma University
Ahmedabad

Director

Institute of Technology
Nirma University
Ahmedabad

ACKNOWLEDGEMENT

First of all, I would like to thank AMTECH Electronics (I) Ltd., Gandhinagar, for giving me an opportunity to perform the project under it premises and give me the industrial exposure.

I wish to express my sincere gratitude to Mr. Vinod Patel, Manager, R&D, AMTECH Electronics (I) Ltd., Gandhinagar, for his guidance and support. His perfectionism has made me improve many details of my work. He challenged me to find technical solutions to realistic problems; many of them are included in this dissertation. He always helped me and encouraged me to make manual of DC motor drive and performance improvement.

I wish to express my deep gratitude to Dr. P. N. Tekwani, for his guidance and advice. I am grateful to him for giving me a valuable guidance throughout my project. He gave me the correct advice when the serious problem arises during hardware testing.

I would like to thank Mr. Bharat Pandya, Chief Engineer-Design for his support and advice. His extensive knowledge and helpful attitude gains my sincere admiration. I would like to thank Mr. Aminesh Gajjar, Mr. Manish Paghada, Mr. Mayur Dhameliya, Mr. Chandresh Patel, Mr. Piyush Dekavadiya, Mr. Vijendra Kharbikar, Piyush Patel, Miss Sejal shah, Mr. Samir, Mr. Hiten and Mr. Atulbhai of the AMTECH Electronics (I) Ltd., for making it easier for me to spend the span of Eleven months. I would like to thank all production staff particularly Kiran Kage, Vipul and Nikunj Patel for their support during the period of my project at Amtech Electronics (I) Ltd.

I am thankful to Prof. A. S. Ranade, HOD, Prof. U.A.Patel, Section Head, Prof. B. B. kadam and Prof. N. K. Sheth, Electrical Engineering Dept, Nirma University for allowing me to do my project work at AMTECH Electronics (I) Ltd., Gandhinagar.

I am grateful to Mr. C. R. Patel, who suggest me some references to solve problem during my project work.

Further I am thankful to Mr. Chanakya Bhatt, Mr. Jignesh Patel and Mr. Amit Sant for their continuous support during their and my project work.

Thanks to my parents and family members for their continuous support and encouragement to strive for my goals.

Finally, I would like to thank all my friends who were always beside me.

THANKS TO ALL OF THEM.

KAUSHAL PATEL

ABSTRACT

DC drives are widely used in application requiring adjustable speed, good speed regulation, frequent starting, breaking and reversing. DC motors have variable characteristic and are used extensively in variable speed drives. The methods of speed control are normally simpler and less expensive than those used for AC drives. DC motor plays a significant role in modern industries. This report demonstrates the DC motor basics and design of the DC motor drive system using TMS320F2811. Simulation of control of DC motor drive with various dynamic performances has been presented. The control strategy to obtain the equidistance pulses has been implemented in the DSP processor with the help of "CODE COMPOSER STUDIO". Inverse cosine scheme was used for triggering of the thyristor. Final testing of the software modules was done with the RL load at low voltage. Prototype of DC motor drive has been built and tested with current control loop using low voltage. The experimental results show close resemblance with simulation results.

LIST OF FIGURES

Fig. 2.1	Cut View of DC Motor	7
Fig. 2.2	Series Connected Motor Circuit	8
Fig. 2.3	Compound Connected Motor Circuit	9
Fig. 2.4	Shunt Connected Motor Circuit	9
Fig. 2.5	Equivalent Circuit of a Separately Excited DC Motor	10
Fig. 2.6	Torque - Speed Characteristic of Separately Excited DC Motor	11
Fig. 2.7	Modes of Operation	12
Fig. 2.8	Ward Leonard Drive	14
Fig. 2.9	Armature Voltage Control using a Transformer with Taps and an Uncontrolled Rectifier	15
Fig. 2.10	Single Phase and Three Phase Controlled Rectifier Circuits	16
Fig. 2.11	Chopper Control of RLE Load	17
Fig. 2.12	Waveform of Chopper Control	17
Fig. 3.1	Three Phase Fully Controlled Rectifier with Resistive Load	19
Fig. 3.2	Waveform of Three Phases	19
Fig. 3.3	Control Circuit of Cosine Wave Firing Scheme	23
Fig. 3.4	Firing Pulse for Thyristor 1 Using Cosine Wave Firing Scheme	24
Fig. 3.5	Synchronizing Signal for Thyristor 1	25
Fig. 3.6	Synchronizing Signal for Triggering Thyristors (1 to 6)	26
Fig. 4.1	Block Diagram of DC Motor Drive with Armature Control	29
Fig. 4.2	Equivalent Model of Separately Excited DC Motor	31
Fig. 4.3	Alternate Representation of the Equivalent Model of DC Motor	32
Fig. 4.4	Equivalent Transfer Function Block Diagram	33
Fig. 4.5	Current Controller Block Diagram	34
Fig. 4.6	Speed Controller Block Diagram	37
Fig. 4.7	Gain Response of Speed Controller	38
Fig. 4.8	Step Response of the Speed Controller	41
Fig. 5.1	Block Diagram of the Hardware Setup for DC Motor Drive System	42

Fig. 5.2	Interfacing Circuit	44
Fig. 5.3	Firing Circuit for Thyristor 1 and Thyristor 4	45
Fig. 5.4	Isolation Circuit for Speed Measurement	46
Fig. 5.5	Block Diagram of the Control Card	48
Fig. 6.1	Timer 0 Interrupt Flow Chart	50
Fig. 6.2	20 ms Routine Flow Chart	50
Fig. 6.3	100 ms Routine Flow Chart	51
Fig. 6.4	Quadrature Encoded Pulses and Decoded Timer Clock	52
Fig. 6.5	Flowchart for Speed Measurement	53
Fig. 6.6	Overload and Timed Overload Protection Flowchart	55
Fig. 6.7	Main Routine Flow Chart for DC Motor Drive	57
Fig. 7.1	Simulation Circuit of Cosine Wave Firing Scheme for Gate Pulse of Thyristor 1 and 4	58
Fig. 7.2	DLL Implementation of Cosine Firing Scheme	59
Fig. 7.3	Simulation Result Synchronizing Voltage with Control Voltage, and Gate Pulse for Thyristor 1 at $\alpha = 90^0$	60
Fig. 7.4	Simulation Result, Synchronizing Voltage with Control Voltage, and Gate Pulse for Thyristor 1 at $\alpha = 0^0$	60
Fig. 7.5	6 Equidistance pulses for Thyristor 1 to 6	61
Fig. 7.6	Simulation Circuit of DC Motor Drive	63
Fig. 7.7	Results of Armature Current and Speed with $\omega^* = 1220$ rpm and $M_L = 29.2$ Nm	64
Fig. 7.8	Magnified Waveform of Armature Current and Speed with $\omega^* =1220$ rpm and $M_L = 29.2$ Nm	64
Fig. 7.9	Results of Current, Torque, Armature Voltage and Speed with $\omega^*=1220$ rpm and $M_L=29.2$ Nm	65
Fig. 7.10	Results of Current and Speed with Speed with ω^* Change from 1159 rpm to 1220 rpm with $M_L = 29.2$ Nm	66
Fig. 7.11	Magnified Waveform of Armature Current and Speed with ω^* Change from 1159 rpm to 1220 rpm with $M_L = 29.2$ Nm	66

Fig. 7.12	Simulation Circuit for the Dynamic Performance with Load Change	67
Fig. 7.13	Results of Current and Speed with Speed with ω* Change from 1159 rpm to 1220 rpm with ML = 29.2 Nm	68
Fig. 7.14	Magnified Waveform of Armature Current and Speed with ω* change from 1220 to 1159 rpm	68
Fig. 7.15	Magnified Waveform of Armature Current and Speed with M_L Change from Rated to 50% of Rated	69
Fig. 7.16	Waveform of ZCD of R-Phase and Firing Pulse of Thyristor - 1 at Vc = 1	71
Fig. 7.17	Waveform of R-Phase and Input to the Pulse Transformer for Thyristor - 1	71
Fig. 7.18	Waveform of Firing Pulses for Thristor 1 and Thyristor- 4 at Vc = 1	72
Fig. 7.19	Waveform of ZCD of R-Phase and Firing Pulse for Thyristor - 4 at Vc = 1	72
Fig. 7.20	Waveform of Firing Pulses for Thyristor - 1 and Thyristor - 2	73
Fig. 7.21	Waveform of ZCD of R-Phase (Input B) and Firing Pulse for Thyristor – 2	73
Fig. 7.22	Waveform of Firing Pulses for Thyristor -6 and Thyristor -1 at Vc = 1	74
Fig. 7.23	Waveform of Firing Pulses for Thyristor - 4 and Thyristor - 6	74
Fig. 7.24	Waveform of DC Voltage V_{DC} and Line Voltage V_{RB} with RL Load and $\alpha = 0^0$	75
Fig. 7.25	Waveform of DC Voltage V_{DC} and Line Voltage V_{RB} with RL Load and $\alpha = 30^0$	76
Fig. 7.26	Waveform of DC Voltage V_{DC} and Line Voltage V_{RB} with RL Load and $\alpha = 60^0$	76
Fig. 7.27	Waveform of DC Voltage V_{DC} and Line Voltage V_{RB} with RL Load and $\alpha = 90^0$	77
Fig. 7.28	Waveform of DC Current in Current Control Mode with RL Load, Current Reference I* = 1.5 A	78

List of Tables

Table 3.1 Thyristor Pair Conduction Table 21

Table 3.2 Synchronizing Signal for Triggering the Thyristors 27

Table 7.1 Output Voltages with Different Firing Angle 75

NOMENCLATURE

C_1	Emf Constant
C_2	Torque Constant
J	Moment of Inertia
K_1	Gain of Speed Sensor
$E_{b,}$ Emf	Back Electromotive Force
I_a^*	Reference Armature Current
I_{amax}	Maximum Armature Current
I_a	Armature Current
K_2	Gain of Current Sensor
K_c	Current Controller Gain
K_N	Speed Controller Gain
K_t	Converter Gain
L_a	Armature Inductance
L_f	Field Inductance
M_d	Motor Developed Torque
M_l	Load Torque
R_a	Armature Resistance
R_f	Field Resistance
T_1	Time Constant of Low Pass Filter in Speed Feedback
T_2	Time Constant of Low Pass Filter in Current Feedback
T_a	Armature Time Constant
T_c	Current Controller Time Constant
T_{em}	Mechanical Time Constant
T_N	Speed Controller Time Constant
T_t	Delay of Converter
V_a	Armature Voltage
V_B	Phase Voltage Across B Phase and Neutral
V_{BR}	Line Voltage Across B and R Phase
V_c	Control Voltage
V_d	DC Voltage
V_f	Field Voltage

V_R	Phase Voltage Across R Phase and Neutral
V_{RY}	Line Voltage Across R and Y Phase
V_Y	Phase Voltage Across Y phase And Neutral
V_{YB}	Line Voltage Across Y and B Phase
ϕ	Air Gap Flux
ϕ_f	Field Flux
α	Firing Angle of Thyristor
θ	Phase Angle
ω	Motor Speed In rad/sec
ω	Natural Oscillation Frequency
ω^*	Speed Reference
ξ	Damping Factor

ABBREVIATION

AC	Alternating Current
DC	Direct Current
ADC	Analog to Digital Controller
Cos	Cosine
DLL	Dynamic Link Library
DSP	Digital Signal Processor
Emf	Electromotive Force
g1	Gate Pulse for Thyristor No. 1
g2	Gate Pulse for Thyristor No. 2
g3	Gate Pulse for Thyristor No. 3
g4	Gate Pulse for Thyristor No. 4
g5	Gate Pulse for Thyristor No. 5
g6	Gate Pulse for Thyristor No. 6
PD	Proportional and Differential
PDF	Pseudo Derivative Controller
PI	Proportional plus Integral
PID	Proportional Integral plus Derivative
PLL	Phase Lock Loop
rpm	Revolution per Minute
Th1	Thyristor No. 1
Th2	Thyristor No. 2
Th3	Thyristor No. 3
Th4	Thyristor No. 4
Th5	Thyristor No. 5
Th6	Thyristor No. 6
ZCD	Zero Crossing Detection

CONTENTS

ACKNOWLEDGEMENT (I)

ABSTRACT (II)

LIST OF FIGURES (III)

LIST OF TABLES (VI)

NOMENCLATURE (VII)

ABBREVIATION (IX)

CONTENTS (X)

Chapter 1. Introduction

1.1 Introduction 1

1.2 Objectives for This Thesis 3

1.3 Outline of Thesis 4

Chapter 2. Basics of DC motor

2.1 History of DC Motor Drives 5

2.2 Basic DC Machine Construction 6

2.3 Types of DC Machine 8

2.3.1 Series Motor 8

2.3.2 Compound Connected DC Motor 8

2.3.3 Shunt Connected DC Motor 9

2.4 Basics of DC Motor 9

2.5 Types of DC Motor Speed Control method 13

2.5.1 Armature Voltage Control Method 13

2.5.1.1 Ward-Leonard Scheme 13

2.5.1.2 Transformer and Uncontrolled Rectifier Scheme 14

2.5.1.3 Controlled Rectifier Fed DC Drive 15

2.5.1.4 Chopper Control 16

2.5.2 Flux Control 17

2.5.3 Armature Resistance Control 17

Chapter 3. Converter Topology and Control Techniques

3.1 Converter Topology 18

3.1.1 Phase Fully Controlled Rectifier 18

3.2 Control Techniques 21

3.2.1 Linear Firing Angle Control 22

3.2.2 Cosine Wave Control 22

3.2.3 Phase Lock Loop Control 24

3.2.4 Synchronizing Signal 25

Chapter 4 Design of Controller

4.1 Basic Block Diagram 28

4.2 Mathematical Modeling of DC Motor 30

4.3 Mathematical Modeling Power converter 32

4.4 Design of a DC Motor Control System 33

4.4.1 Current Controller Design 34

4.4.2 Design of Speed Control Loop 37

4.2.1.1 General Considerations For Optimization 38

4.2.1.2 Symmetric Optimization by Computation or Modulus Hugging Method 40

Chapter 5 Hardware Design

5.1 Hardware design 42

5.2 Power supply for Control Card 43

5.3 Control Card 43

5.3.1 Interfacing Circuit 44

5.3.2 Firing Circuit 44

5.3.3 QEP Circuit 45

5.3.4 Serial Communication 46

5.3.5 DSP Processor 46

5.3.6 Power Modules 46

5.3.7 Programmable Terminals 47

5.4 Keypad and Display unit 48

Chapter 6 Software Design
6.1 Software Development 49
6.2 Flowchart for the Speed Measurement 51
6.2.1 Quadrature Encoded Pulses Circuit 51
6.2.2 Flowchart for Speed Measurement 53
6.3 Flow chart for the protection 54
6.3.1 Over Current and Timed Overload protection 54
Chapter 7 Simulation and Experimental Results
7.1 Simulation Results and Discussion 58
7.1.1 Firing Pulse Generation 58
7.1.2 Simulation of DC Motor Drive 61
7.2 Actual results and Discussion 70
7.2.1 Inverse Cosine Firing Scheme using DSP 70
7.2.2 Results of Controlled Rectifier 75
7.3 Current Control 77
Chapter 8 Conclusions and Scope for Future Work
8.1 Conclusions 79
8.2 Scope for Future work 80
Chapter 9 Bibliography 81

APPENDIX - A 82
APPENDIX - B 84

Chapter 1
Introduction

1.1 Introduction

A rotational load that is to be run over a wide scope of speeds is often called an ‘infinitely adjustable speed drive’ or more commonly, a ‘variable speed drive’. These drives may be in the form of hydraulic or mechanical means, not being restricted to electrical drives. Electrical drives are very common and of great interest within this composition. Manual speed controllers have become near extinct and the use of analog systems for speed control is now becoming obsolete. The use of digitally controlled systems, which automatically set the motor speed, is finding increasing use in industry.

DC drives are widely used in application requiring adjustable speed, good speed regulation and frequent starting, breaking and reversing. Some important applications are rolling mills, paper mills, machine tools, traction, printing presses, and mine winders. Direct current motors have variable characteristics and are used extensively in variable speed drives. DC motors can provide a high starting torque and it is also possible to obtain speed control over a wide range. The methods of speed control are normally simpler and less expensive than those of AC drives. DC motors play a significant role in modern industrial drives. Both series and separately excited DC motors are normally used in variable drives, but series motors are traditionally employed for traction applications. In case of a separately excited motor, the field and armature voltage can be controlled independent of each other. In a shunt motor, the field and armature are connected to a common source. Therefore, an independent control of the armature voltage and field current can be done only be inserting a resistance in the appropriate circuit; however this is an inefficient method of control. In the case of a series motor, the field flux is function of armature current. The alternative to inserting a resistance is to provide variable DC voltage supply. There are no. of methods to get variable DC voltage. But due the growing number of power electronic devices, variable DC voltage can be obtained without much loss of power. The phase controlled rectifier and chopper are widely used for getting the variable DC voltage from AC source and DC source respectively. For the motor control, controlled rectifiers are classified as fully controlled and half controlled rectifier. Single phase fully controlled rectifier are widely used up to a rating of 10 kW and in some special cases up to 50 kW. For higher power ratings three phase-controlled rectifiers are employed.

The use of power electronics for the control of electric machines offers not only better performance caused by the precise control and fast response, but also a remarkable improvement of reliability service life, maintenance etc. In parallel with the advance in power electronics there have been great advances in digital electronics. Digital electronics are widely used in motor control. These controllers are more accurate, flexible in terms of software and less expensive following the rapid development in integrated circuit technology. In addition protection functions for the reliable operation of drive circuits are easily implemented in digital controllers. While the controllers are digital, the motors are analog and, therefore, signals between the controller and motor are linked to each other using analog to digital converters.

Due to commutator, DC motors are suitable for very high-speed applications and require more maintenance than AC motors. With the recent advancements in power conversions, control techniques and microcomputers, the AC motor drives are becoming increasingly competitive with DC motor drives. Although the future trend is toward AC drives, DC drives are widely used in many industries.

1.2 Objectives for This Thesis

The objective of this thesis is to design and construct the closed loop control system for the DC motor. The 6-pulse controlled converter is used to get variable DC voltage. The control strategy for the firing the 6 Thyristors is implemented using DSP. Various controlling modes of the DC drive are provided. A man-machine interface (MMI) system is designed to set various parameters and display the required parameter and various conditions. The project also includes start/stop of the drive, speed control, current control, monitoring of control variable and initiative protection. Various protections of drives like field failure and over-current, motor over-temperature, Thyristor stack over-temperature, stall protection etc., are also provided. A manual for the DC motor drive system explaining the various programmable parameters and their limits as well as the quantities that can be displayed and their selection is prepared.

The simulation work is carried out in PSIM 6.0. In hardware model, the firing signals are generated with the help of DSP TMS320F2811. Software for the DC drive is written in the code composer studio using C language. The software development for the DC motor drive is first separated in the small module. After completing the modules, these software modules are checked using the RL load at the low voltage. After testing of the software at low voltage, software is checked with the DC motor.

1.3 Outline of Thesis

The rest of thesis is organized as follows:

Chapter 2 describes the basic of the DC motor. It includes the basic construction, types of DC motor and methods of DC motor speed control.

Chapter 3 contains the converter topology and control techniques for DC motor drive system. It includes theory of linear firing scheme, cosine firing scheme and synchronizing signal used for thyristor triggering.

Chapter 4 contains the mathematical derivation for the design of the DC motor speed control system. It includes basic block diagram of DC motor drive system, the design of speed controller and current controller.

Chapter 5 contains hardware design of the DC motor drive system. It includes the various interfacing circuit used to interface the Analog input with TMS320F2811.

Chapter 6 contains the software design of the TMS320F2811. It describes the flow chart for the software development of DC motor drive.

Chapter 7 contains the simulation and experimental results. Simulation results are obtained in steady state and various dynamic conditions like change in speed reference and load change. Experimental results are taken on RL load at low voltage.

Chapter 2
Basic of DC Motor

2.1 History of DC Motor Drives

During the last century, industry has boomed and the DC motor has been an integral part of the electrical industry's history. Most power at the beginning of the century was constant voltage direct current because of it's ease of use and it only requires two transmission buses, unlike the three phase transmission of today.

Last century DC drives were typically constant speed, due to the limited of knowledge of commutation. This caused problems with commutator sparking and reduced life of brushes. The variation of speed was only possible through adjustment in field flux of the most durable motors. However with improvements in commutation then came improvements in speed control.

Last century DC motor drives were typically constant speed, due to the limited of knowledge of commutation. This caused problems with commutator sparking and reduced life of brushes. The variation of speed was only possible through adjustment in field flux of the most durable motors. However with improvements in commutation then came improvements in speed control.

In the 1890's, a more successful method of speed control was introduced, the Ward-Leonard method. The system utilized a motor generator set to vary the power supplied to the DC machine by varying the generator excitation. This consequentially varied the voltage and then provided continuous control of the motor of a wide range. This system was the first to provide better performance in machine speed control. Meanwhile, the development of AC systems continued to become more attractive due to their durability. They also exhibited no problem with commutation as current was passed to the machine via a set of slip rings located on the rotor.

In the late 1940's, electronic control gas filled rectifiers brought a significant change to the speed control industry. They provided advantages of electronic control by possessing faster response, increased accuracy and allowed the first automatic closed loop system to operate. This began the move of electronic drives, a movement, which is still increasing accuracy, response and controllability of motors.

As the decades rolled on the use and new innovation of solid-state electronic devices took over, with the introduction of the thyristor. The thyristor was a semi-controlled device, which allowed greater control, rugged systems.

Today the electronic drives are increasing smaller and able to handle larger currents and voltages. And with the introduction of micro-controller drives the limits seem endless. The direction into the new millennium is uncertain but all the same assured for the use of electronic drives. Perhaps the next step will be into cheaper electric cars.

2.2 Basic DC Motor Construction

The processes, which take place within DC motors, and generators, are the same, and as a result the same machine can perform both functions. To produce a rotational torque from a motor, an arrangement of conductors is required to generate magnetic fields that interact to cause a resultant force or torque. The DC machine consists of three essential items: the stator, the rotor and the commutator (not shown) illustrated in Fig. 2-1.

The stator, so called because it is stationary, consists of salient poles that carry the main field coils, commonly called the field windings. These coils are connected in series to ensure that each coil carries the same current and the same magneto-motive force (mmf). The current through each conductor must be equal, as the magnitude is a function of current.

The stator yoke, pole shoes and rotor are constructed from ferromagnetic materials to enhance the flux of the machine. The pole shoes are used to increase the output of the machine by placing more armature windings, on the rotor, under strong influence from a magnetic field. With the rotation of the armature there will be eddy currents present in the pole shoe material. Therefore laminated steel sections are used to reduce eddy current loss.

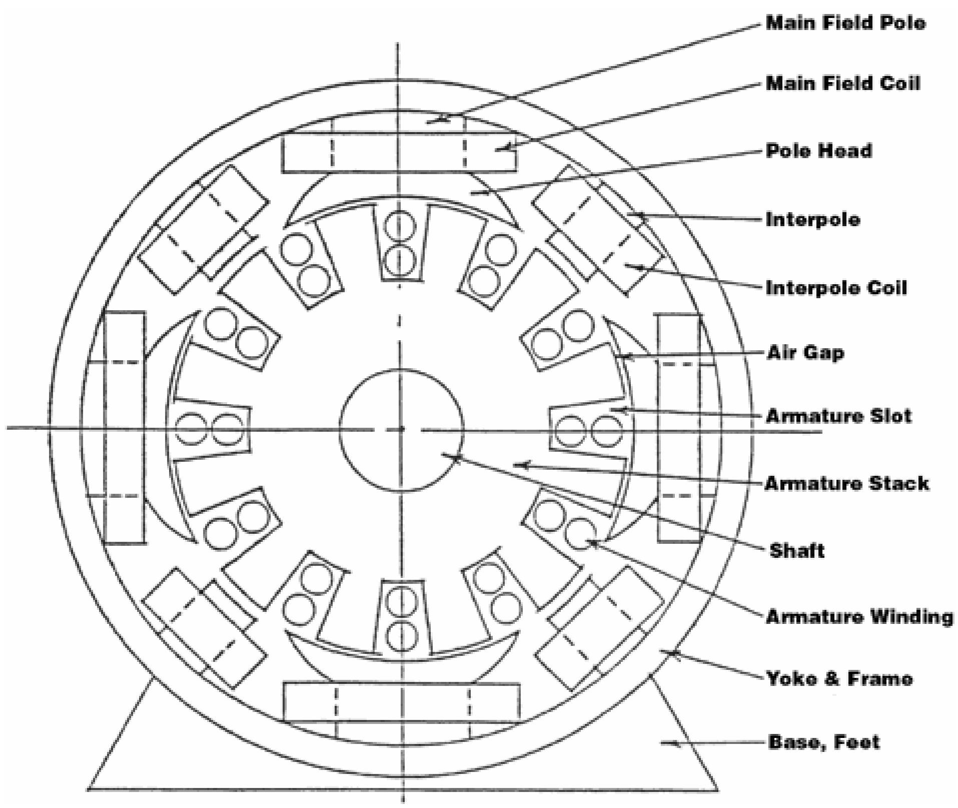

Fig 2.1 Cut View of DC Motor

The armature, or rotor, named so because it rotates, caries the armature windings that under the influence from the field windings. It is this interaction between the armature windings and the field windings that causes rotational torque to be produced. The rotor should possess a uniform small air gap (typically 0.05 cm to 0.25 cm) between the pole shoes and the armature to reduce losses due to the reluctance torque, TR. The reluctance can be described simply as the unwillingness of the magnetic circuit to be at a point other than equilibrium (un-aligned with the poles).

This reluctance torque is the force required overcoming the reluctance of the armature when it is not aligned with the pole faces (at minimum reluctance). It reduces the maximum possible output and efficiency of the motor. The commutator converts the direct current of the supply voltage to an alternating current to develop a unidirectional torque within the rotor. The commutator is a series of small copper conducting segments around the rotor shaft, and a stationary set of brushes.

2.3 Types of DC Motor

The DC motors are classified according the way, which the field winding is connected. According to this, DC Motor is classified as follows [1].

2.3.1 Series Connected Motor

This motor has its field winding connected in series with the armature. The armature current and the field current are therefore the same. A DC series motor can be distinguished by windings consisting of heavy gauge wire with few turns. The equivalent circuit is illustrated in Fig. 2-2.

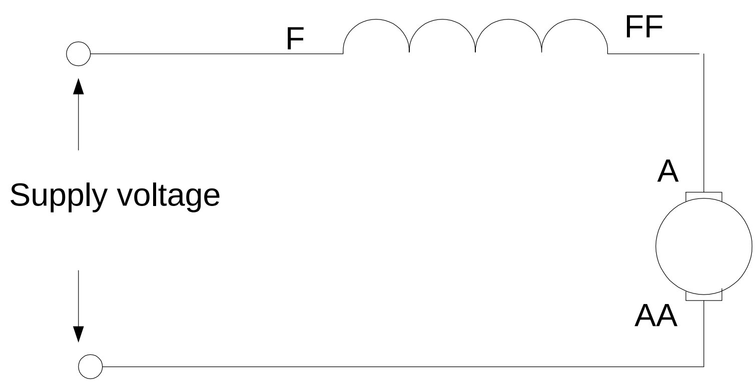

Fig 2.2 Series Connected Motor Circuit

The series motor is used mainly in traction systems, where the motor is always near full-load. This is a resultant of the fact that series motors accelerate to dangerous speeds at no-load.

2.3.2 Compound Connected DC Motor

This motor is a combination of the shunt and series connected motors with a winding connected in series and another winding connected in parallel with the armature. These machines exhibit greater speed regulation than shunt motors but does not obtain high speeds at low loads like series connected. They are found in traction drives, such as mining dump trucks.

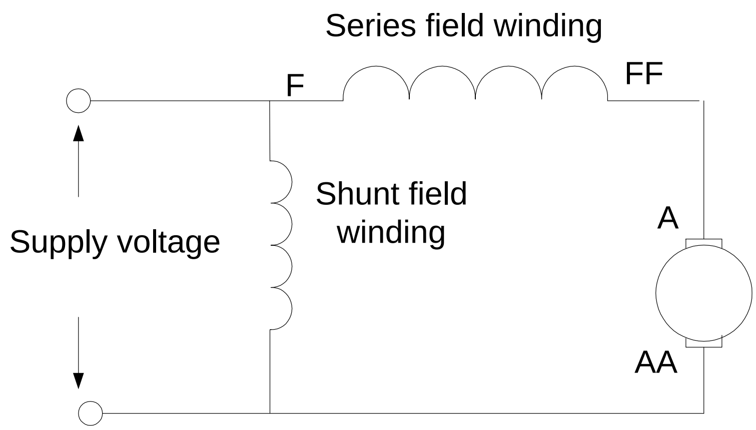

Fig. 2.3 Compound Connected Motor Circuit

2.3.3 Shunt Connected DC Motor

The shunt-connected motor is characterized by the field winding placed in parallel with the armature. The winding resistance is large to draw a small field current in comparison to the armature current. The equivalent circuit is shown below in Fig. 2-4.

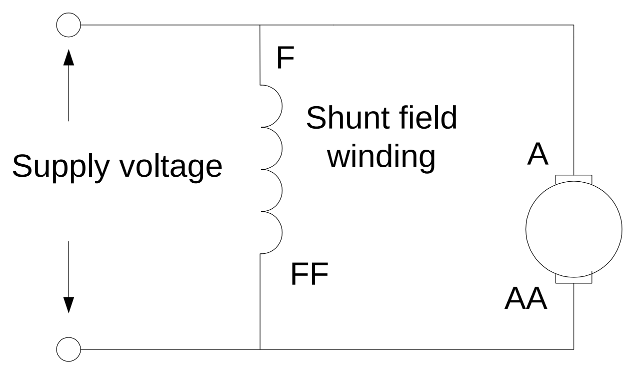

Fig. 2.4 Shunt Connected Motor Circuit

Shunt motors have easily controllable speed. This machine finds use in situations where speed control is required from no to full-load speed.

2.4 Basics of DC Motor

In a DC motor, the static field flux is established using either permanent magnets or a stator field winding. The armature winding, on the rotor of a DC machine, carries the main motor current. The armature winding is a series of coils, each connected to segments of a commutator. In order that the motor develops constant torque as the rotor moves, successive armature coils must be connected to the external DC circuit. This is achieved using a pair of stationary brushes held in contact with the commutator. The motor torque is produced by the interaction of the field flux and the armature current and is given by,

$$M_d \alpha I_a I_f \qquad \text{………2.4.1}$$

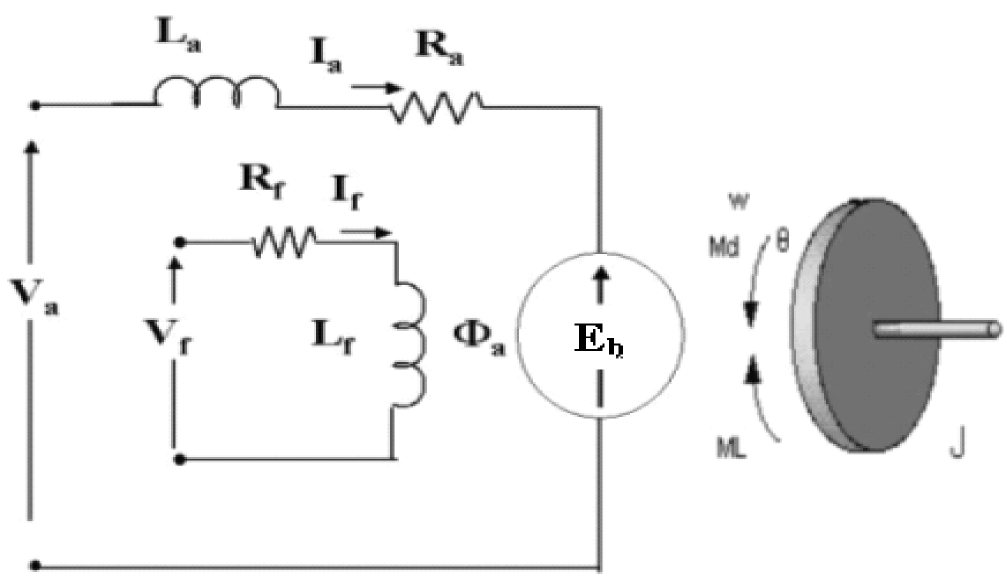

Fig. 2.5 Equivalent Circuit of a Separately Excited DC Motor

The back emf developed across the armature conductors increases with the motor speed,

$$E_b \alpha \omega_m \qquad \text{………2.4.2}$$

For field wound DC motors the field current controls the flux and hence the motor torque and speed constants. The field winding can be connected in series with the armature winding, in shunt with it, or can be separately excited. The separately excited DC motor, shown in Fig. 2.5 can be made to operate in two distinct modes: constant torque operation up to the rated speed of the motor, and then constant power operation above rated speed, as shown in Fig.2.6 The steady state operation of the motor is described by,

$$V_a = E_b + I_a R_a \qquad \text{………2.4.3}$$

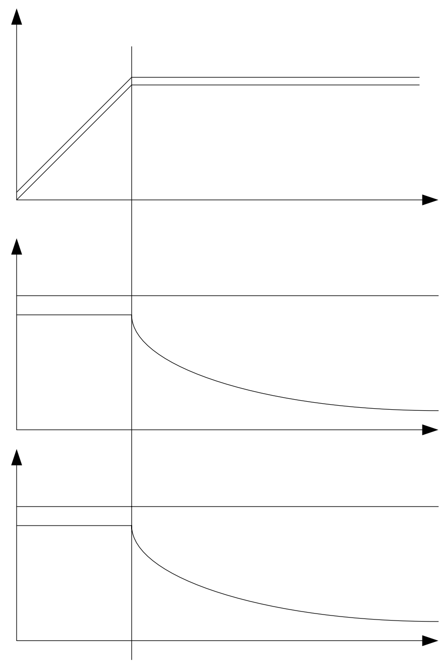

Fig. 2.6 Torque - Speed Characteristic of Separately Excited DC Motor

For normal motor operation E_b and I_a are positive and the motor is operating in its 'first quadrant'. The motor is said to be operating in its second quadrant that is braking or regenerating, by reducing V_a below Ea such that I_a is negative. These two quadrants are shown in Fig.2.7 a) [1]. If the polarity of the applied voltage is reversed then motoring and regenerating operation can occur with the direction of rotation reversed. Thus by controlling the armature voltage and current polarities, full four-quadrant operation, as shown in Fig.2.7 b), can be achieved. The speed can be varied by controlling the armature voltage V_a known as voltage control method and controlling the field current I_f known as field control method. The speed, which corresponds to the rated armature voltage, rated field voltage, rated field current and rated armature current is known as base speed.

In practice, for a speed less than the base speed, field current is maintained constant to meet the torque demand, and the armature voltage V_a varied to control the speed. For speed higher than the base speed, the armature voltage is maintained at the rated value and the field current is varied to control the speed. However, the power developed by the motor remains constant [2].

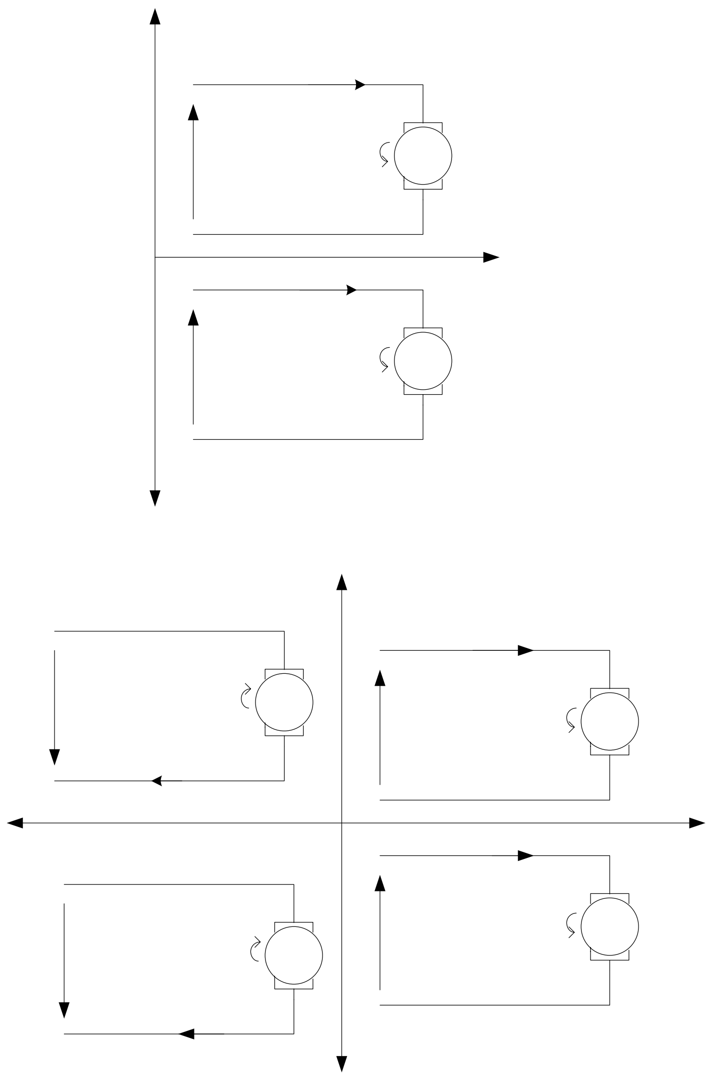

Fig. 2.7 Modes of Operation

The DC machine has many advantages:

- High starting torque (good for traction systems)
- Good braking torque
- Quickly reversible direction
- Maintain constant mechanical power output

- Maintain constant torque
- Permit continuous speed variation (as large as 4:1, is only really limited by continuity of current)

2.5 Types of DC Motor Speed Control Method

Speed of the DC motor can be controlled by any of the following methods

i) Armature Voltage control

ii) Flux control

iii) Armature resistance control

Armature voltage control is preferred because of high efficiency, good transient response and good speed regulation. But it can provide speed control below base speed because the armature voltage cannot be allowed to exceed rated value. For speed above the base speed field flux control is employed. In normally, the maximum speed can be allowed up to twice rated speed and in specially designed machines it can be six times rated speed.

2.5.1 Armature Voltage Control Method

Variable armature voltage for speed control, starting, breaking and reversing of DC motor can be obtained by the following methods

When the supply is AC

i) Ward-Leonard scheme

ii) Transformer with taps and uncontrolled rectified bridge

iii) Static Ward-Leonard scheme or Controlled rectifier

When supply voltage is DC

iv) Chopper control

2.5.1.1 Ward-Leonard Scheme

It consists of a separately excited generator feeding the DC motor to be controlled. The generator is driven at a constant speed by an AC motor connected to 50 Hz AC mains. The driving motor may be an induction motor or a synchronous motor. When the source of power is not electrical, generator is driven by a non-electrical prime mover such as a diesel engine of gas turbine. Motor terminal voltage can be control by adjusting the field current of the generator. When field voltage is smoothly varied in either direction, the motor terminal voltage and therefore speed can be steplessly varied from full positive to full negative. Figure 2.8 shows the Ward Leonard control scheme for DC motor [3].

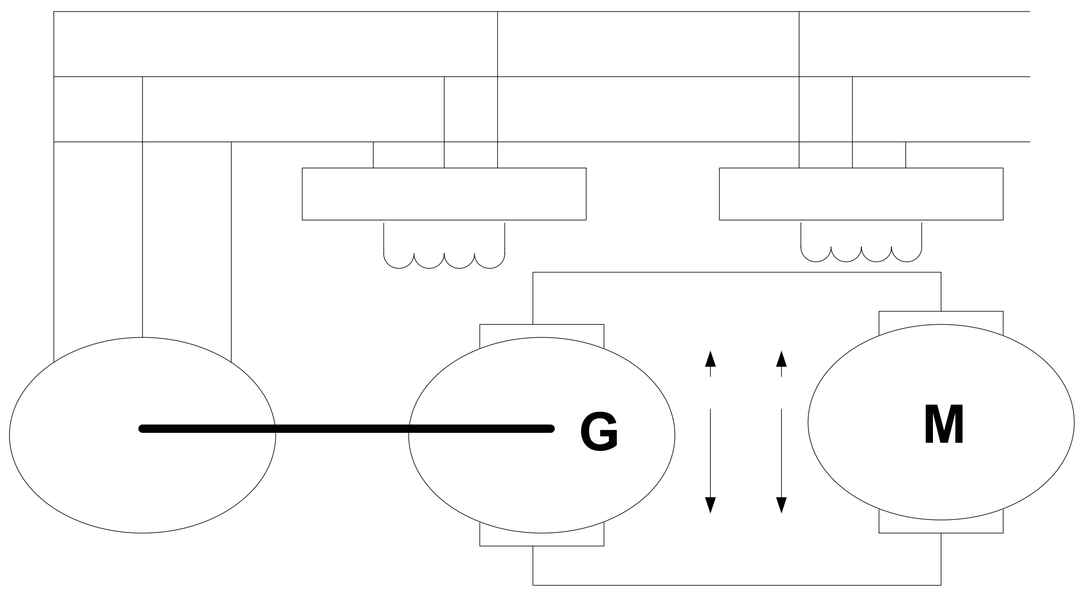

Fig. 2.8 Ward Leonard Drive

This system has the following advantages:

i) Full forward and reverse speed is achievable

ii) Armature current is smooth

iii) Overload capacity is large

Although it also exhibits the following disadvantages:

i) High cost – due to cost of 2 motors and a generator

ii) Large components needing space

iii) Maintenance issues

2.5.1.2 Transformer and Uncontrolled Rectifier Scheme

Variable voltage for the DC voltage can be obtained by either using auto transformer or using a transformer with tapings followed by an uncontrolled rectifier as shown in Fig. 2.9. A reactor is connected in the armature circuit to improve armature current waveform.

Autotransformer can be employed for low power ratings. For higher applications a transformer with tapings is employed and tap changing is done with the help of the on load tape changer.

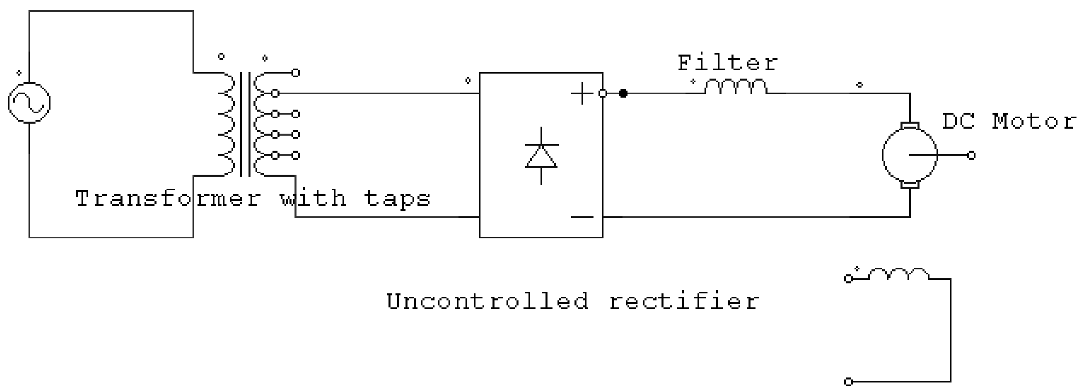

Fig. 2.9 Armature Voltage Control using a Transformer with Taps and an Uncontrolled Rectifier

The important feature of the this scheme are as follows

i) Out put voltage can be changed by in steps
ii) Rectifier output voltage waveform does not change as the output voltage in reduced. A good power factor is maintained at the source and current harmonics introduce in the supply lines do not increase abnormally, like in the case of a controlled rectifier when motor voltage is reduced to small value.
iii) Because of the use of diode circuit is not capable of regeneration.

2.5.1.3 Controlled Rectifier Fed DC Motor Drive

Controlled rectifiers are used to get variable DC voltage from an AC source of fixed voltage. The controlled rectifier fed DC motor drive is also known as static ward Leonard drive. Fig.2.10 shows commonly used controlled rectifier circuits. As thyristors are capable of conducting only in one direction, all these rectifier are capable of providing current only in one direction, rectifiers of Fig.2.10 a) and c) provide control of DC voltage in either direction and therefore, allow motor control in quadrant I and IV. They are known as fully controlled rectifiers. Figure 2.10 b) and d) are called half controlled rectifiers, as they allows the DC voltage control in one direction.

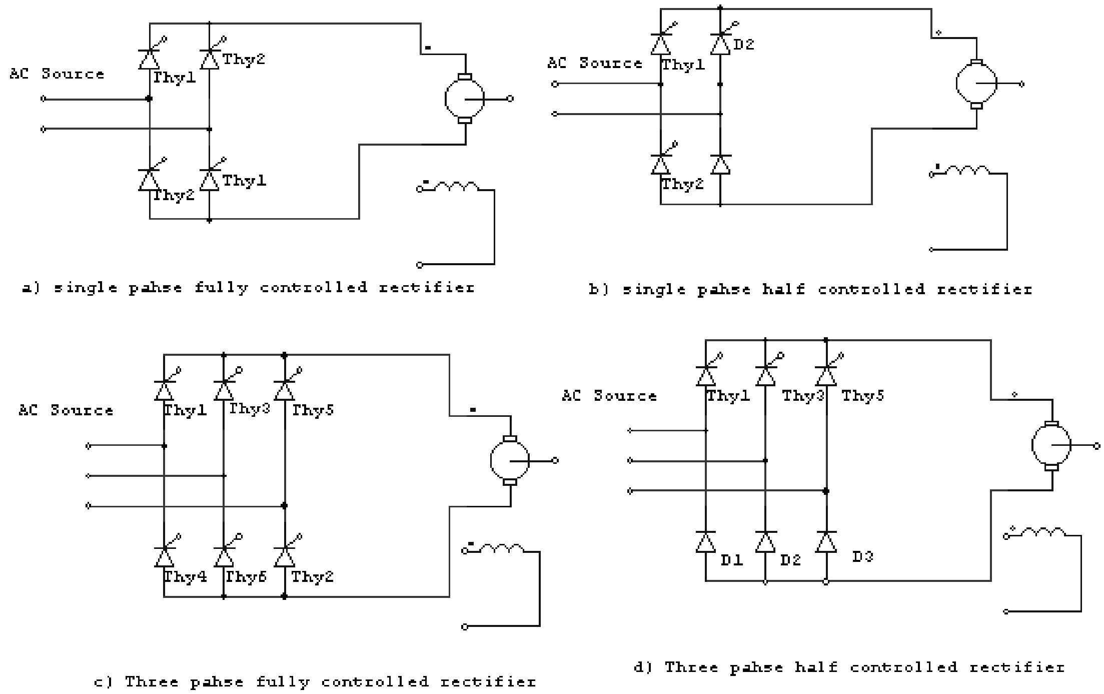

Fig. 2.10 Single Phase and Three Phase Controlled Rectifier Circuits

2.5.1.4 Chopper Control

Now a days chopper based DC motor drive is widely used. In chopper based DC motor drive input supply is DC. With the help of the self-commutated devices like MOSFET, GTO, and IGBT, this DC voltage is converted in to the variable DC voltage. A transistor chopper controlled RLE load is shown in Fig. 2.11 [3]. Transistor T_r is operated periodically with period T and remains on for a duration t_{on} . During on period the motor terminal voltage is V_a is given by

$$V_a = \delta V \qquad \text{...........2.2.1}$$

Where V = Supply Voltage.

δ = Duty Cycle

$$= \left(\frac{t_{on}}{T}\right)$$

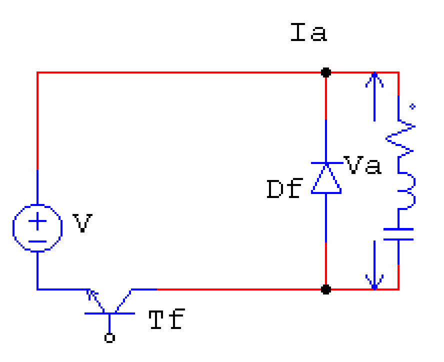

Fig.2.11 Chopper Control of RLE Load

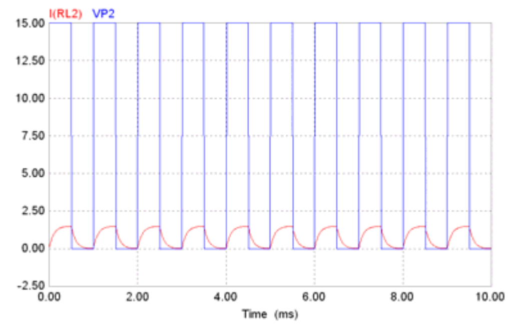

Fig.2.12 Waveform of Chopper Control

By changing the duty cycle, variable DC voltage for armature supply can be obtained. This method is generally use when supply is DC. But when supply is AC, first of all AC is converted in to the DC and then Chopper control can be use. It requires two stages of conversion from AC to DC and then DC-to-DC, thus efficiency of the method is less then controlled AC to DC converter. And also due to the limitations in rating of the self-commutated switches, it cannot be use for high power drives.

2.5.2 Field Control

For speed above the base speed flux control is employed. In this method field voltage is varied to control the field flux. When speed is below the based speed, rated field voltage is apply to the field and when speed above the base speed is required field voltage is reduced. The variable field voltage is obtained by using any of the armature control method. As speed is increase above the base speed, motor developed torque is reducing.

2.5.3 Armature Resistance Control

Armature resistance control method is generally not use in industries. In this method external resistance is inserted in to the armature circuit and by varying the resistance armature voltage can be reduced. Hence speed of the DC motor can be controlled. Efficiency of this method is poor because there is a power loss occurs in the resistance. Due to these reason this method is not use.

Chapter 3
Converter Topology and Control Techniques

3.1 Converter Topology

For low cost, low power applications (up to about 10 kW) a single-phase rectifiers can be used. Low-power, economical drives can also be constructed using single-phase half-wave rectifier with freewheeling diodes. For higher power drives (up to MW range), three-phase supply with three-phase rectifier is normally employed. For low to medium power DC supplied drives (such as battery), a chopper (DC-DC converter) is used. It is also common to find in some applications (especially locomotives), choppers are used in conjunction with uncontrolled bridge rectifiers. They are normally rated at medium power (100s of kW)

For obtaining the variable DC voltage there are no. of topologies are available such as,

i) Using Switched-mode:

Full bridge DC-DC converter: 4-quadrant operation

Half bridge: 2 quadrants

Simple single-quadrant converter (buck): 1 quadrant

ii) Using line-frequency Controlled Rectifier

Normally in high power drives thyristor are use. The controlled DC voltage can be obtained by varying the firing angle of the thyristor. In phase controlled rectifier the line current is unidirectional, but the output voltage can be reverse. Hence two-quadrant operation is possible.

3.1.1 Three Phase Fully Controlled Rectifier

A three-phase fully controlled bridge rectifier can be constructed using six thyristors as shown in Fig. 3.1.

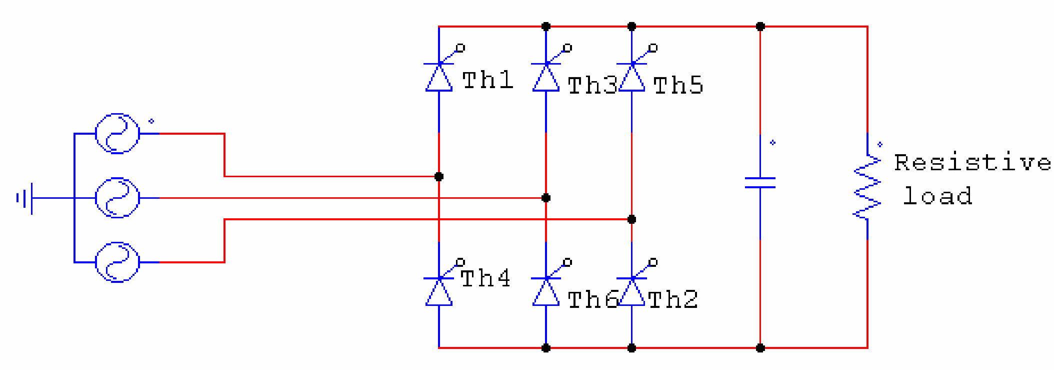

Fig. 3.1 Three Phase Fully Controlled Rectifier with Resistive Load

The three-phase bridge rectifier circuit has three-legs, each phase connected to one of the three phase voltages. Alternatively, it can be seen that the bridge circuit has two halves, the positive half consisting of the Thyristors Th1, Th3 and Th5 and the negative half consisting of the thyristors Th2, Th4 and Th6. At any time, one Thyristor from each half conducts when there is current flow. If the phase sequence of the source be RYB, the Thyristors are triggered in the sequence Th1, Th2, Th3, Th4, Th5, Th6 and Th1 and so on.

The operation of the circuit is first explained with the assumption that diodes are used in place of the Thyristors. The three-phase voltages vary as shown in Fig. 3.2

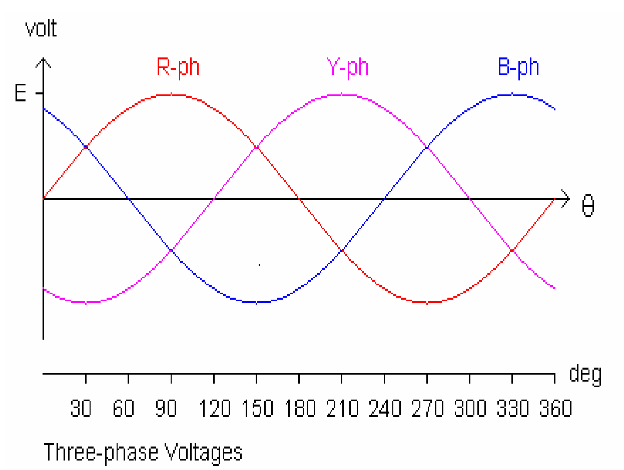

Fig. 3.2 Waveform of Three Phases

It can be seen that the R-phase voltage is the highest of the three-phase voltages when θ is in the range from 30^o to 150^o. It can also be seen that Y-phase voltage is the highest of the three-phase voltages when θ is in the range from 150^o to 270^o and that B-phase voltage is the highest of the three-phase voltages when θ is in the range from 270^o to 390^o or 30^o in the next cycle. We also find that R-phase voltage is the lowest of the three-phase voltages when θ is in the range from 210^o to 330^o. It can also be seen that Y-phase voltage is the lowest of the three-phase voltages when θ is in the range from 330^o to 450^o or 90^o in the next cycle, and that B-phase voltage is the lowest when θ is in the range from 90^o to 210^o. If diodes are used, diode D_1 in place of Th1 would conduct from 30^o to 150^o, diode D_3 would conduct from 150^o to 270^o and diode D_5 from 270^o to 390^o or 30^o in the next cycle. In the same way, diode D_4 would conduct from 210^o to 330^o, diode D6 from 330^o to 450^o or 90^o in the next cycle, and diode D_2 would conduct from 90^o to 210^o. The positive rail of output voltage of the bridge is connected to the topmost segments of the envelope of three-phase voltages and the negative rail of the output voltage to the lowest segments of the envelope.

At any instant barring the changeover periods, when current flow gets transferred from one diode to another diode, only one of the following pairs conducts at any time. If Thyristors are used, their conduction can be delayed by choosing the desired firing angle. When the Thyristors are fired at 0^o firing angle, the output of the bridge rectifier would be the same as that of the circuit with diodes. For instance, it is seen that D_1 starts conducting only after $\theta = 30^o$. In fact, it can start conducting only after $\theta = 30^o$, since it is reverse-biased before $\theta = 30^o$. The bias across D_1 becomes zero when $\theta = 30^o$ and diode D_1 starts getting forward-biased only after $\theta =30^o$. When $V_R(\theta) = E \times Sin(\theta)$, diode D_1 is reverse-biased before $\theta = 30^o$ and it is forward-biased when $\theta =30^o$. When firing angle of Thyristor is zero degree, Th1 is triggered when $\theta = 30^o$. This means that, if a synchronizing signal is needed for triggering Th_1, that signal voltage would lag $V_R(\theta)$ by 30^o and if the firing angle is α then Thyristor Th1 is triggered when $\alpha = \theta + 30^o$. Given that the conduction is continuous, the following Table 3.1 presents the Thyristors pair in conduction at any instant.

TABLE 3.1.
THYRISTOR PAIR CONDUCTION TABLE

Period, range of θ	Thyristor Pair in conduction
$\theta + 30^o$ to $\theta + 90^o$	Th1 and Th6
$\theta + 90^o$ to $\theta + 150^o$	Th1 and Th2
$\theta + 150^o$ to $\theta + 210^o$	Th2 and Th3
$\theta + 210^o$ to $\theta + 270^o$	Th3 and Th4
$\theta + 270^o$ to $\theta + 330^o$	Th4 and Th5
$\theta + 330^o$ to $\theta + 360^o$ and $\theta + 0^o$ to $\theta + 30^o$	Th5 and Th6

3.2 Control Techniques

There are no. of techniques for firing the Thyristors for 1-phase & 3-phase controlled rectifier, some of the most popular methods are as follows.

i) Linear firing angle control

ii) Cosine wave control

iii) PLL based control

The function of controller is to control the firing angle α of a converter symmetrically in response to a demand of output DC voltage or current. Any other control loop can be applied as desired. The controller usually incorporates the following function [3].

- Line synchronization
- Control of firing angle α
- Advance limit of angle α
- Retard limit of angle α

Line synchronization permits the establishment of a symmetrical firing angle control to all thyristors with respect to the fixed position of line AC voltage wave. The firing angle controller alters angle α in response to a variable input control voltage. The advance and retard limit controls restrict the angle α within safe limits. Theoretically, the advance limit angle can be establishment as early as $\alpha = 0$, but the retard limit angle must provide a sufficient margin so that a minimum turn-off angle γ is maintained to avoid commutation failure.

3.2.1 Linear Firing Angle Control

The line supply voltage V_{RY} is stepped down through a transformer and converted to a square wave through a zero-crossing detector. A saw-tooth wave of twice the supply frequency can be generated such that it remains synchronized with the square wave. The saw-tooth wave stars with an initial voltage at zero angle, linearly decreases to zero at angle Π, and restarts again. The control voltage V_c is compared with the saw-tooth wave and firing angle is generated at the crossover point by the following linear relation,

$$\alpha = \frac{\Pi}{A} \times V_c + \Pi \qquad \text{.........3.2.1}$$

The long firing pulse train in the interval Π - α is created for the respective thyristor through a steering circuit. As the control voltage V_c is increase, α advances, giving a higher DC voltage at the output until α approaches zero at $V_c = A$. On the other extreme, α approaches Π at $V_c = 0$ in the absence of a retard limit control. The relation between control voltage V_c and output

$$V_d = V_{d0} \cos\alpha \qquad \text{..........3.2.2}$$

$$V_d = V_d \cos\left(\Pi - \frac{\Pi}{A} \times V_c\right) \qquad \text{.........3.2.3}$$

Because of nonlinear transfer characteristics, linear firing angle control is hardly used.

3.2.2 Cosine Wave Control

A popularly used control method where linearity of transfer characteristic is achieved is known as the cosine wave-crossing method. Figure 3.3 shows the cosine wave crossing control method for a three-phase bridge converter. The derivation of firing logic signals for thyristor Th1 is shown only, but the principle can be easily extended to the other firing angle range voltage V_{RB} is reference wave in which the angle 0 to Π corresponds to the firing angle range of Th1. The phase voltage $-V_Y$ leads the V_{RB} by $\frac{\Pi}{2}$ and constitutes the cosine reference wave for thyristor Th1. the phase and line voltages are stepped down through the transformers and connected to the comparators, as shown. The comparator 1, which compares the control voltage V_c with phase voltage $-V_Y$, transitions to logic 1 at firing angle α. The output of comparators 1 and 2 are logically ANDed to trigger flip flop at the leading edge, which in turn couples a pulse train to the gate of Th1. the flip flop is reset at the firing of Th3, thus limiting the gate pulse duration to $2\frac{\Pi}{3}$. The firing angle of Th1 can be advanced or retarded by increasing of decreasing, respectively, the magnitude of V_c. The advance limit notch, as indicated, is coupled to AND gate and the retard- limit pulse is coupled to OR gate. Fig 3.3 shows the practical implementation circuit for the cosine wave control and fig 3.4 shows how the firing pulse is generate for the thyristor 1. When the control voltage $-V_Y$ is less than V_c the firing pulse is generate. By varying this control voltage, the firing angle of thyristor can be vary.

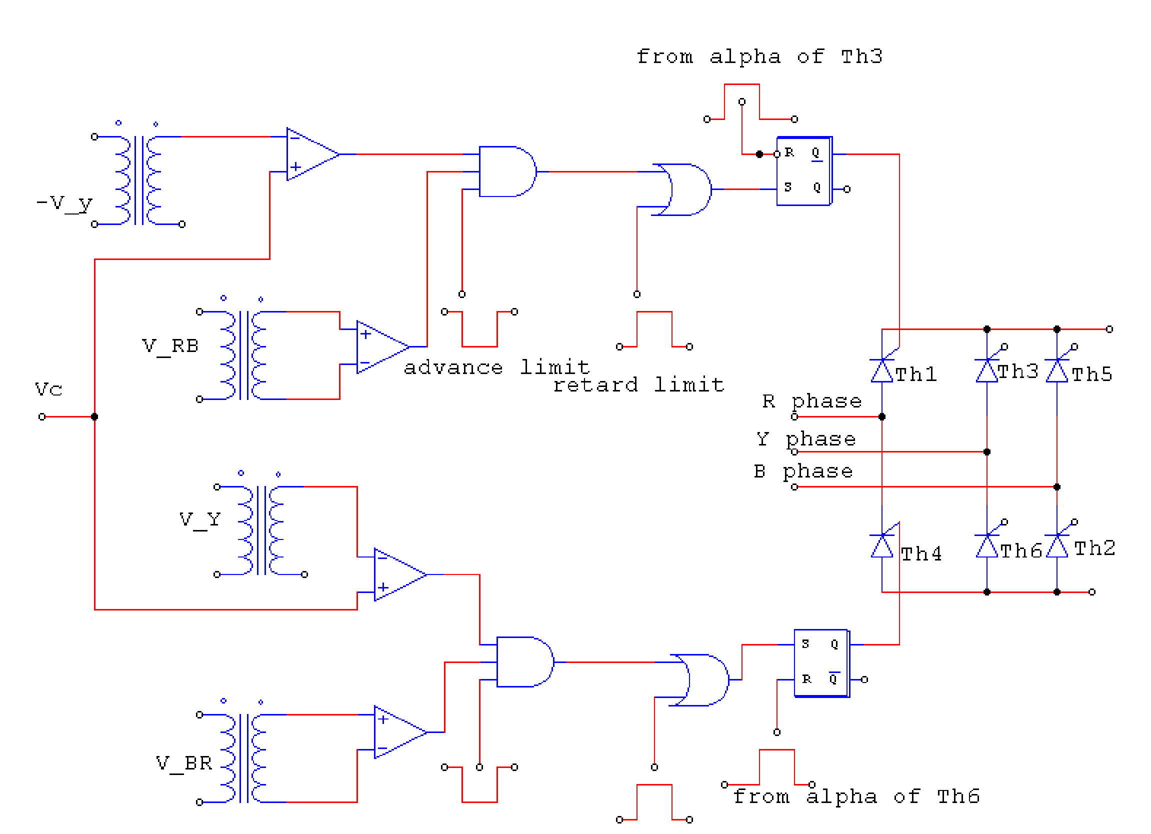

Fig. 3.3 Control Circuit of Cosine Wave Firing Scheme

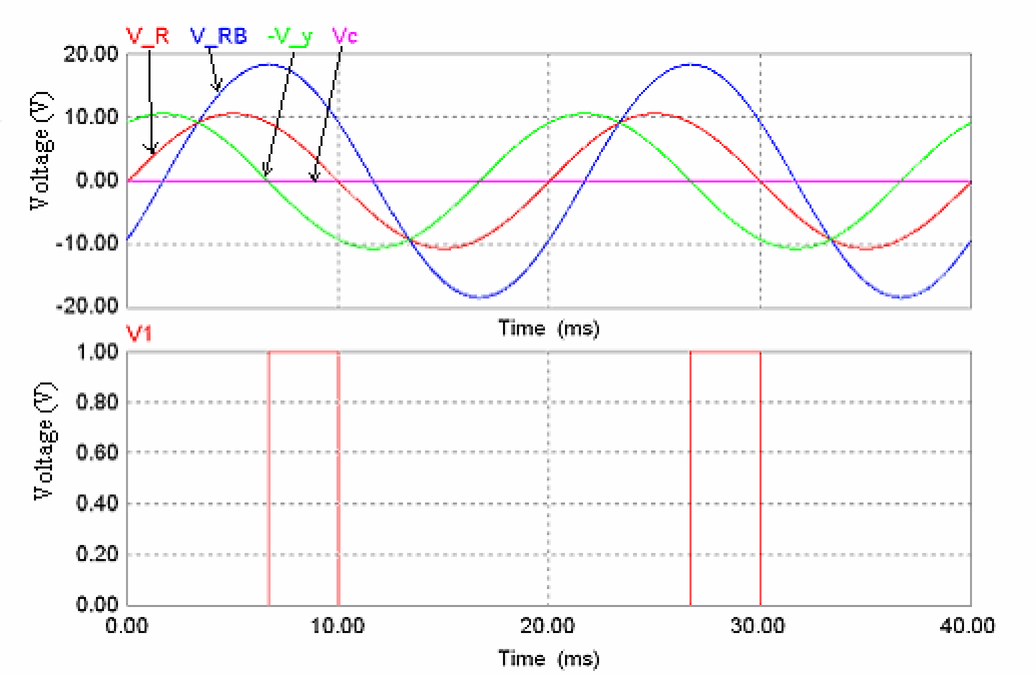

Fig. 3.4 Firing Pulse for Thyristor 1 Using Cosine Wave Firing Scheme

3.2.3 Phase Lock Loop Control

For precise speed control of servo systems, closed loop control is normally used. The speed is compared with the reference speed to generate the error signal and to vary the armature voltage of the motor. These analog devices for speed sensing and comparing signals are not ideal and the speed regulation is more than .2%. The speed regulator can be improved by using PLL controlled method. In phase lock loop control system, the motor speed is converted to a digital pulse train by a speed encoder. The output of the encoder acts as the speed feedback signal of frequency f_o. The phase detector compares the reference pulse train f_r with the feedback frequency f_o and provides a pulse width modulated output voltage V_e Which is proportional to the difference in phase and frequencies of the reference and feedback pulse trains. The phase detector is available in integrated circuits. A low pass loop filter converts the pulse train V_e to a continuous DC level V_c which varies the output of the power converter and in turn the motor speed.

When the motor runs at the same speed as the reference pulse train, the two frequencies would be synchronized together with a phase difference. The output of the phase detector would be constant voltage proportional to the phase difference and the steady-state motor speed would be maintained at a fixed value irrespective of the load on the motor. Any disturbances contributing to the speed change would result in a phase difference and the output of the phase detector responds immediately to vary the motor in such a direction and magnitude as to retain the locking of the reference and feedback frequencies. The response of the phase detector is very fast. As long as the two frequencies are locked, the speed regulation should ideally be zero. However in practice the speed regulation is limited to 0.002% and this represents a significant improvement over the analog speed control system [3].

3.2.4 Synchronizing Signal

To vary the output voltage, it is necessary to vary the firing angle. In order to vary the firing angle, one commonly used technique is to establish a synchronizing signal for each Thyristors. It has been seen that zero degree firing angle occurs 30^o degrees after the zero crossing of the respective phase voltage. If the synchronizing signal is to be a sinusoidal signal, it should lag the respective phase by 30^o. When the 3-phase source supply connected to the rectifier is star-connected, the line voltages and the phase voltages have a 30^o phase angle difference between them, as in Fig. 3.5.

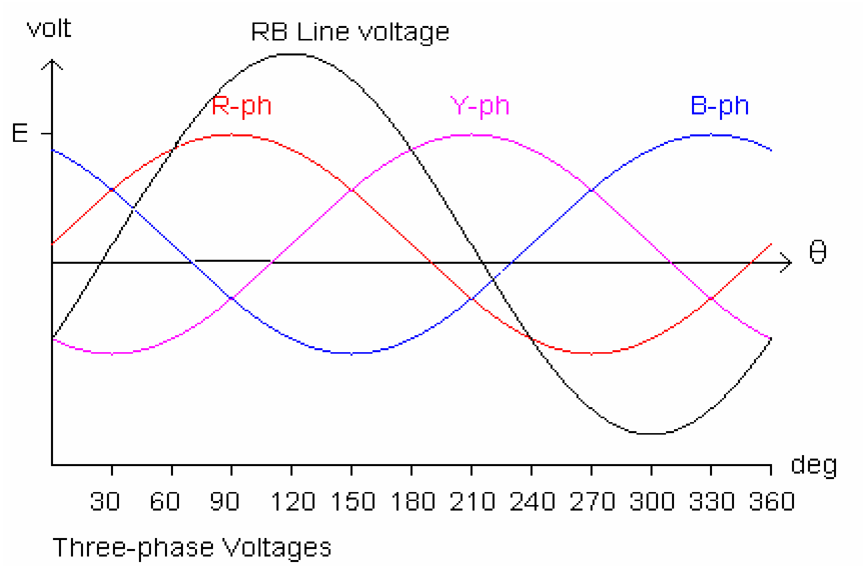

Fig. 3.5 Synchronizing Signal for Thyristor 1

This line voltage lags the R-phase voltage by30^o and has amplitude, which is 1.732 times the amplitude of the phase voltage. The synchronizing signal for Thyristors Th1 can be obtained based on V_{RB} line voltage. The synchronizing signals for the other Thyristors can be obtained in a similar manner.

To get the synchronizing signals, three control transformers can be used, with the primaries connected in delta and the secondary in star. For Th1, voltage V_{RB} is used as the synchronizing signal. Voltage V_{YB} is used as the synchronizing signal for Thyristor Th2 and so on. The waveforms presented by the synchronizing signals are as shown Fig. 3.6. The waveforms do not show the effect of turns ratio, since any instantaneous value has been normalized with respect to its peak value. For example, let the primary phase voltage be 240 V and then its peak value is 339.4 V. The primary voltage is normalized with respect to 339 V. If the peak voltage of each half of secondary is 10 V, the secondary voltages are normalized with respect to 10 V. Table 3.2 shows the synchronizing signal required for the thyristors [4].

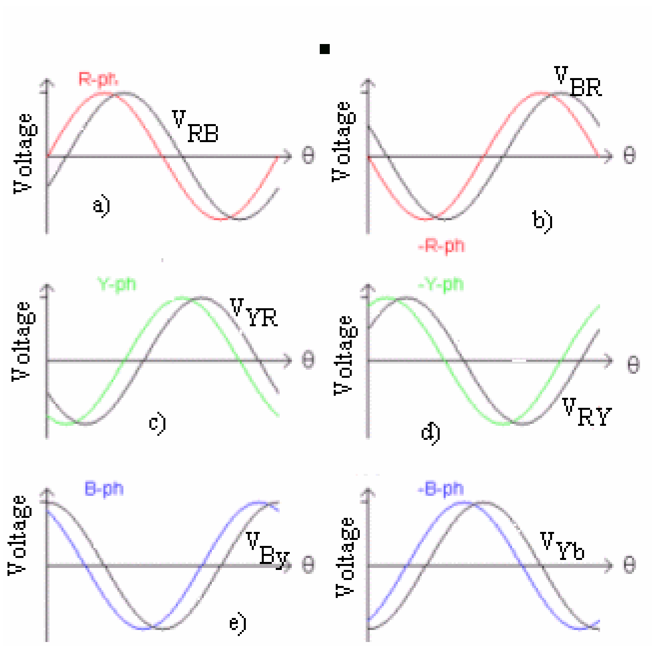

Fig. 3.6 Synchronizing Signal for Triggering a) Thyristors 1 b) Thyristor 4 c) Thyristor 3 d) Thyristor 6 e) Thyristor 5 and f) Thyristor 2

TABLE 3.2
SYNCHRONIZING SIGNAL FOR TRIGGERING THE THYRISTORS

Thyristor no.	Reference line voltage
Thyristor 1	V_{RB}
Thyristor 4	V_{BR}
Thyristor 3	V_{YR}
Thyristor 6	V_{RY}
Thyristor 5	V_{BY}
Thyristor 2	V_{YB}

Chapter 4
Design of Controller

DC motor control system consists of DC motor, converter and controller, to obtain controller parameter it is necessary to convert all the component in the equivalent transfer function. This chapter include the basic block diagram of DC Drive, mathematical modeling of DC motor, mathematical modeling of power converter include with control circuit and design of the speed and current controller.

4.1 Basic Block Diagram

A separately excited DC motor is considered to be a multi-input, multi-output system. This machine is widely used in many variable speed drives. Open-loop operation of the motor can be unsatisfactory in some industrial applications. If the drive requires constant-speed operation under changing load torque, closed loop control is necessary. The closed loop speed control system consists of a separately excited DC motor; three phase fully controlled converter, and proportional integral type (PI) speed and current controllers. The block diagram representation of the system is given in Figure 4.1. The closed-loop control of the motor has basically two feedback loops. The outer loop is a speed feedback loop and the inner loop is the current feedback loop. The controllers used in these loops are both of PI type. The speed controller output is the reference for the current controller. The output of the current controller is the input to the fully controlled converter that controls the motor input voltage

The speed controller is usually a PI controller and serves three purposes – stabilizes the drive and adjusts the damping ratio at the desired value, makes the steady state speed-error close to zero by integral action, and filters out noise again due to the integral action. In close loop control systems PD (proportional and differential) and PID (proportional integral and differential) controller are often used. But they are not preferred in converter drives because of the presence of substantial noise and ripple in the current and speed feedback signals. The output of the speed controller e_c is applied to the current limiter which set the reference I_a^* for the inner current control loop. The output signal of the speed controller should be limited at the upper as well as the lower end $0 <= I_a^* <= I_{amax}$ [2]. The armature current is sense by a current sensor, filtered to remove ripple, and compared with the current reference I_a^*. The current is processed through a PI controller which enables to achieve the just mentioned three objectives, through it is not necessary to make the steady state current error close to zero. The output of the current controller V_c adjust the converter firing angle such that the actual speed is brought to a value set by the speed command wm^*. Any positive speed error, caused by either an increased in speed command or an increased in load torque produces a higher current reference I_a^*. The motor accelerates due to an increase in I_a, to correct the speed error and finally settles at a new I_a^* which makes the motor torques equal to the load torque and speed error close to zero. For large positive error , the current controller saturates and the current reference I_a^* is limited to a value I_{amax} (maximum armature current), and the drive current is not allowed to exceed the maximum permissible armature current until the speed error becomes small and the current limiter comes out of saturation. Now the speed error is corrected with I_a less than the permissible value [1] [5] [6].

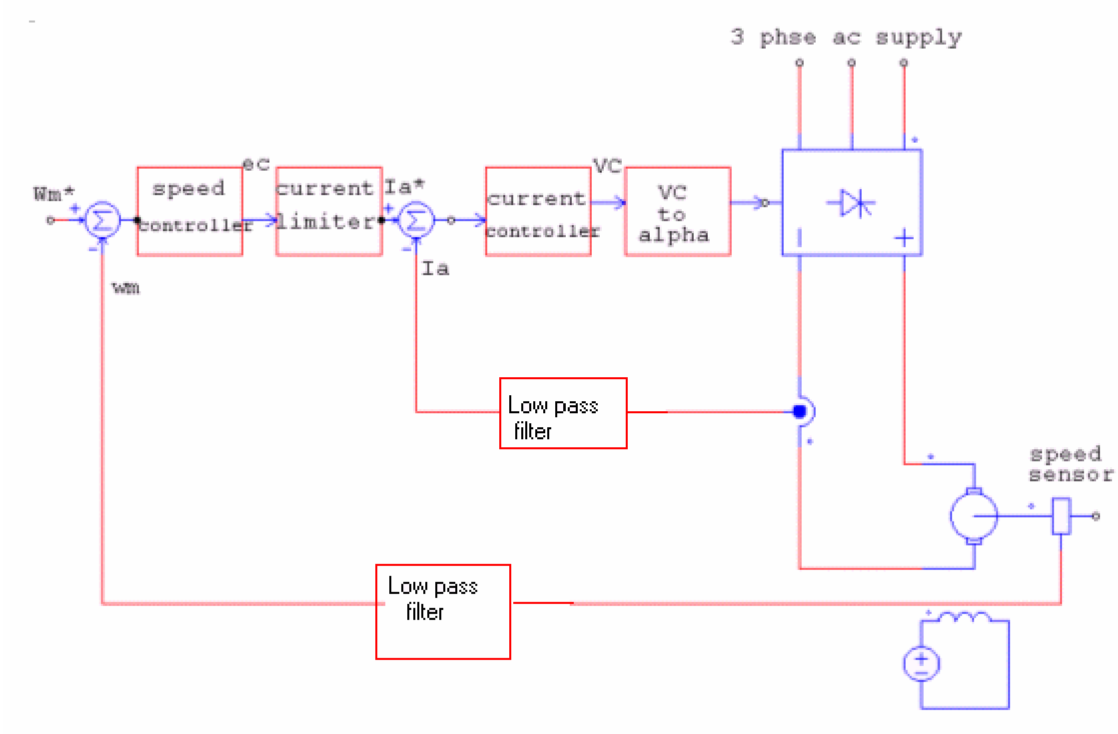

Fig. 4.1 Block Diagram of DC Motor Drive with Armature Control

4.2. Mathematical Modeling of DC Motor

The equivalent circuit of separately excited DC machine can be represented in schematic form as shown in Fig. 2.7 [7]. The armature is modeled as circuit with a resistance R_a in series with an inductance L_a and a voltage source E_b representing a back emf in the armature when the rotor rotates. The wound field is represented by a resistance R_f in series with an inductance L_f. The air-gap flux is designated by ϕ. The pertinent dynamic equations for the DC motor are as follows

$$R_a I_a(t) + L_a \frac{di_a(t)}{dt} + E_b(t) = V_a(t) \quad \text{.........4.2.1}$$

$$E_b(t) = C_1 \phi \omega(t) \quad \text{.........4.2.2}$$

$$J \frac{d\omega(t)}{dt} = M_d(t) - M_L(t) \quad \text{.........4.2.3}$$

$$M_d(t) = C2\phi i_a(t) \quad \text{.........4.2.4}$$

$$\frac{d\varepsilon(t)}{dt} = \omega(t)$$

It is assumed that the field flux Φf is constant and the dynamics associated with the field circuit is slow as compared to the armature circuit. From (4.2.2) and (4.2.4), it can be seen that

$$E_a(t) i_a(t) = \frac{C_1}{C_2} M_d(t) \omega(t) \quad \text{.........4.2.5}$$

Therefore $C_1 = C_2 = C$. The armature voltage V_a and field voltage V_f are assumed to be independently controllable. The machine model can be built from the dynamic equations as described above, and is shown in Fig. 4.2.

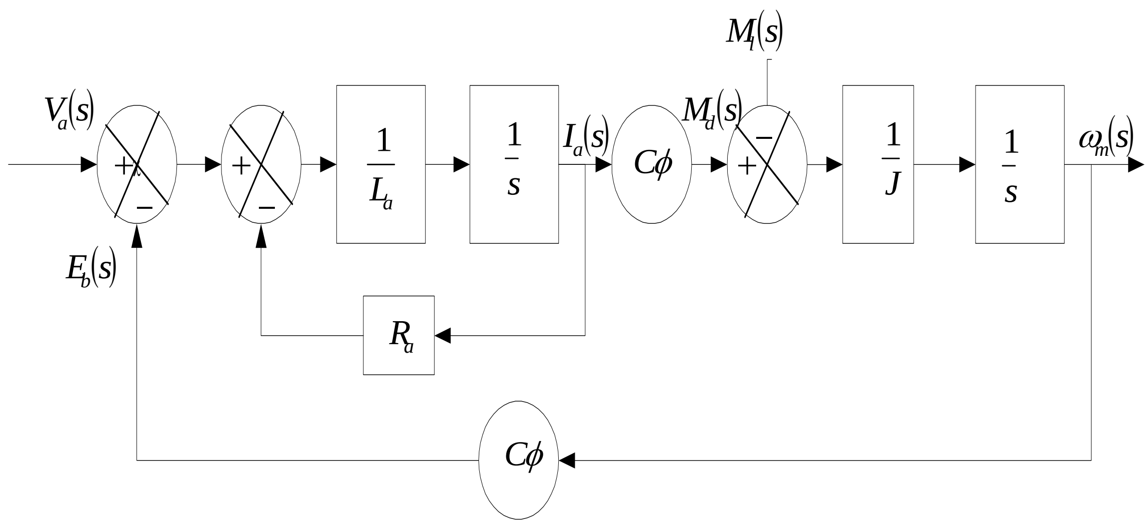

Fig. 4.2 Equivalent Model of Separately Excited DC Motor

The input output relationship can be determined for the above model in terms of transfer functions. Here the inputs to the system are $M_L(s)$ and $V_a(S)$ while the outputs are $I_a(s)$ and $w_m(s)$.

$$\frac{\mathrm{Ia(s)}}{\mathrm{Va(s)}} = \frac{(1/R_a)sT_{em}}{1+sT_{em}(1+sT_a)} \qquad \text{……….4.2.7}$$

$$\frac{\omega_{\mathrm{m}}(\mathrm{s})}{\mathrm{Va(s)}} = \frac{(1/C\phi)}{1+sT_{em}(1+sT_a)} \qquad \text{……….4.2.8}$$

$$\frac{Ia(s)}{M_L(s)} = \frac{(1/C\phi)}{1+sT_{em}(1+sT_a)} \qquad \text{……….4.2.9}$$

$$\frac{\omega_{\mathrm{m}}(\mathrm{s})}{\mathrm{Va(s)}} = \frac{(R_a/C\phi)^2(1+sT_a)}{1+sT_{em}(1+sT_a)} \qquad \text{..…….4.2.10}$$

The current loop can be represented as a simple lag with a time constant $T_a=L_a/R_a$ (called electrical time constant of motor). Similarly the mechanical time constant is defined as $T_{em} = JR_a/(C\phi)^2$. The equivalent model may be presented as shown in Fig. 4.3.

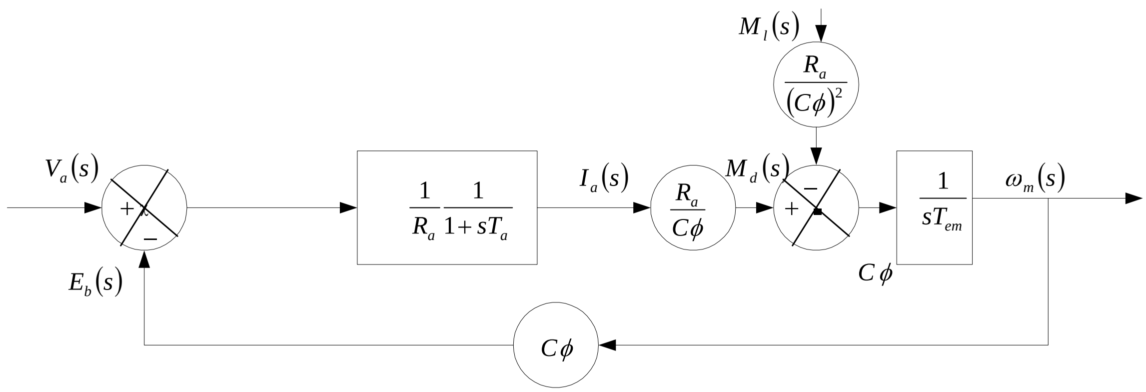

Fig. 4.3 Alternate Representation of the Equivalent Model of DC Motor

4.3 Mathematical Modeling Power converter

The output of the current controller is often a voltage, which sets the firing angle for the fully controlled bridge circuit. The firing of a rectifier is a discrete process. A variation in the output of the current controller does not change the firing angle instantaneously since the Thyristors in the bridge are triggered in a sequence at an interval of 60^o on the average and there is a delay before the change in the output of the current controller has an effect on the firing angle. The transfer function of a control unit is often is selected to match the transfer function of the converter. For conventional operation of 3 phase rectifiers under continuous conduction output voltage can be express as [1] [7],

$$V_d = 1.35 \times V_m \times \cos\alpha \qquad \text{..........4.3.1}$$

the maximum average output voltage that can be obtained at 0^o firing angle . Then the amplitude of line voltage of 3-phase supply is described by,

$$V_d = 1.35 \times V_m \qquad \text{..........4.3.2}$$

A variation in the output of the current controller does not change the firing angle instantaneously since the Thyristors in the bridge are triggered in a sequence at an interval of 60^o on the average and there is a delay before the change in the output of the current controller has an effect on the firing angle. This delay can be classified as a transportation lag and it can be approximated by a first-order transfer function, as shown in equation 4.3.3. In equation 4.3.3, y has been used in place of sT_t.

$$e^{-Y} = 1 - y + ... \approx \frac{1}{1+y} \qquad \text{……….4.3.3}$$

so the equivalent transfer function of the converter and control circuit can be express as

$$G_c(s) = \frac{K_t}{1 + sT_t} \qquad \text{……….4.3.4}$$

Where K_t = Gain of the converter

$$= 3 \times \frac{V_{rms}}{\Pi}$$

$$= 1.35 \times \frac{V_{rms}}{\Pi}$$

For a system with 50 Hz input source, one-sixth of a cycle is about 3.3 ms and then the delay T_t can be set to be half of that value, which is 1.67 ms [8].

4.4 Design of a DC Motor Control System

Block diagram shown in Fig. 4.1 is represented in to the equivalent transfer function block diagram as shown in Fig. 4.4.

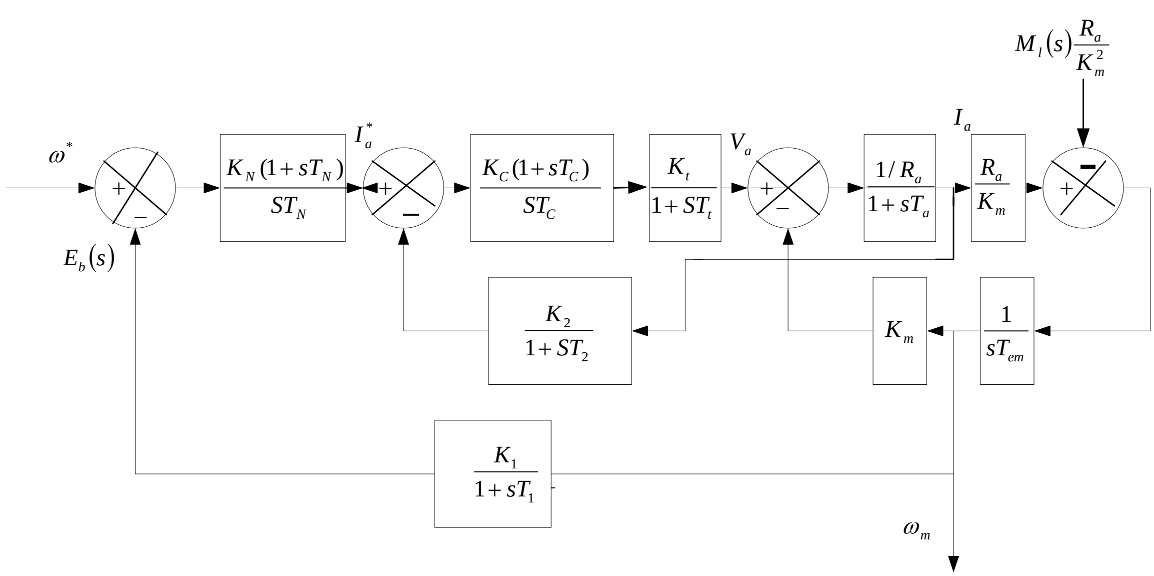

Fig. 4.4 Equivalent Transfer Function Block Diagram

4.4.1 Current Controller Design

The two output parameters of interest are the torque and the speed. The armature current is selected as one of the state-variables to be controlled in closed-loop, since the torque output varies linearly with it. It is preferable that the variable to be controlled by negative feedback is a variable that reflects some energy stored in a system. Here the armature current reflects the energy stored in the inductance in the armature circuit. If the motor has a compensating winding and/or a compound winding, the inductance of this winding should be added to L_a. In some drives, an additional inductor is used in series with the armature and this value should also be added to L_a. The part of the closed loop system that is usually used for controlling the armature current is shown in Fig. 4.5.

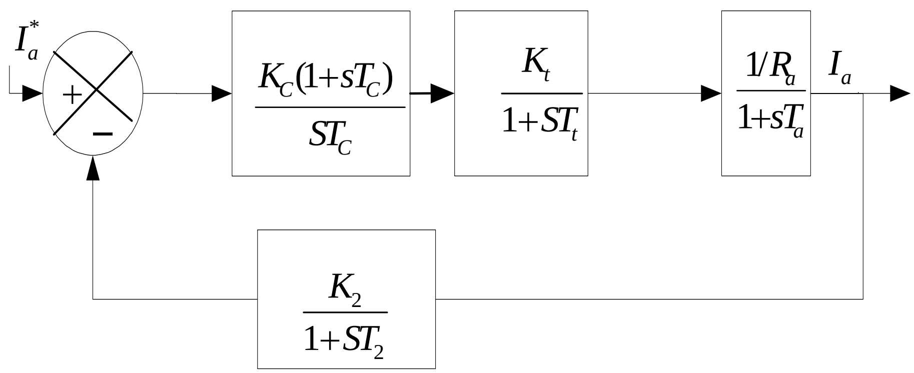

Fig. 4.5 Current Controller Block Diagram

The block diagram in Fig. 4.5 is now described. If the armature current is to be controlled in closed loop, it is necessary to have a current reference signal, marked as Ia^* in Fig. 4.5. This signal is internally generated; most often as the output of the controller for speed it is possible to use a controller other than a proportional plus integral (PI) controller. A PDF controller (a pseudo-derivative controller) or a PID-controller can be used. But a PI controller is often sufficient, since the integrating part of the PI controller leads to zero steady-state error for a step input and the proportional gain can be adjusted to yield fast response and stability [9]. The output of the current controller is often a voltage, which sets the firing angle for the fully controlled bridge circuit.

The closed loop transfer function of the current loop is

$$\frac{I_a^*(s)}{I_a(s)} = \frac{k_c\,(1+T_c s)\frac{k_t}{R_a}(1+T_2 s)}{T_c s\,(1+T_t s)(1+T_2 s)(1+T_a s)+k_c k_t \frac{1}{R_a} k_2\,(1+T_c s)}, \qquad \text{……….4.4.1}$$

The larger time constant T_a will be compensated by T_c.

So, $$\frac{I_a^*(s)}{I_a(s)} = \frac{k_c \frac{k_t}{R_a}(1+T_2 s)}{T_c s\,(1+T_t s)(1+T_2 s)+k_c k_t \frac{k_2}{R_a}},$$

The smaller time constant can be approximated as $\sigma = T_t + T_2$ and let $k_0 = \frac{k_c k_t}{R_a T_a}$ so that,

$$\frac{I_a^*(s)}{I_a(s)} = \frac{k_0\,(1+T_2 s)}{s^2\sigma + s + k_2 k_0} \qquad \text{……….4.4.2}$$

Now the gain k_c of the controller has to be chosen for the required transient response.

$$\frac{I_a^*(s)}{I_a(s)} = \frac{\frac{k_0}{\sigma}(1+T_2 s)}{s^2 + \frac{s}{\sigma} + \frac{k_2 k_0}{\sigma}}, \qquad \text{……….4.4.3}$$

The characteristic equation is of the form, $s^2 + 2\xi\,\omega_n s + \omega_n{}^2$.

Here, $2\xi\,\omega_n s = \frac{1}{\sigma}$, $\omega = \sqrt{\frac{k_2 k_0}{\sigma}}$.

$$\xi = \frac{1}{2\sigma\omega_n} = \frac{1}{2\sigma\sqrt{\frac{k_2 k_0}{\sigma}}}. \text{ Let } \xi = \frac{1}{\sqrt{2}}, \text{ then}$$

$$\frac{1}{\sqrt{2}} = \frac{1}{2\sqrt{k_2 k_0 \sigma}},$$

$$\sqrt{2} = \frac{1}{\sqrt{k_2 k_0 \sigma}} \quad i.e.\ k_0 = \frac{1}{2k_2\sigma}$$

$$k_0 = \frac{k_c k_t}{R_A T_A} = \frac{1}{2k_2\sigma}$$

So $k_c = \dfrac{R_a T_a}{2k_t k_2 (T_t + T_2)}$ and $T_C = I_a^*$ ……….4.4.4

The transfer function is

$\dfrac{I_a^*(s)}{I_a(s)} = \dfrac{K_t}{s\, T_t}$, Substituting for $k_0 = \dfrac{1}{2k_2\sigma}$

$$\frac{I_a^*(s)}{I_a(s)} = \frac{\frac{1}{2k_2\sigma}(1+T_2 s)}{s^2\sigma + s + k_2 k_0}$$

$$= \frac{\frac{1}{k_2}(1+T_2 s)}{1+2\sigma s+2\sigma^2 s^2}$$ ……….4.4.5

If the current reference is also smoothened by a filter having a transfer function, $\dfrac{1}{(1+T_2 s)}$, the resulting current loop is,

$$k_2 \frac{I_a^*(s)}{I_a(s)} = \frac{1}{1+2\sigma s+2\sigma^2 s^2}\ .$$ ……….4.4.6

The characteristic equation is of the form $1+\dfrac{2\xi s}{\omega_n}+\dfrac{s^2}{\omega_n^{\,2}}$. The transient response for a step input is,

$$y(t) = 1e^{-\frac{t}{2\sigma}}\left(\cos\frac{2}{2\sigma}+\sin\frac{t}{2\sigma}\right)$$ ……….4.4.7

The current loop is much faster than the speed loop, so this can be further approximated as,

$$\frac{I_a^*(s)}{I_a(s)} = \frac{(1+T_2 s)}{k_2(1+2\sigma s)}$$ ……….4.4.8

4.4.2 Design of Speed Control Loop

The design of the speed controller is carried out based on the assumption that the motor is on no load.[8] A variable drive system tends to exhibit oscillatory behavior under no load conditions and hence the design based on no load condition has been assumed to be justified. Here the output of the speed controller is not clamped, whereas there would be limits on the output of speed controller. The output of speed controller corresponds to armature current and it is necessary to limit the peak value of speed controller in order to protect the thyristors used in the bridge. The closed loop system that is usually used for the speed control of DC motor is shown in Fig. 4.6.

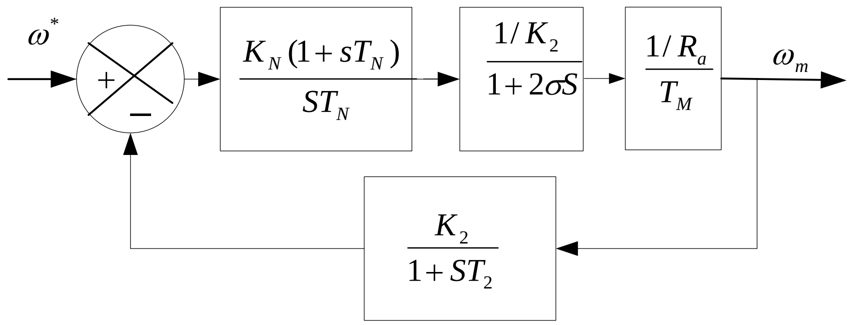

Fig. 4.6 Speed Controller Block Diagram

The equivalent transfer function of Fig. 4.6 is

$$\frac{\omega^*(s)}{\omega_m(s)} = \frac{\frac{k_N R_a}{T_m T_N k_2 k_m}\left(\frac{1}{s}\ \frac{1}{(1+2\sigma s)}\ \frac{1}{s}\right)(1+T_N s)}{1+\frac{k_N R_a}{T_m T_N k_2 k_m}\left(\frac{1}{s^2}\ \frac{1}{(1+2\sigma s)}\ \frac{k_1}{1+T_1 s}\right)(1+T_N s)} \qquad \text{……….4.4.9}$$

If the zero $(1+T_N s)$ is used to cancel the larger time constant of $\frac{1}{(1+2\sigma s)}$, the resulting transfer function is,

$$\frac{\omega^*(s)}{\omega_m(s)} = \frac{\frac{k_N R_a}{k_2 k_m}(1+T_1 s)}{s^3 T_N T_m T_1 + s^3 T_N T_m + \frac{k_N R_a k_1}{k_2 k_m}} \qquad \text{…….4.4.10}$$

Here the 's' term is missing in the characteristic equation, hence the speed control system is unstable. So the loop should be optimized using a different technique.

4.4.2.1 General Considerations for Optimization

The dynamic performance of a control system is good if the controlled variable very rapidly reaches the reference input. Ideally, for any frequency of input variation, the output should track the input variable, instantaneously. So for a practical system, in terms of frequency range, the modulus of the output gain should be very close to one, over a wide range of frequency (band width).

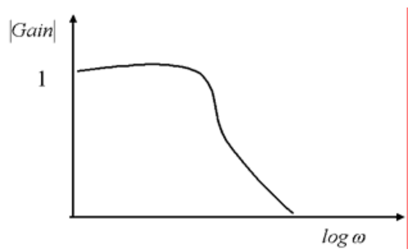

Fig. 4.7 Gain Response of Speed Controller

Optimization aims at bringing the modulus of the frequency characteristic as close to 1, over wide frequency range (modulus hugging).

Let us consider a second order system with the closed loop transfer function given by,

$$\frac{b_0}{a_0 + j\omega a_1 + (j\omega)^2 a_2}$$

if $a_0 = b_0$, $F(j\omega) = \dfrac{a_0}{a_0 - a_2\omega^2 + j\omega a_1}$. ………4.4.11

Multiplying the numerator and the denominator with the complex conjugate of the denominator,

$$F(j\omega) = \frac{a_0\left(a_0 - a_2\omega^2 - j\omega a_1\right)}{\left(a_0 - a_2\omega^2\right)^2 + \omega^2 a_1^2} \qquad \text{………4.4.12}$$

$$|F(j\omega)| = \frac{a_0\sqrt{\left(a_0 - a_2\,\omega^2\right)^2 + \omega^2\,a_1^{\,2}}}{\left(a_0 - a_2\,\omega^2\right)^2 + \omega^2\,a_1^{\,2}} = \frac{a_0}{\sqrt{\left(a_0 - a_2\,\omega^2\right)^2 + \omega^2\,a_1^{\,2}}}$$

$$= \sqrt{\frac{a_0^{\,2}}{a_0^{\,2} - 2a_0a_2\,\omega^2 + a_2^{\,2}\,\omega^4 + \omega^2\,a_1^{\,2}}} = \sqrt{\frac{a_0^{\,2}}{a_0^{\,2} + \omega^2\left(a_1^{\,2} - 2a_0a_2\right) + a_2^{\,2}\,\omega^4}}$$

………4.4.13

If the modulus is to approach to 1 at low frequency, the term in parenthesis must be zero.

i.e. $a_1^{\,2} - 2a_0a_2 = 0 \quad or \quad a_1^{\,2} = 2a_0a_2$.

Therefore, $|F(j\omega)|_{optimum} = \sqrt{\dfrac{1}{1 + + \left(\dfrac{a_2}{a_0}\right)^2 \omega^4}}$ ………4.4.14

Let us consider a third order system with the closed loop transfer function given by,

$$F(j\omega) = \frac{b_0 + j\omega\,b_1}{a_0 + j\omega\,a_1 + (j\omega)^2 a_2 + (j\omega)^3 a_3}$$ ………4.4.15

if $a_0 = b_{0,}$

$$F(j\omega) = \frac{a_0 + j\omega\,a_1}{a_0 + j\omega\,a_1 - \omega^2 a_2 - j\omega^3 a_3} = \frac{a_0 + j\omega\,a_1}{a_0 - \omega^2 a_2 + j\omega\left(a_1 - \omega^2 a_3\right)}$$ ………4.4.16

Multiplying the numerator and the denominator with the complex conjugate of the denominator,

$$F(j\omega) = \frac{a_0 + j\omega a_1\left(a_0 - \omega^2 a_2 - j\omega\left(a_1 - \omega^2 a_3\right)\right)}{\left(a_0 - \omega^2 a_2\right)^2 + \omega^2\left(a_1 - \omega^2 a_3\right)^2} = F_1(j\omega)F_2(j\omega)$$ ………4.4.17

$$|F_1(j\omega)| = \sqrt{a_0^{\,2} + \omega^2\,a_1^{\,2}}$$ ………4.4.18

$$|F_2(j\omega)| = \frac{\sqrt{\left(a_0 - \omega^2 a_2\right)^2 + \omega^2\left(a_1 - \omega^2 a_3\right)^2}}{\left(a_0 - \omega^2 a_2\right)^2 + \omega^2\left(a_1 - \omega^2 a_3\right)^2}$$

$$= \frac{1}{\sqrt{\left(a_0 - \omega^2 a_2\right)^2 + \omega^2\left(a_1 - \omega^2 a_3\right)^2}}$$ ………4.4.19

Therefore,

$$\left|F\ (j\omega)\right| = \frac{\sqrt{a_0{}^2 + \omega^2\, a_1{}^2}}{\sqrt{\left(a_0 - \omega^2 a_2\right)^2 + \omega^2\left(a_1 - \omega^2 a_3\right)^2}} = \sqrt{\frac{a_0{}^2 + \omega^2\, a_1{}^2}{a_0{}^2 + \omega^2(\, a_1{}^2 - 2a_0 a_2\,) + \omega^4(\, a_2{}^2 - 2a_1 a_3\,) + \omega^6 a_3{}^2}} \qquad \text{.........4.4.20}$$

For modulus hugging, $(\, a_1{}^2 - 2a_0 a_2\,) = 0 \;\; and \;\; (\, a_2{}^2 - 2a_1 a_3\,) = 0$, so that the optimized transfer function magnitude is,

$$\left|F\ (j\omega)\right| = \sqrt{\frac{1+\omega^2\left(\frac{a_1}{a_0}\right)^2}{1+\omega^6\left(\frac{a_3}{a_0}\right)^2}}$$

4.4.2.2 Symmetric Optimization by Computation or Modulus Hugging Method

The closed loop transfer function of the speed loop is,

$$\frac{\omega^*(s)}{\omega_m(s)} = \frac{\frac{k_N R_a}{k_2 k_m}\left(1+T_N s\right)\left(1+T_1 s\right)}{T_m T_N s\,(1+2\sigma s)\left(1+T_1 s\right) + \frac{k_N R_a k_1}{k_2 k_m}\left(1+T_N s\right)} \qquad \text{.........4.4.21}$$

Let $\frac{k_N R_a}{k_2 k_m} = k_0 \;\; and \;\; \left(2\sigma + T_1 s\right) = \delta$ then,

$$\frac{\omega^*(s)}{\omega_m(s)} = \frac{k_0\left(1+T_N s\right)\left(1+T_1 s\right)}{T_m T_N \delta\, s^3 + T_m T_N\, s^2 + k_0 k_1 T_N\, s + k_0 k_1} \qquad \text{.........4.4.22}$$

As a result of the non-cancellation of the poles, the terms s^0 and s^3 are present, thus ensuring the damping of the oscillations. Now referring to the previous equation,

$$\left(k_0 k_1 T_N\right)^2 = 2k_0 k_1 T_m T_N \quad and$$

$$\left(T_m T_N\right)^2 = 2k_0 k_1 T_m T_N{}^2 \delta$$

Simplifying, $T_N = 4\delta = 4(\,2\sigma + T_1\,) \;\; and \quad k_0 = \frac{T_m}{2k_1\delta}$, i.e. $\frac{k_N R_a}{k_m k_2} = \frac{T_m}{2k_1\delta}$

i.e. $k_N = \frac{T_m k_m k_2}{2k_1 R_a (2T_t + 2T_2 + T_1)}$ and 4.4.23

$$T_N = 4[2(T_t + T_2) + T_1] \quad \text{………4.4.24}$$

Substituting these in the transfer function equation 4.4.12,

$$\frac{\omega^*(s)}{\omega_m(s)} = \frac{(1+4\delta s)(1+T_1 s)}{8\delta^3 s^3 + 8\delta^2 s^2 + 4\delta s + 1} \quad \text{………4.3.25}$$

If the speed reference is smoothened with a filter $\frac{1}{(1+4\delta s)(1+T_1 s)}$, the resulting transfer function is, $\frac{\omega^*(s)}{\omega_m(s)} = \frac{1}{8\delta^3 s^3 + 8\delta^2 s^2 + 4\delta s + 1}$ ………4.4.26

The transient solution for the step input is $\omega(t) = 1 - e^{\frac{-t}{2\delta}} - \frac{2}{\sqrt{3}} e^{\frac{-t}{4\delta}} \sin\frac{\sqrt{3}}{4\delta} t$ ………4.4.27

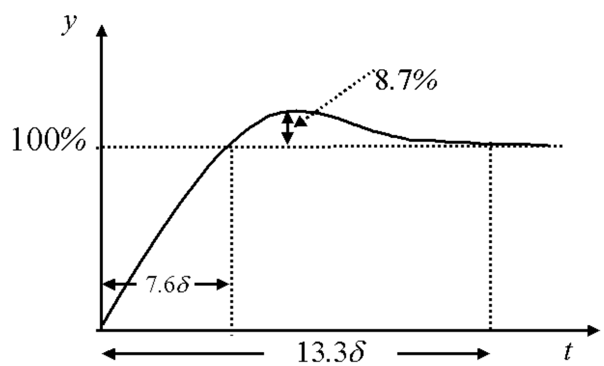

Fig. 4.8 Step Response of the Speed Controller

The smoothing input reference filter can be approximated as $\frac{1}{1+(T_1+4\delta)s}$. If the encoder is use for speed measurement than low pass filter in speed feed back loop is not require.

Chapter 5
Hardware Design

5.1 Hardware Design

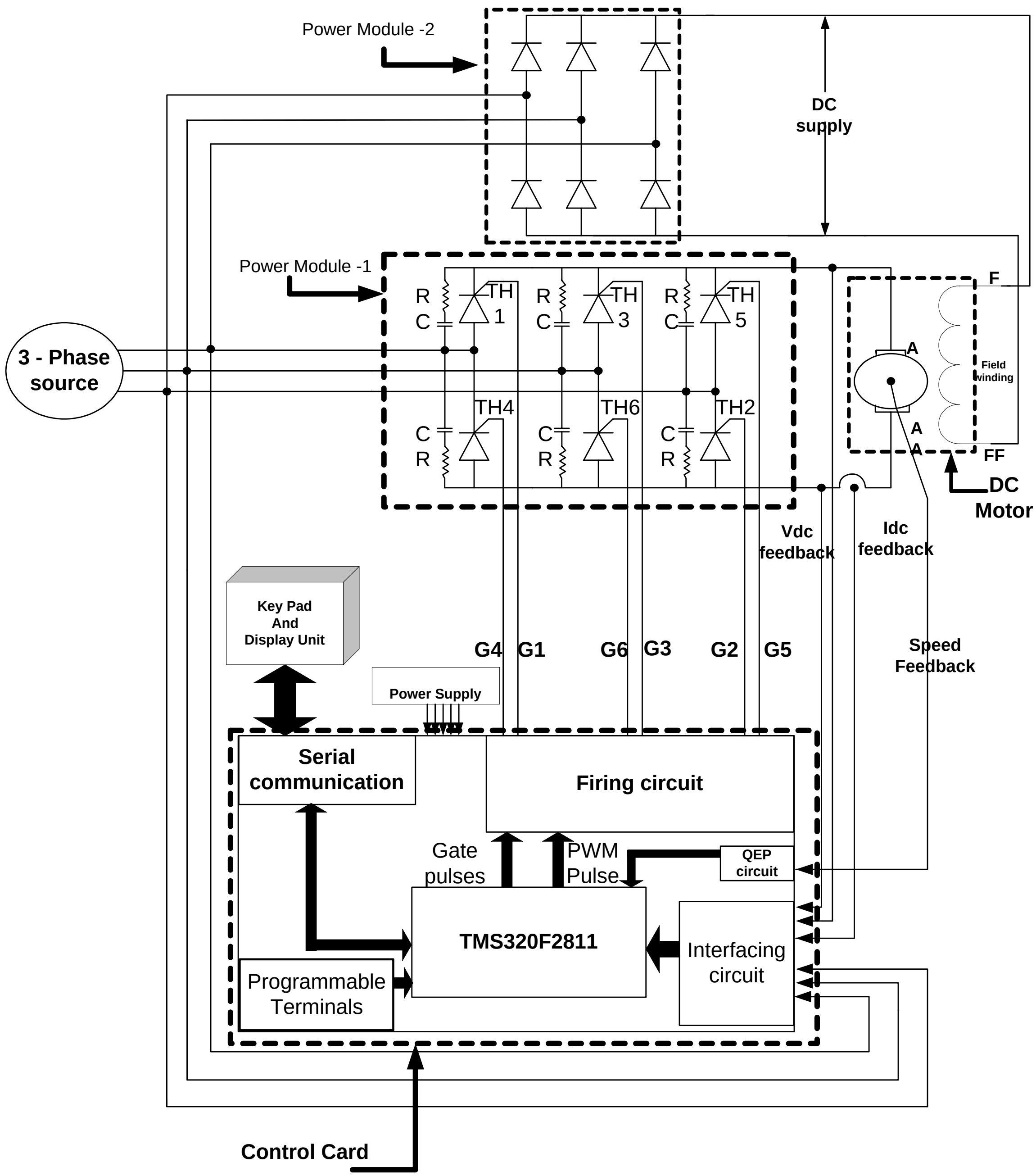

Fig. 5.1 Block Diagram of the Hardware Setup for DC Motor Drive System

Figure 5.1 shows the block diagram of the complete DC motor drive system. This is composed of four blocks. The first block is the DSP controller, which samples the feedback DC current and the encoded position signal to produce six independent gate signals for the controlled rectifier converter. This controller can realize the PI and pulse modulator function. The second block is the power supply card. The function of this block is to generate supply voltage for the control card and display. The third block is the Power module, which provides current to each winding to produce desired torque for DC motor. The fourth block is the Keypad and Display, one of the functions of this block is to display various parameters on the LCD. It also allows user to change the parameter like motor voltage, motor current, maximum current limit, maximum overload, time for the overload etc.

5.2 Power Supply for Control Card

Power supply to the control card is given by an external SMPS with capability to generate +24V, +15V, -15V and +5 V supply. +24 V supply is given to the control terminals, which are programmable with capability to give of take signals to DSP processor. The Keypad and Display unit get supply from the same source, +15 Vand-15 V supply are used as power supply to Driver IC’s and also as Biasing voltages for OP-amps. The DSP processor requires 3.3 V supply and is obtained from +5V supply using potential Divider.

5.3 Control Card

The control card includes interfacing circuit, Serial communication, Firing circuit, programmable terminals, QEP circuit and DSP processor TMS320F2811. DSP TMS320F2811 is the heart of the control card, which performs all the control actions of the DC drive. It comprises of inbuilt ADC, General-purpose I/o port, Timer etc. The main function of the control card is to generate firing pulses, which are used to drive thyristors in order to get speed control of the DC motor.

5.3.1 Interfacing Circuit

The interfacing circuit is used for the Interfacing the Analog input like Supply voltage, DC voltage, DC current with the DSP processor. The ADC of the DSP processor requires only positive voltage. In order to obtain the positive voltage at ADC, supply voltages are first drop to 1.5 V peak to peak using the Resistor network. These reduce level of the supply voltage are clamp to +1.5 V by using the Op-amp based adder circuit. Figure 5.2 shows the interfacing circuit. The same concept is used for the interfacing the DC current and DC voltage.

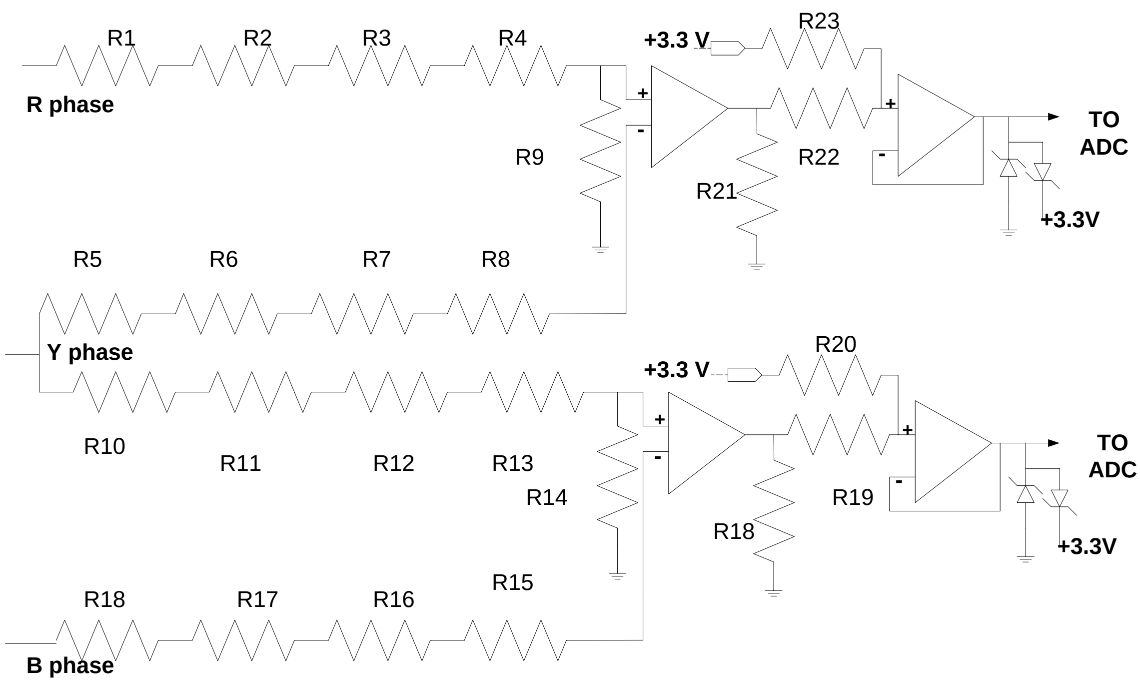

Fig 5.2 Interfacing Circuit

5.3.2 Firing Circuit

Figure 5.3 shows firing pulses and PWM pulse form the DSP processor. The firing pulses are “NORing” with the PWM pulse. The output of the NOR gate is applied to the Driver IC, Further this output of the driver IC is applied to primary side of the pulse transformer.

The secondary of the pulse transformer is connected across the Gate-cathode terminal of the thyristor.

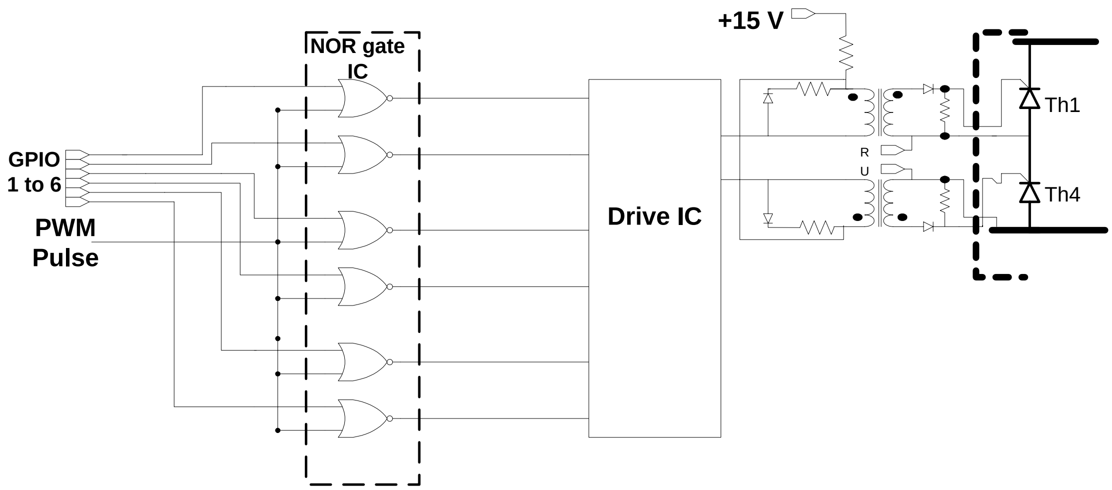

Fig. 5.3 Firing Circuit for Thyristor 1 and Thyristor 4

5.3.3 QEP Circuit

The QEP circuit has been used for interfacing the encoder with the DSP processor. It receives two 90 deg. phase shifted pulses from the encoder. These pulses are applied to the DSP processor using the opto-coupler. The opto-coupler is used for the isolation purpose. Figure. 5.4 shows the isolation circuit for speed measurement.

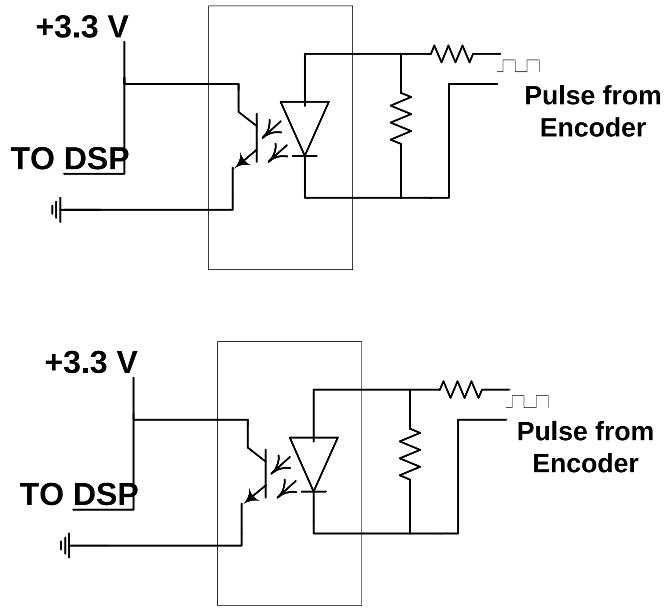

Fig. 5.4 Isolation Circuit for Speed Measurement

5.3.4 Serial Communication

The Keypad and Display unit are connected with the DSP processor using serial communication. The DSP processor has two pins stated as Tx and Rx, which are connected with the keypad and display unit through the serial communication IC.

5.3.5 DSP Processor

DSP processor is the hart of the Control card. It receives various input form the circuit and according to the programming, it generate firing pulses for the thyristor. The TMS320F2811 is used as the DSP processor. It has 52 GPIO pins, which can be use for the general purpose or for the special purpose like PWM, QEP input etc. It has inbuilt 12 bit ADC, two Event manager modules. These Event manager modules are used for controlling the motor, to generate the PWM pulses etc.

5.3.6 Power Modules

DC motor drive requires two power modules; one is for the field winding and another for the armature winding. The 3-phase uncontrolled rectifier is used for the field winding supply, which receive the supply from the 3-phase supply. The line commutated fully controlled rectifier is used for the armature supply. Variable DC voltage can be obtained by changing the firing angle of the thyristor. Series combinations of the RC networks are used as the Snubber for the thyristor. The output of the controlled rectifier is connected with the armature of the DC motor.

5.3.7 Programmable Terminals

The control card of the DC motor drive includes programmable terminals, which controls the operation of control card externally. These terminals include programmable sequence output terminals, programmable sequence input terminals, analog input & output terminals and interfacing terminals. When signal is applied to the any programmable pin, the signal enables the corresponding DSP processor pin and thus performs the corresponding control action. The interfacing terminals are used to interface the control card with display card. Figure 5.5 shows the block diagram of the control card.

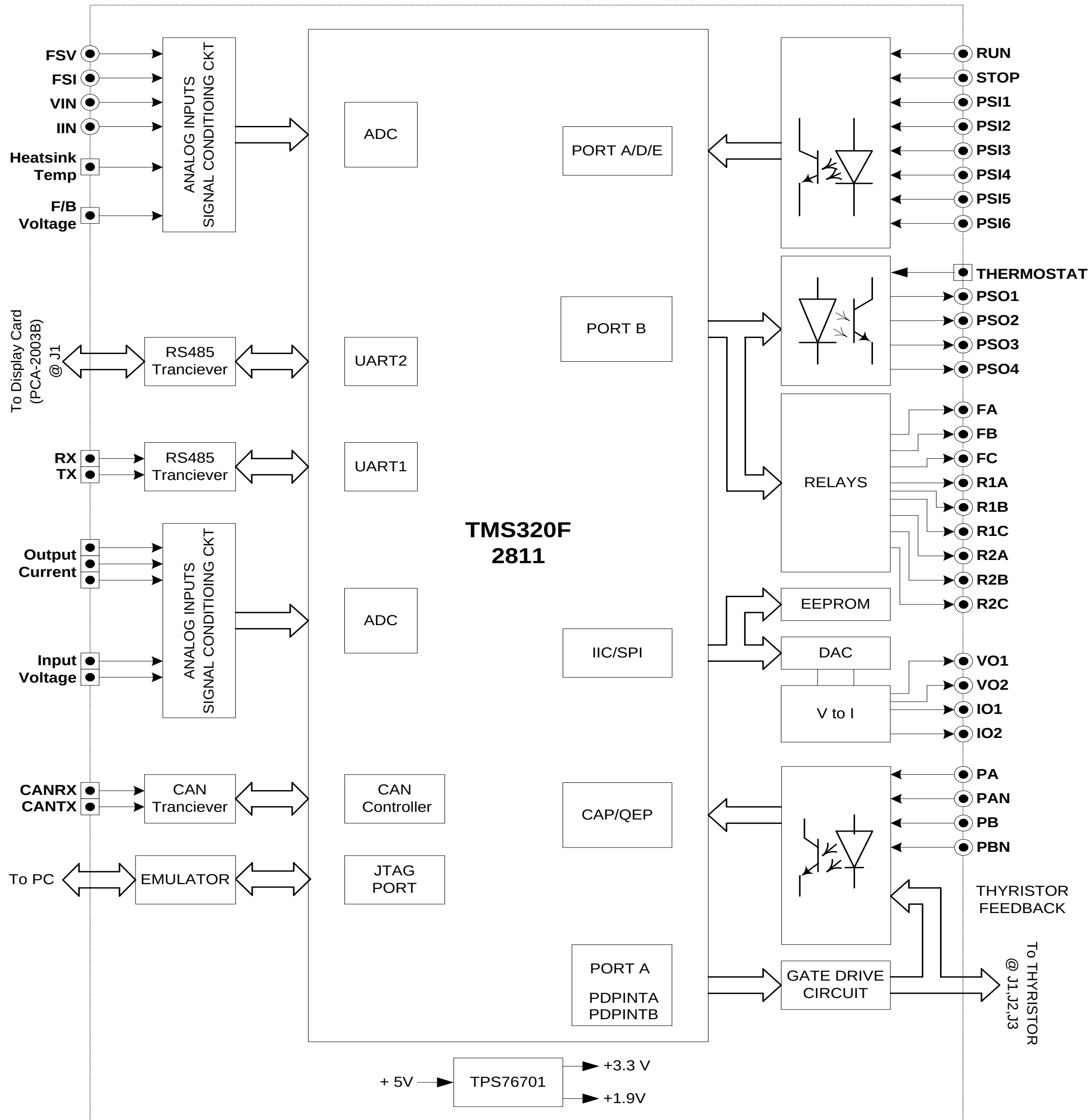

Fig. 5.5 Block Diagram of the Control Card

5.4 Keypad and Display Unit

The display cum Keypad has been used to enter the various parameters such as Reference speed, Reference Current, Reference Torque, Motor parameter etc. It also allows to change the parameter value. The same card equipped with LCD, which shows the different parameter to the user. For the testing purpose, the same program used in Soft-starter is installed in the Card for the DC motor drive. The program is transferred to the card through JTAG

Chapter 6
Software Design

6.1 Software Development

The main consideration in designing the software for the DC motor drive is to achieve a performance, which is comparable to that of the analog or continuous controller and to maintain a good flexibility since that is an important merit of the digital controller. In order to attain this goal the sampling time is made small is made as small as possible and the controller effort is obtained by on-line calculation [7]. A simple but effective prediction procedure was developed which is necessary for an executable control algorithm [7] [10].

The main circuit of the digital controller is as shown in Fig.5.1. The operator sets the required speed reference through the KEYPAD. The line voltage V_{RY}, V_{YB}, armature current and speed are taken as feedback. These are applied to the ADC of DSP TMS320f2811. In the ADC, the signal is converted in to binary digit form. The DSP is programmed such that it read the ADC to get update information of the feedback. According to the V_{RY} and V_{YB} the phase voltage are calculated by using the α-β transformation [11] and form that information, the control efforts for maintain the reference speed is calculated. The inverse cosine method has been used to obtain the firing pulses for the thyristor [1]. The thyristor must be triggered synchronously to the ac supply voltage in an appropriate sequence. The speed controller, current controller (PI controller) and low pass filter must be converted in to the digital (Discrete) mode to obtain our goal [7] [12]**.** Timer 0 interrupt has been used for calculation of time. Figure 6.1, 6.2 and 6.3 shows the flow chart of the timer 0 interrupt, 20ms routine and 100ms routine respectively.

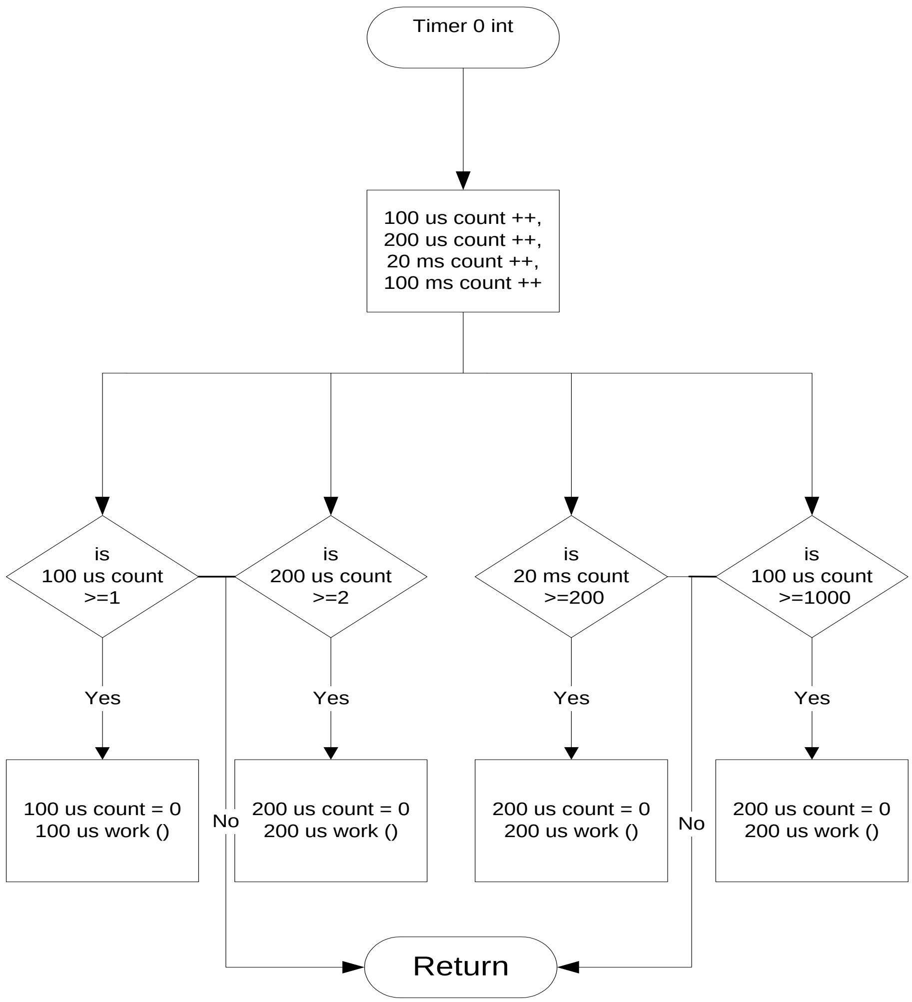

Fig. 6.1 Timer 0 Interrupt Flow Chart

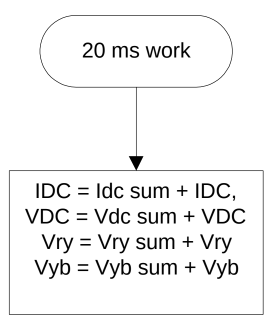

Fig.6.2 20 ms Routine Flow Chart

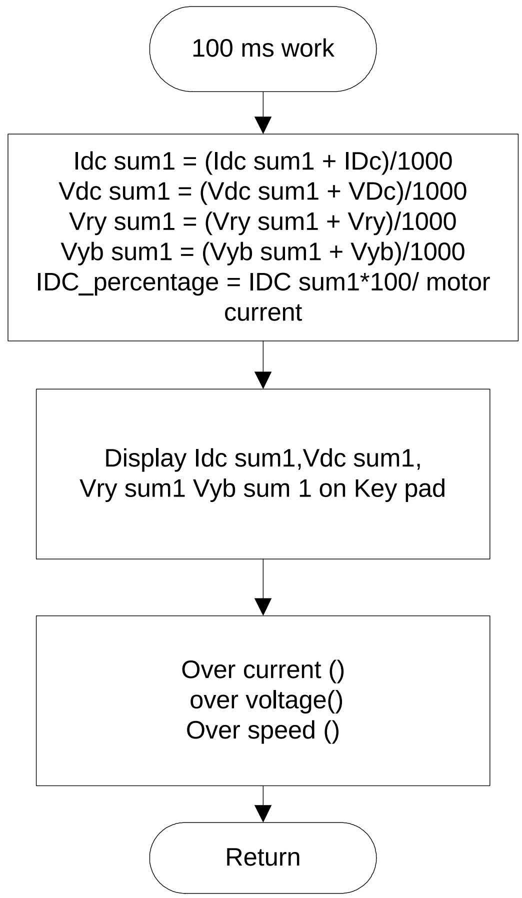

Fig. 6.3 100 ms Routine Flow Chart

6.2 Flow Chart for the Speed Measurement

The closed loop control of the DC motor drive requires the feedback of armature current and speed of the DC motor. The speed feedback has been used for the further calculation to control the DC motor. The Encoder is generally used as the speed sensor. The encoder gives the square pulses, which is used for the speed measurement. TMS320f2811 has the QEP circuit, which can be use for the speed measurement.

6.2.1 Quadrature Encoded Pulses Circuit

TMS320f2811 contain two Event manager (EVA & EVB) modules Each Event Manager module has a quadrature encoder pulse (QEP) circuit. The QEP circuit decodes and counts the quadrature encoded input pulses on pins QEP1 and QEP2 (in case of EVA) or

QEP3 and QEP4 (in case of EVB). These QEP circuit is use to interface with an optical encoder to get position and speed information from a rotating machine.

Quadrature encoded pulses are two sequences of pulses with a variable frequency and a fixed phase shift of a quarter of a period (90 degrees). When optical encoder is connected with the motor shaft, it generates these 90^o phase shifted pulses as shown in Fig 6.4. The direction of rotation of the motor can be determined by detecting which of the two sequences is the leading sequence. The angular position and speed can be determined by the pulse count and pulse frequency. The General-purpose timer is provided with each EVM for counting the pulses. The counter must be put in directional up down mode with QEP as clock source. The QEP circuit counts both edges of the pulses of the two quadrature-encoded inputs. Therefore, the frequency of the clock generated by the QEP logic to GP timer is four times that of each input sequence. This quadrature clock is connected to the clock input of GP timer. Because of these, timer updates its value four times faster than the actual. So to get actual speed, timer count are divided with the (4*ppr of encoder), Where ppr is pulse per revolution. Reading the counter value does the speed measurement.

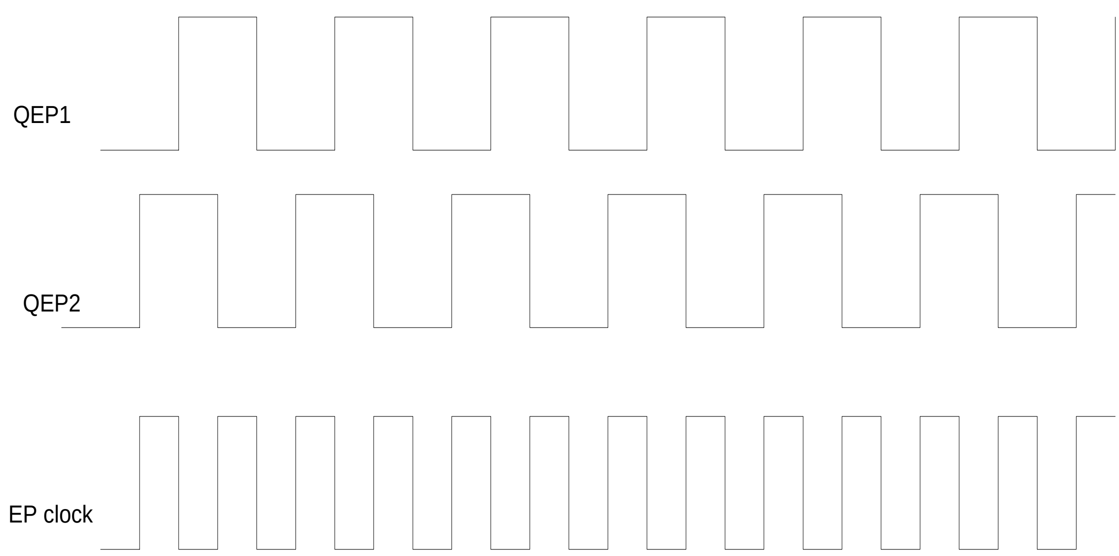

Fig. 6.4 Quadrature Encoded Pulses and Decoded Timer Clock

6.2.2 Flow Chart for Speed Measurement

The speed of the DC motor can be measure with the help of the Encoder or Techogenerator or using back emf sensing method. In industries encoder is use as the Speed sensor. Figure 6.5 shows the flow chart for speed measurement using encoder.

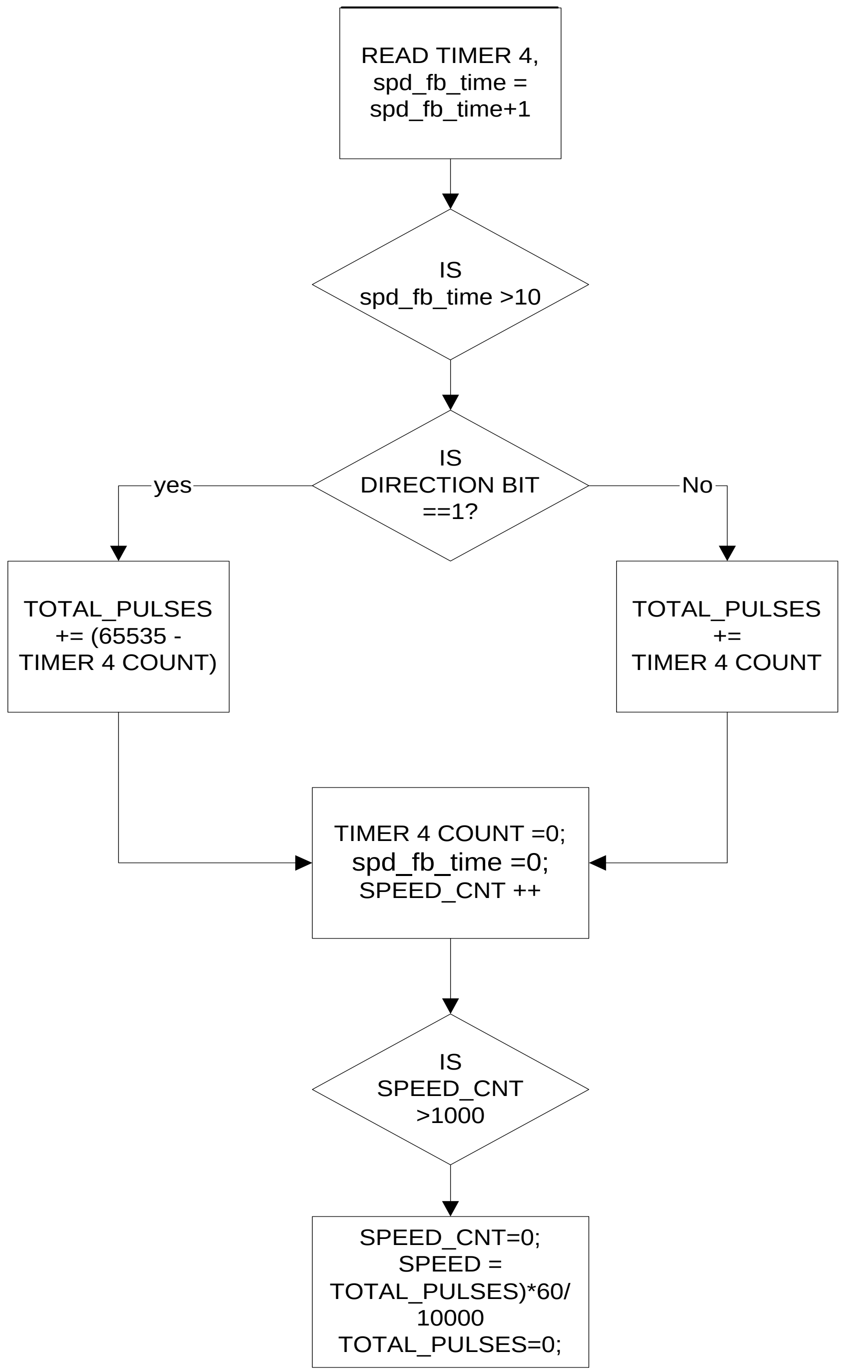

Fig. 6.5 Flowchart for Speed Measurement

6.3 Flow Chart for the Protection

6.3.1 Over Current and Timed Overload Protection

The over current and Timed overload protection has been provided for the protection of the motor. The DC motor draws the more current during the starting and at the time of the overload. In some cases 150 % overload has been allowed for the 60s only [4]. Above this time, Fault has been display on the display. The firing pulses have been seized in faulty conditions. Figure 6.6 shows the flow chart for the Over current and Timed over current. This routine has been called at every 200µs. When motor current is 105 % more than the rated current, it is considered as the minimum overload condition. Figure No. 6.7 Shows the flow chart of the main routine. The main routine has been called at every 100µs.

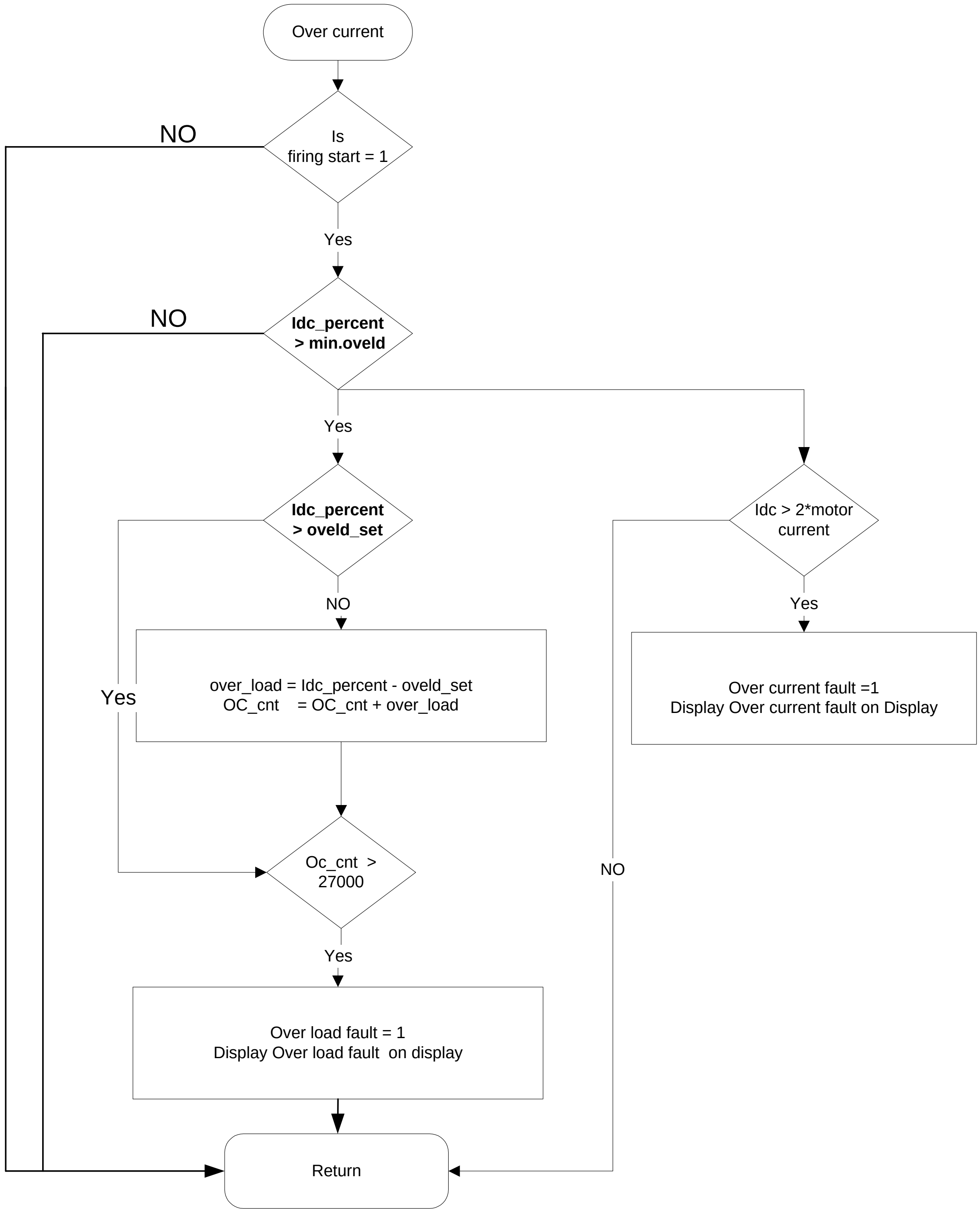

Fig. 6.6 Overload and Timed Overload Protection Flowchart

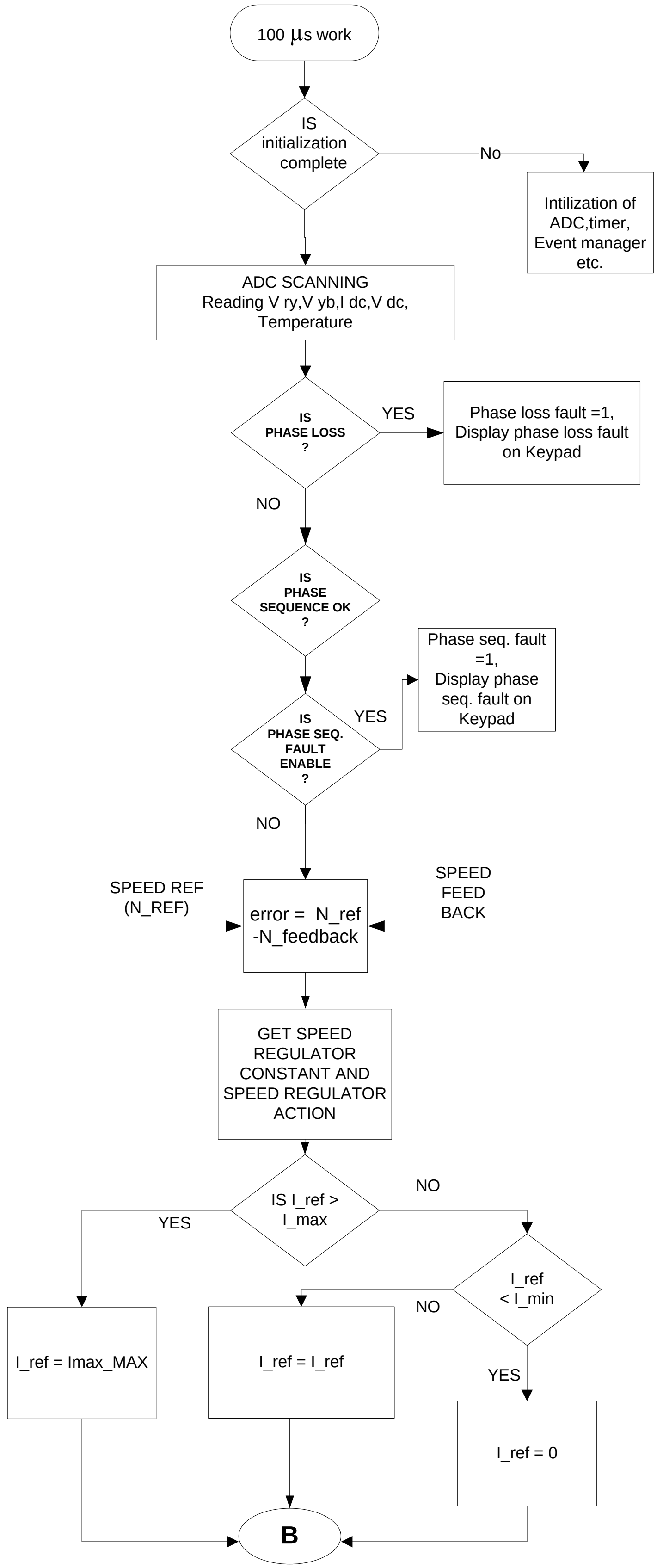

a) Main Routine Flow Chart for DC Motor Drive

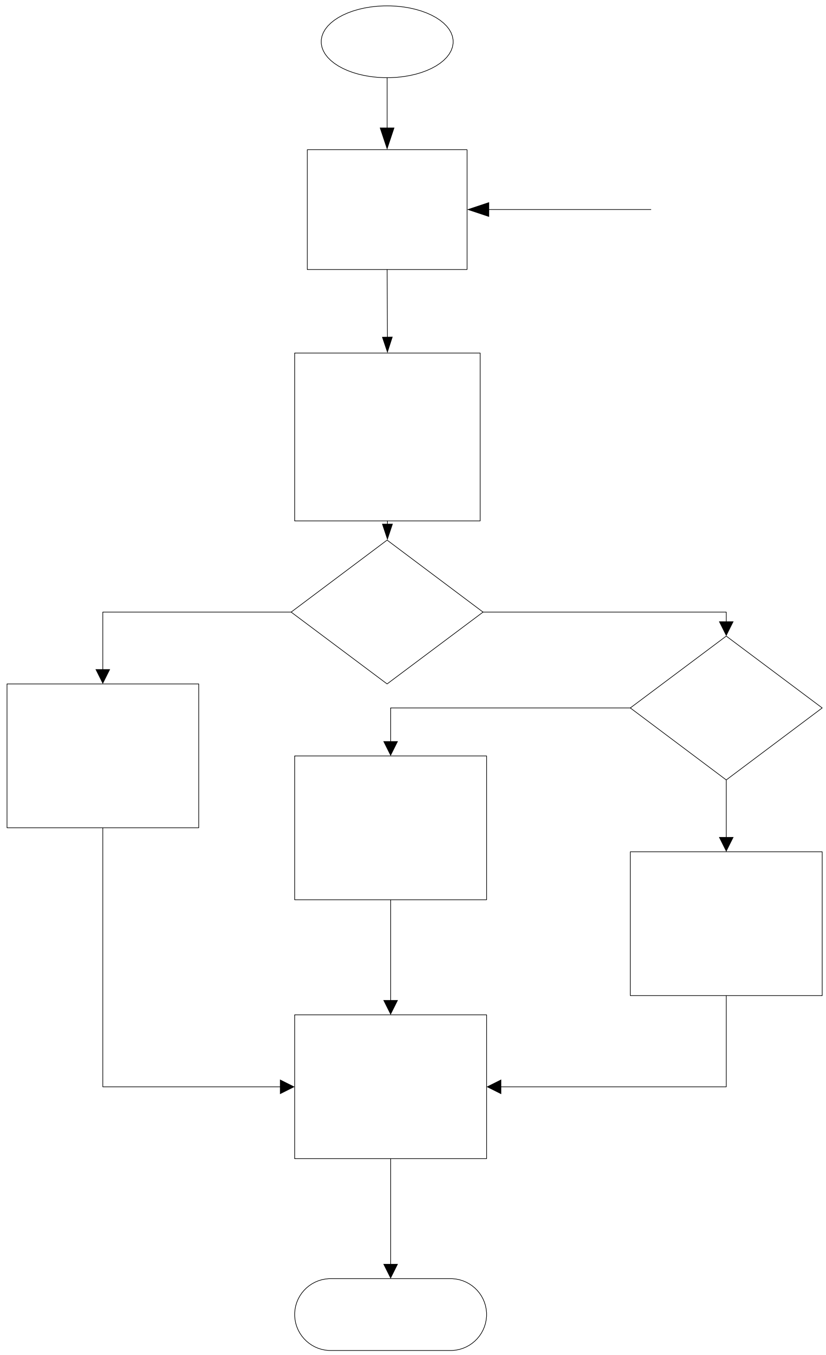

Fig. 6.7 Main Routine Flowchart for DC Motor Drive

Chapter 7
Simulation and Experimental Results

7.1 Simulation Results and Discussions

The simulation of the DC drive has been performed with the Commercial simulation tool PSIM 6.0® and PSIM 5.0®, and the results obtained are presented in the present chapter.

7.1.1 Firing Pulse Generation

In DC motor control, the triggering pulses must be synchronous with the voltage of power supply to ensure that the thyristors are triggered on a sequence to avoid fault and damage to the converter, namely the trigger signal must keep a fixed phase difference with the voltage of power supply.

The trigger pulses are generated in such a way that to get pulses for each phase with the 60^0 displacement between two pulses and 120^0 displacement between pulses of respective phases. Cosine wave firing scheme is use to turn on the thyristor as shown in Fig. 7.1 [3].

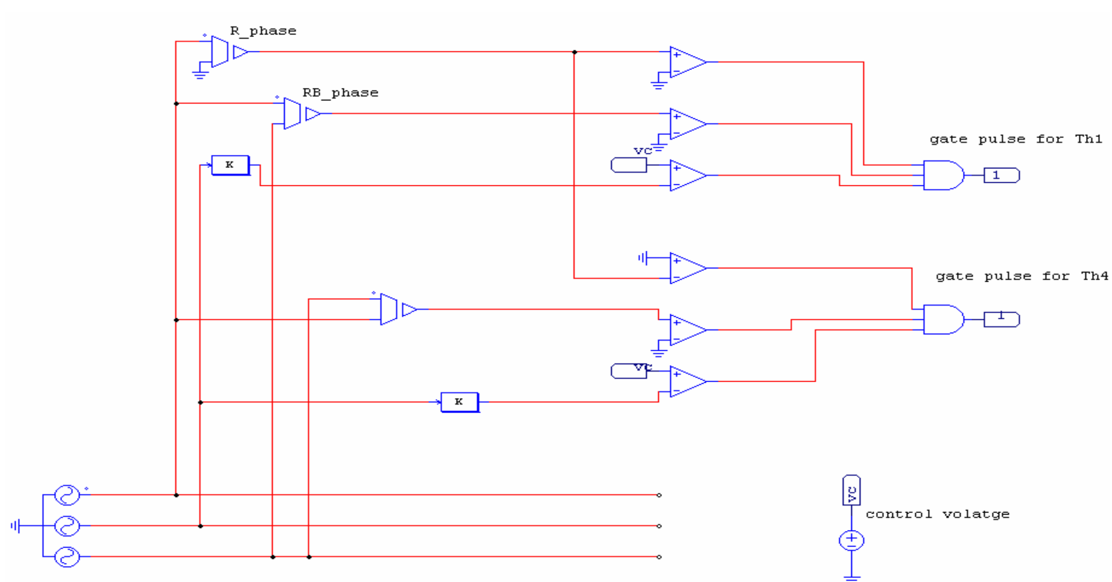

Fig. 7.1 Simulation Circuit of Cosine Wave Firing Scheme for Gate Pulse of Thyristor 1 and 4

The control circuit works on the low voltage side so the gain of the voltage sensors are selected such that its output voltage is with in the 10 to 15 volt. The gain of voltage sensor has been selected .054 to step down the 240V supply voltage to 10.58 Volt. The control scheme as shown in Fig 3.3 is converted in to the program and run it in PSIM with the help of DLL block as shown in the Fig. 7.2

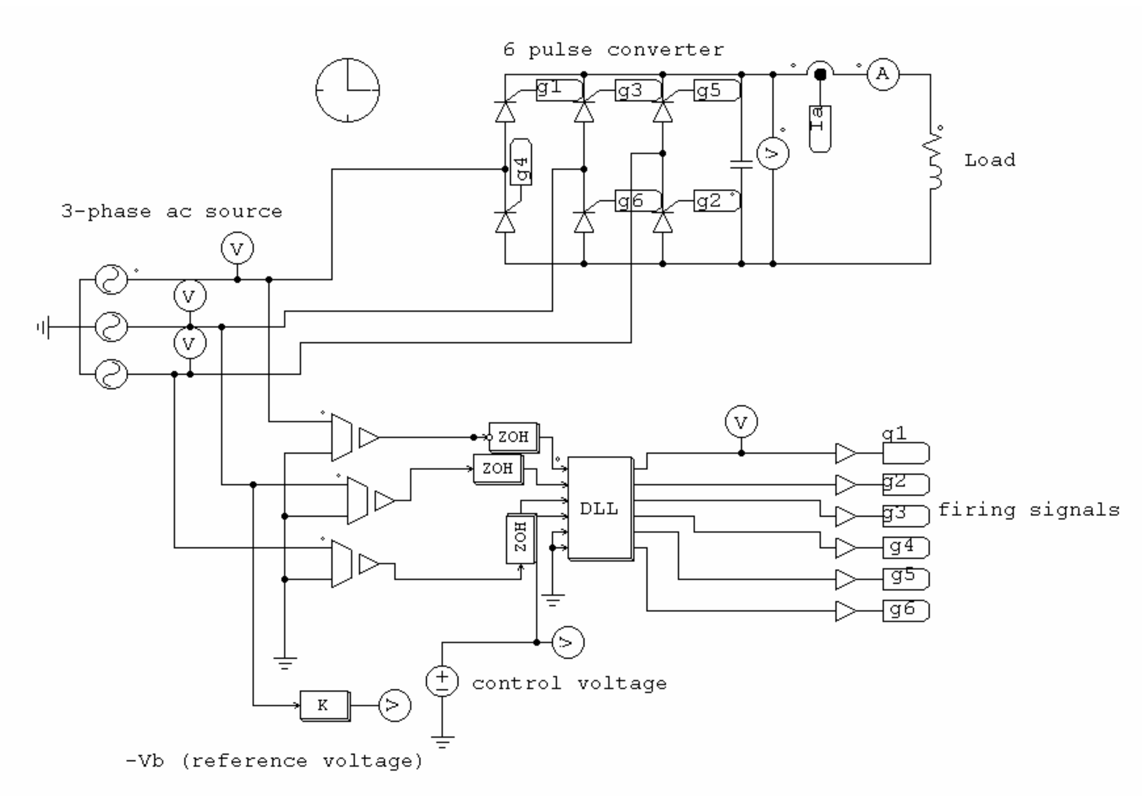

Fig. 7.2 DLL Implementation of Cosine Firing Scheme

Figure 7.3 and Fig. 7.4 shows the firing pulse generation for the thyristor 1 (g1). Here V_c is controlled voltage compare with the –Y phase, which is ANDed with the square pulse of the R phase and V_{RB} phase. The square pulses of R phase voltage and line voltage V_{RB} are generated by comparing it with the ground.

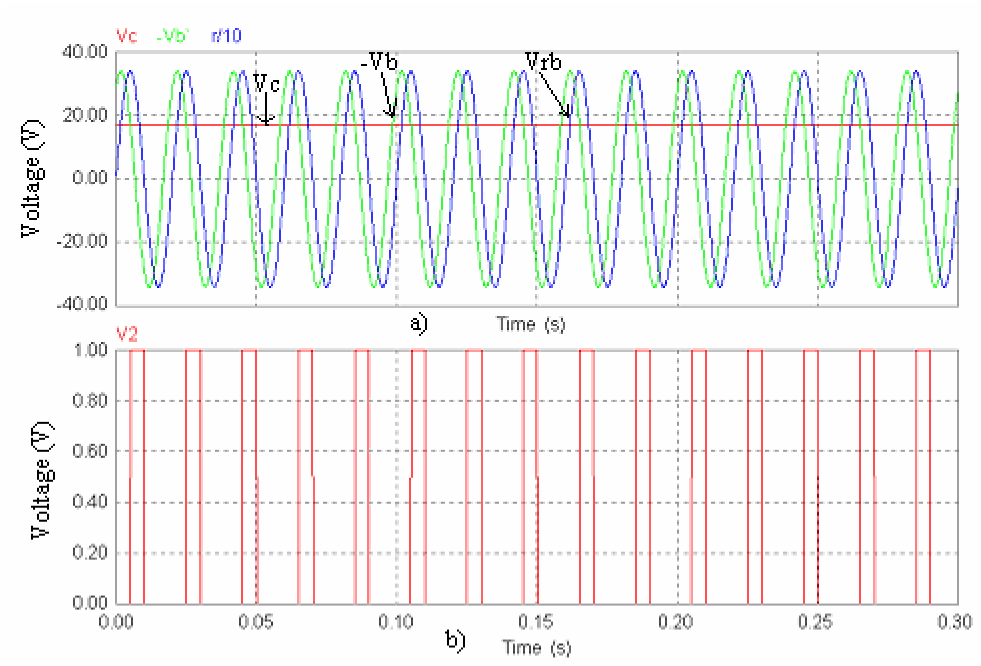

Fig. 7.3 Simulation Result a) Synchronizing Voltage with Control Voltage, Scale X - axis - 0.05 sec/Div & Y - axis – 20 V/Div and b) Gate Pulse for Thyristor 1 at α = 90^0, Scale X - axis - 0.05 sec/Div & Y - axis – 0.20 V/Div

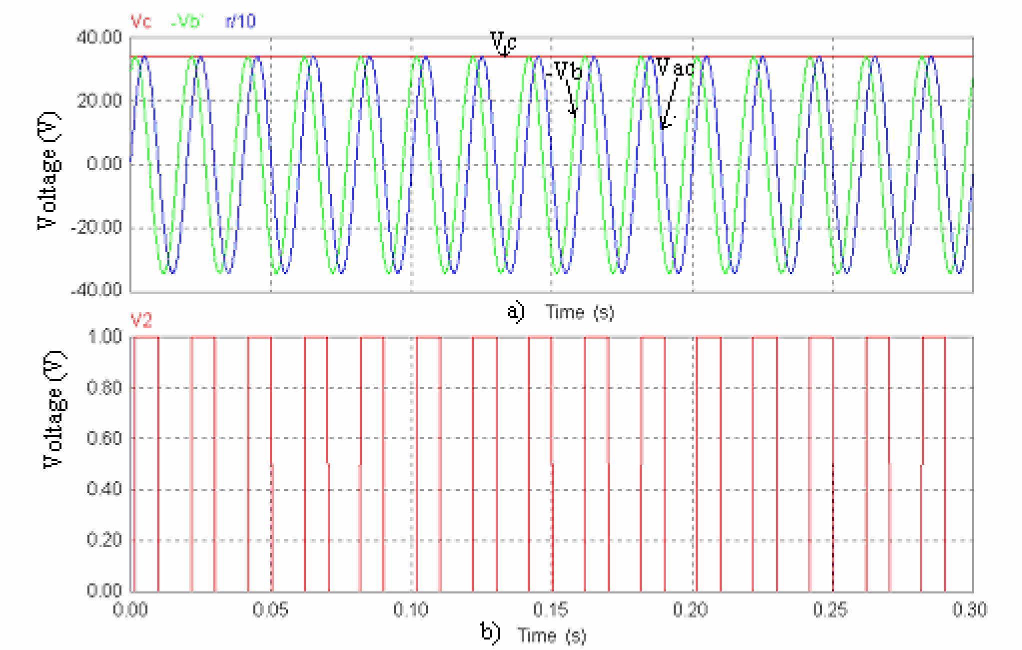

Fig. 7.3 Simulation Result a) Synchronizing Voltage with Control Voltage, Scale X - axis - 0.05 sec/Div & Y - axis – 20 V/Div and b) Gate Pulse for Thyristor 1 at α = 0^0, Scale X - axis - 0.05 sec/Div & Y - axis – 0.20 V/Div

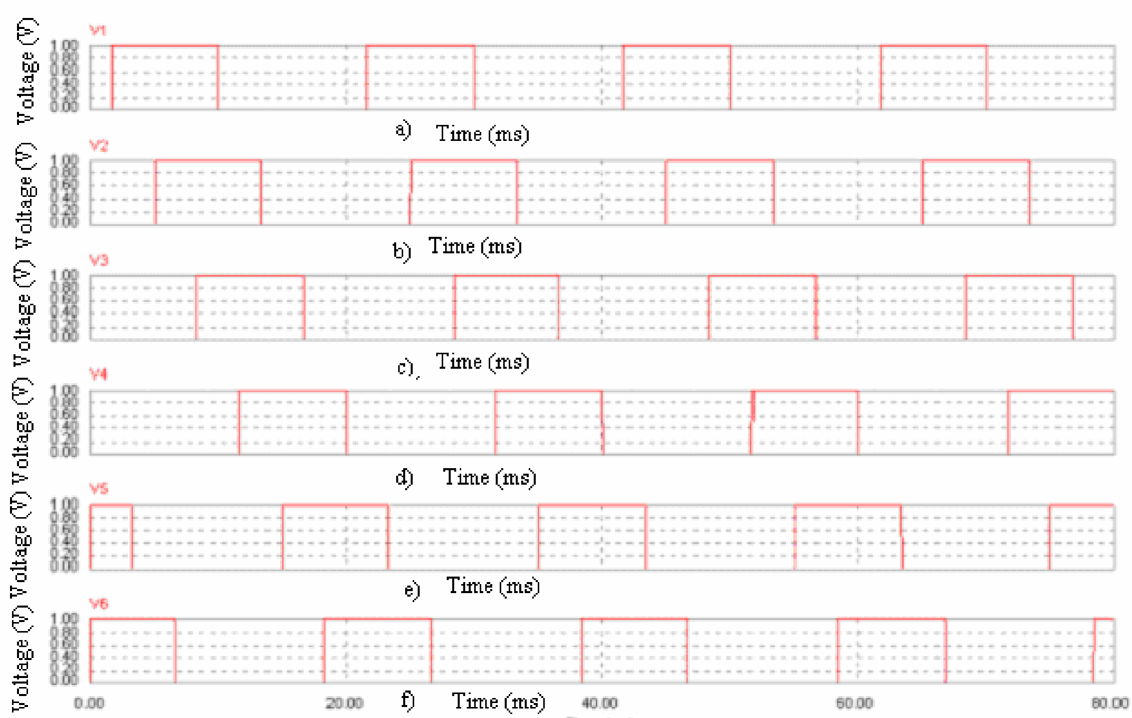

Fig. 7.5 6 Equidistance pulses for a) Thyristor 1,b) Thyristor 2, c) Thyristor 3, d) Thyristor 4, e) Thyristor 5 and f) Thyristor 6, Scale X - axis – 20 msec/Div & Y - axis – 0.20 V/Div

7.1.2 Simulation of DC Motor Drive

For the simulation purpose following parameters of DC machine are consider.

Machine Parameter

5HP, Voltage 240 V

$R_a = 0.6\ \Omega$ $L_a = .012$ H

$R_f = 240\ \Omega$ $L_f = 120$ H

I_a rated = 16.2 A

Rated speed = 1220 rpm

Load torque = 29.2 NM

Moment of inertia = 1 $Kg.m^2$

In the simulation parameter of the current controller and speed controller are as follows

Parameter of current controller:

Proportional gain = 1.9804

Time constant = 0.258 sec

Parameter of speed controller:

Proportional gain = 80.599

Time constant = 0.4358 sec

In the simulation steady state and dynamic performance of the DC motor drive has been checked with this parameter. The steady state performance has been checked by setting the speed reference at 1220 rpm and found that starting current has been with in the limit. DC Motor achieve the reference speed at 6.2 sec with the full load on the motor as shown in Fig. 7.6

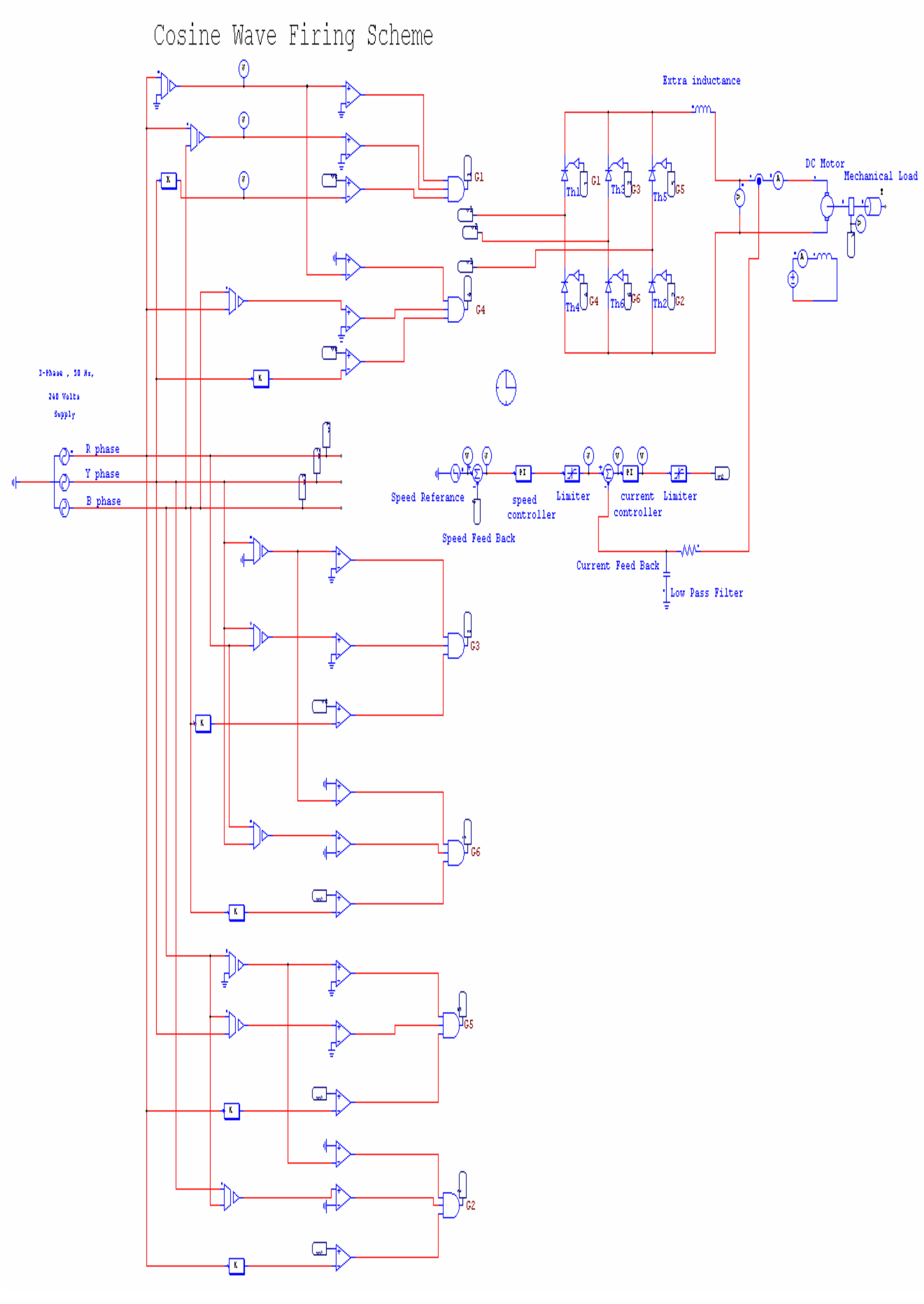

Fig. 7.6 Simulation Circuit of DC Motor Drive

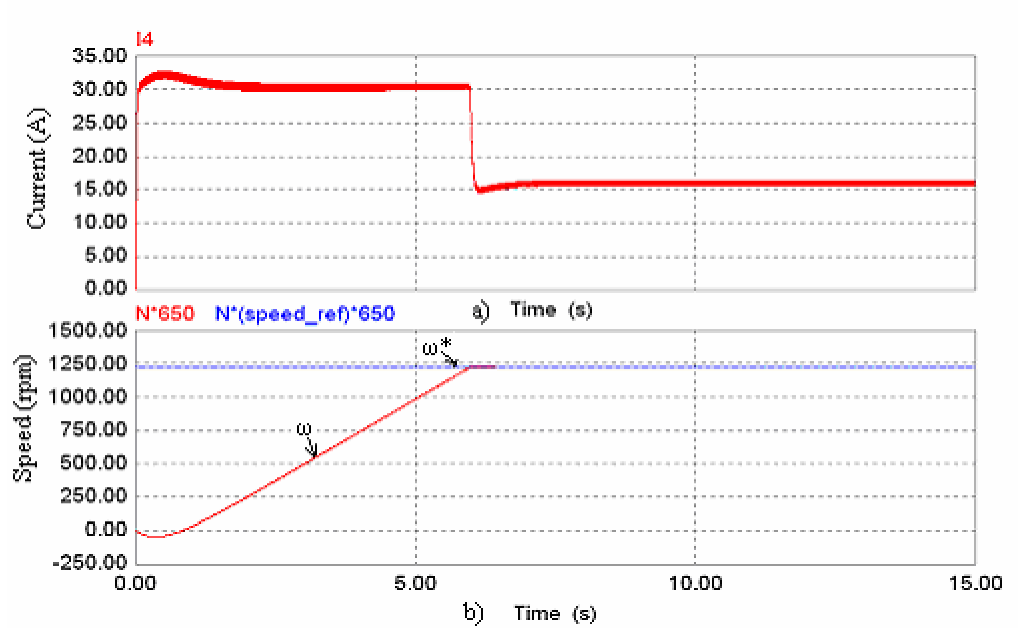

Fig. 7.7 Results of a) Armature Current,
Scale X - axis – 5 sec/Div. & Y - axis – 5 A/Div. and
b) Speed with ω^* =1220 rpm and M_L = 29.2 Nm,
Scale X - axis – 5 sec/Div. & Y - axis – 250 rpm/Div.

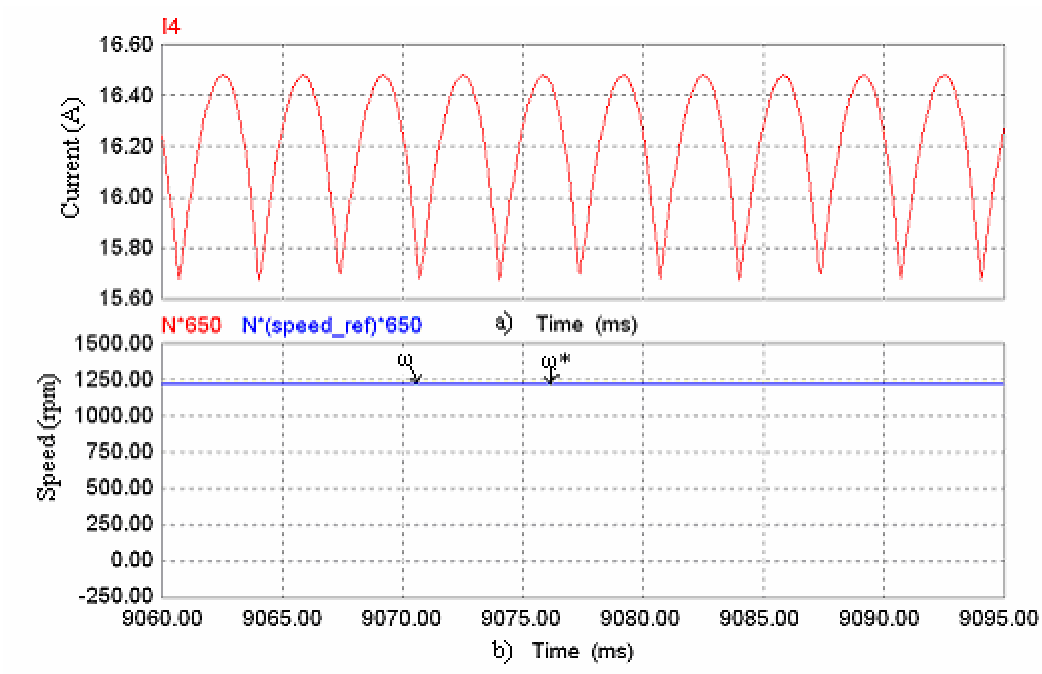

Fig. 7.8 Magnified Waveform of a) Armature Current,
Scale X - axis – 5 msec/Div. & Y - axis – 0.20 A/Div. and
b) Speed with ω* =1220 rpm and M_L = 29.2 Nm
Scale X - axis – 5 msec/Div. & Y - axis – 250 rpm/Div.

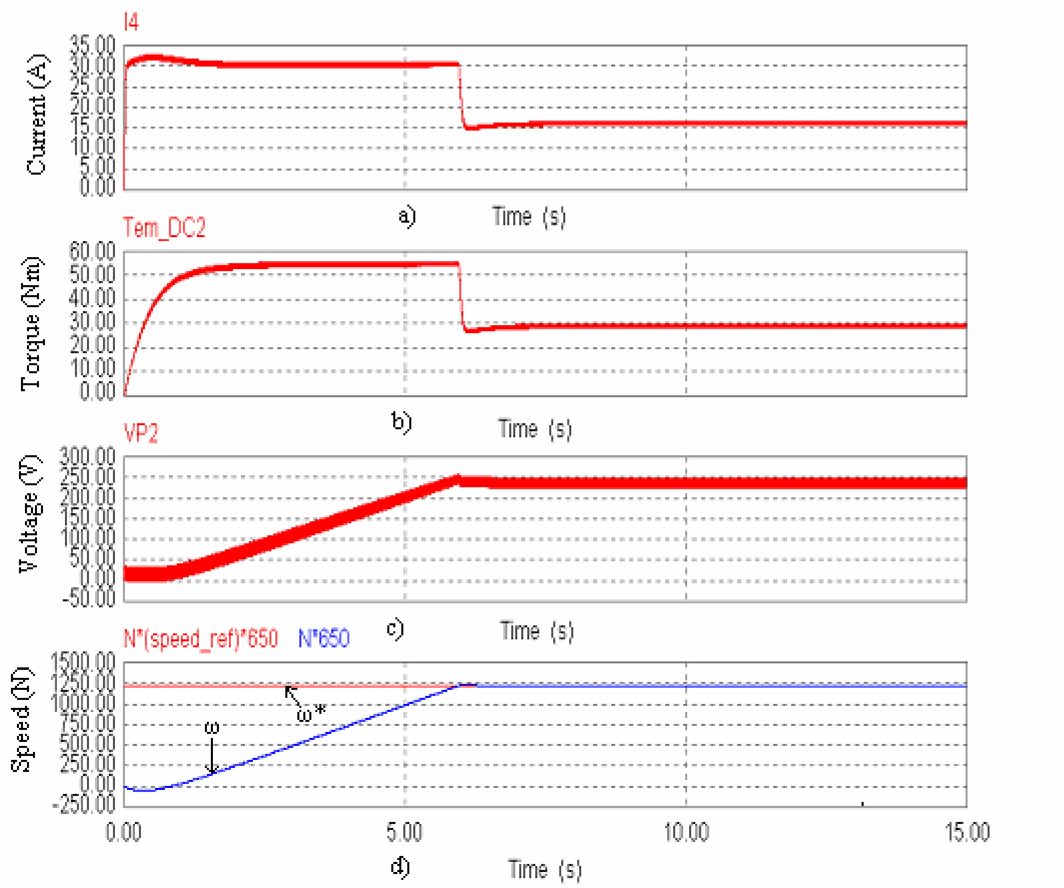

Fig. 7.9 Results of a) Current, Scale X - axis – 5 sec/Div. & Y - axis – 5 A/Div. b) Torque, Scale X - axis – 5 sec/Div. & Y - axis – 10 Nm/Div., c) Armature voltage, Scale X - axis – 5 sec/Div. & Y - axis – 50 V/Div. and d) Speed with ω^*=1220 rpm and M_L=29.2 Nm, Scale X - axis – 5 sec/Div. & Y - axis – 250 rpm/Div.

The dynamic performance of DC motor has been checked with the either of speed reference change or with the change of load torque on the DC motor. The reference speed has been changed from 95% of the rated (1159) to the rated speed (1220) at 12 second. Figure 7.10 shows the armature current at the transient.

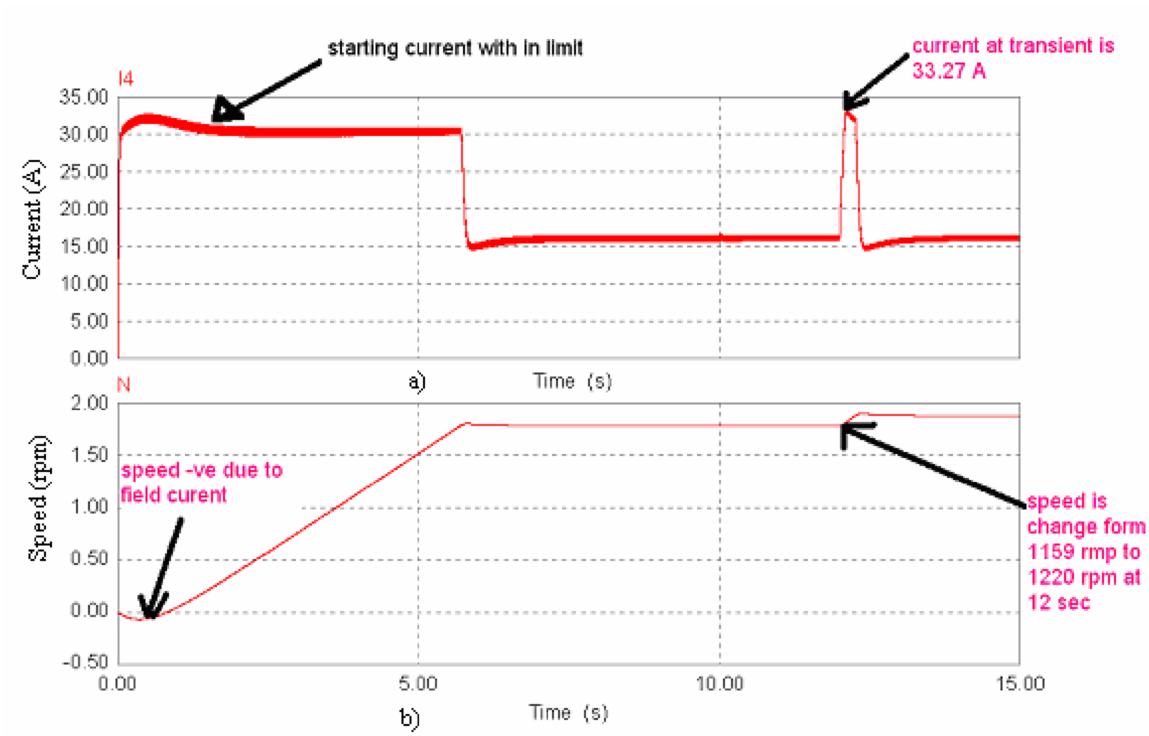

Fig. 7.10 Results of a) Current, Scale X - axis – 5 sec/Div. & Y - axis – 5 A/Div. and b) Speed with ω* Change from 1159 rpm to 1220 rpm with M_L = 29.2 Nm, Scale X - axis – 5 sec/Div. & Y - axis – 1 rpm/Div.

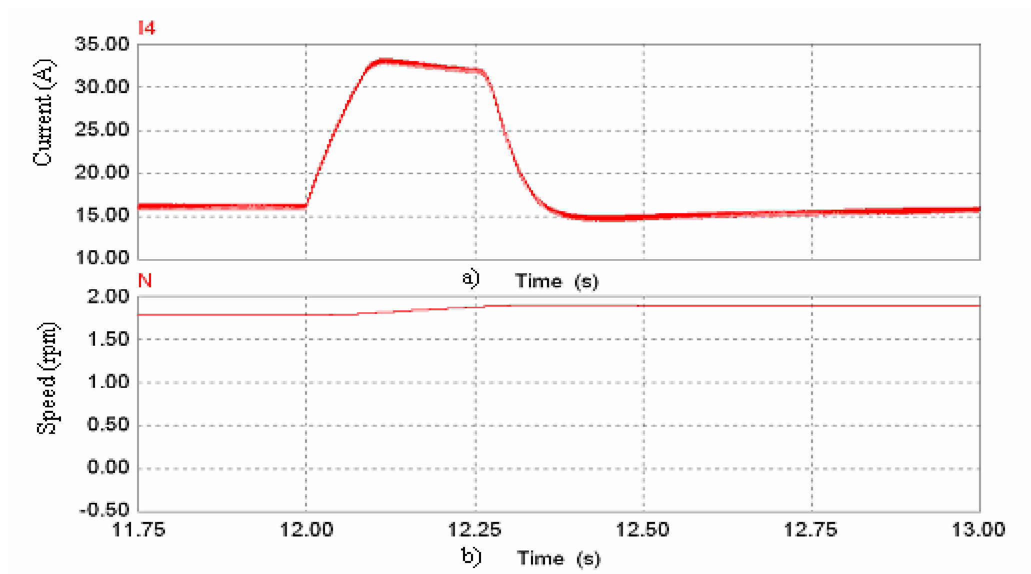

Fig. 7.11 Magnified Waveform of a) Current, Scale X - axis – 0.05 sec/Div. & Y - axis – 5 A/Div., and b) Speed at Transient with Speed Reference Change, Scale X - axis – 0.05 sec/Div. & Y - axis – 0.5 rpm/Div.

The dynamic performance with the load change has been checked by connecting the generator with the DC motor as shown in Fig. 7.12 [12]. The load on the generator has been changed by changing the connected resistance to the output side of the generator.

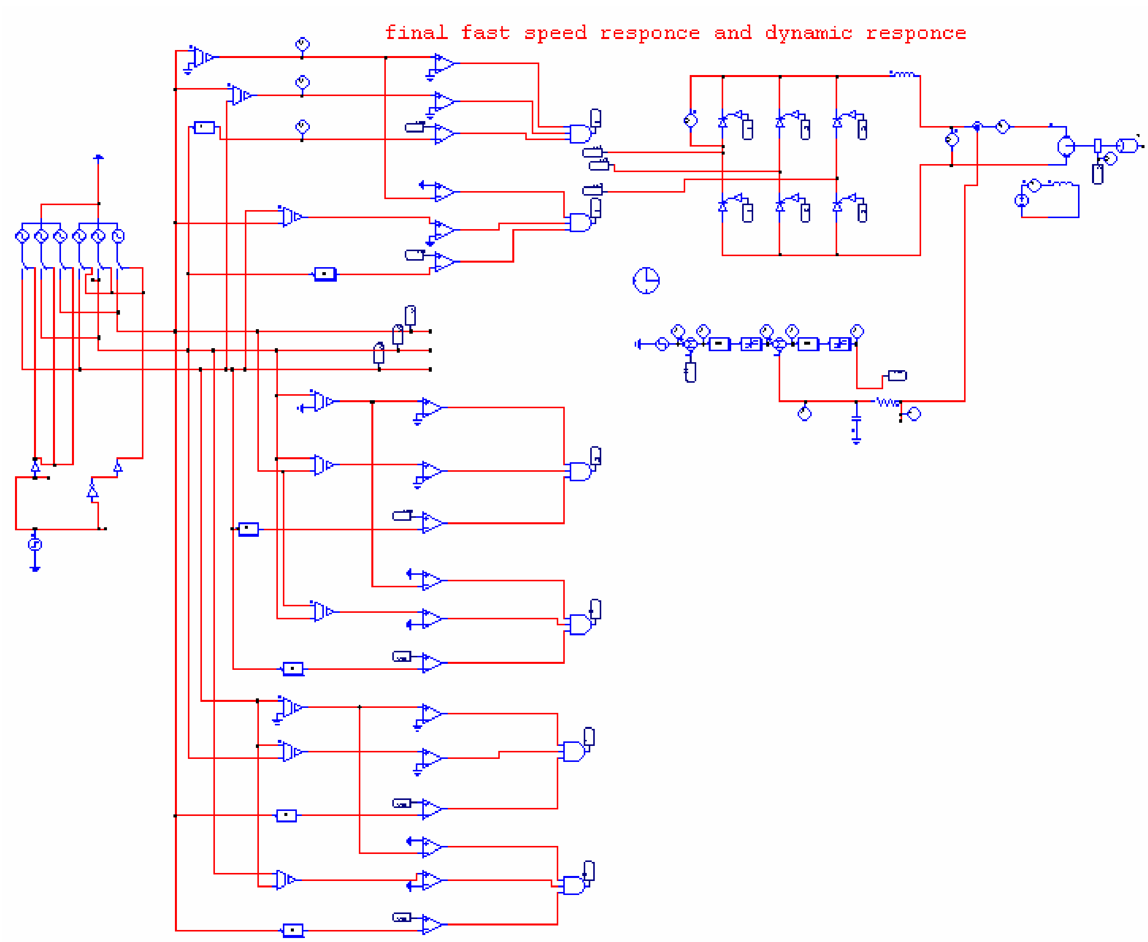

Fig. 7.12 Simulation Circuit for the Dynamic Performance with Load Change

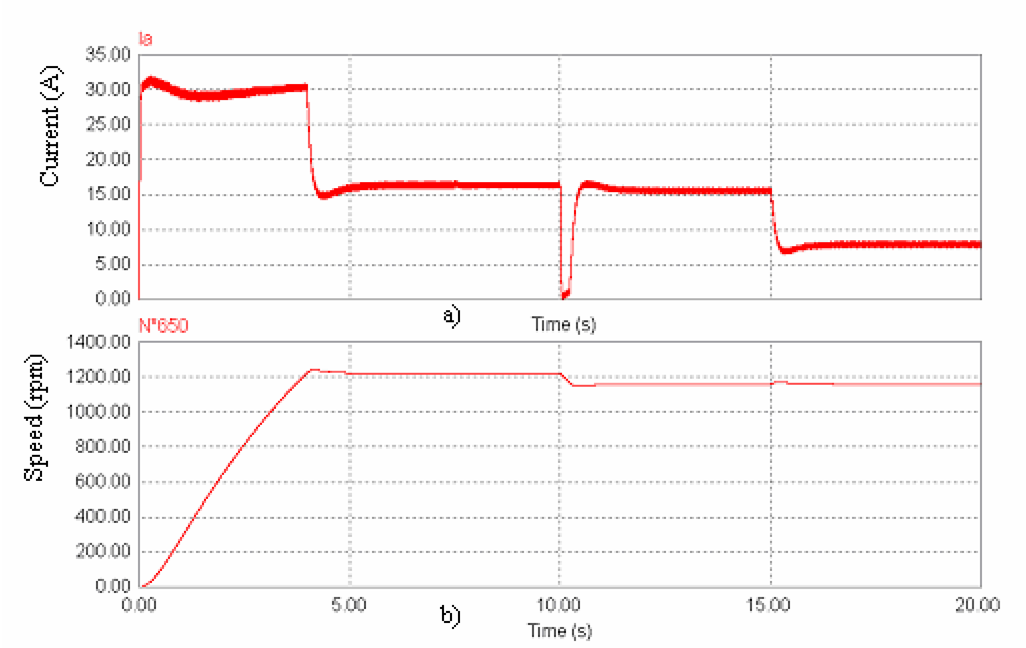

Fig. 7.13 Results of a) Current, Scale X-axis – 5 sec/Div. & Y-axis – 5 A/Div. and b) Speed with ω^* change from 1220 to 1159 rpm, M_L Change from Rated to 50% of Rated, Scale X - axis – 5 sec/Div. & Y-axis – 200 rpm/Div.

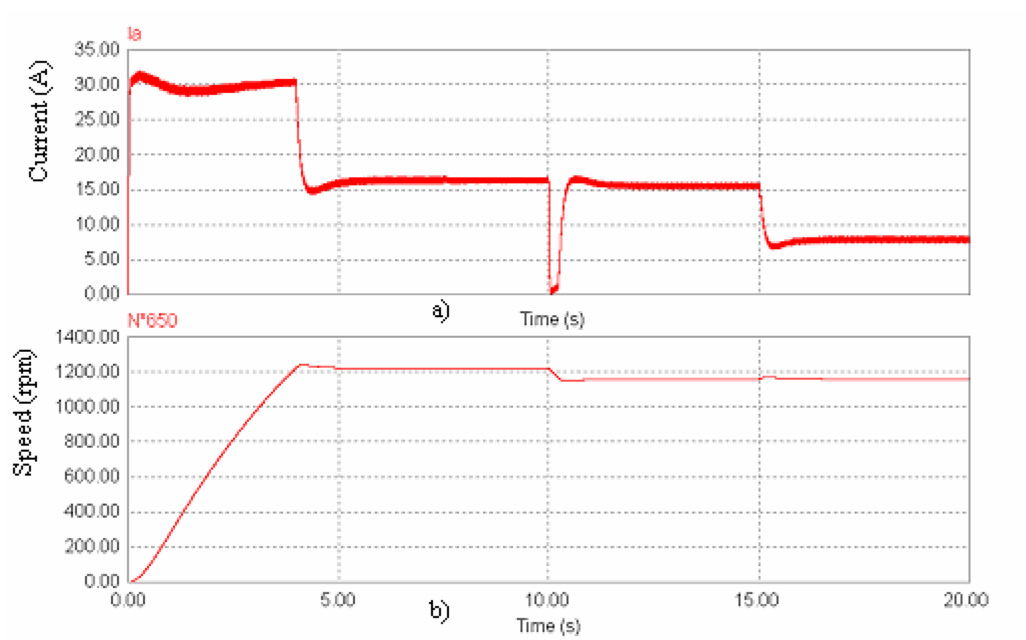

Fig. 7.14 Magnified Waveform of a) Current, Scale X - axis – 5 sec/Div. & Y-axis – 5 A/Div. and b) Speed with Speed Change from 1220 to 1159 rpm, Scale X - axis – 5 sec/Div. & Y - axis – 200 rpm/Div.

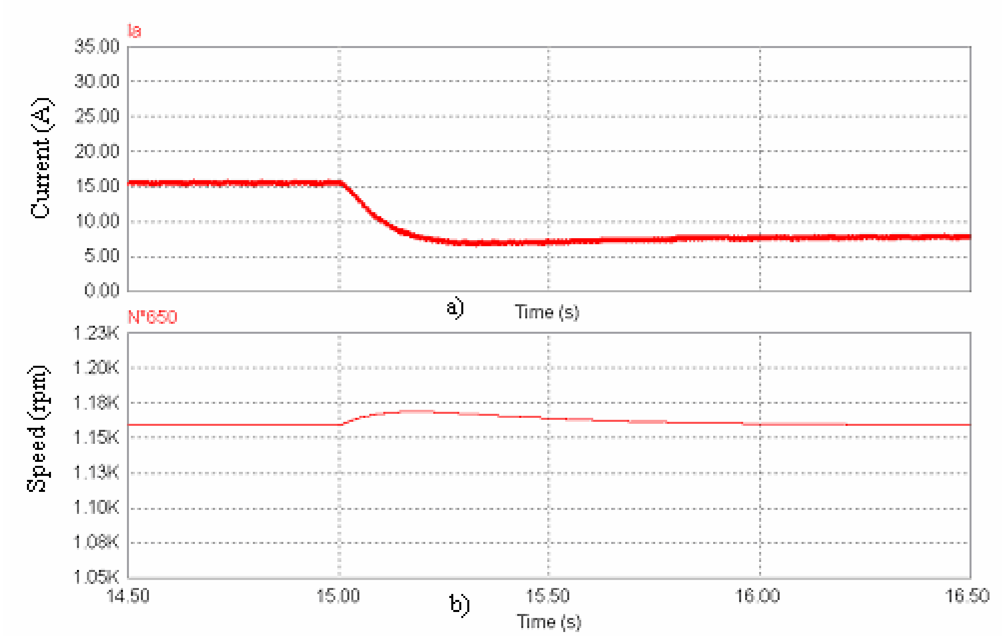

Fig. 7.15 Magnified Waveform of
a) Current, Scale X - axis – 0.5 sec/Div. & Y - axis – 5 A/Div.
and b) Speed with Load Change,
Scale X - axis – 0.5 sec/Div. & Y - axis – 30 rpm/Div.

7.2 Experimental Results and Discussion

The software development has been done as per the flowchart. The software for TMS320f2811 has been written in the Code composer studio using C language. The software development for the DC motor drive has been first separated in the small modules. After completing the modules, these software modules have been checked using the RL load at the low voltage. The software has been checked with 30 V AC supply and RL load. The testing of the complete software has been done step by step. First of all, inverse cosine logic has been checked, after that the measurement (scanning) of the current using Hall sensor has been checked. The gain and the offset of for the ADC have been set according the requirement. The measurement of the speed using QEP circuit has been checked. The following data was used for the testing of the software.

AC supply: 31 V (line to line)

Resistive load: 150 Ω (3 resistance in parallel)

Inductive load: r = 1 Ω and L = 2 H

The RL load was connected in the parallel.

7.2.1 Inverse Cosine Firing Scheme using DSP

The inverse cosine has been implemented using the DSP TMS320F2811. The inverse cosine scheme is implemented as describe above. The gate pulses for different thyristor are as shown in following Fig.

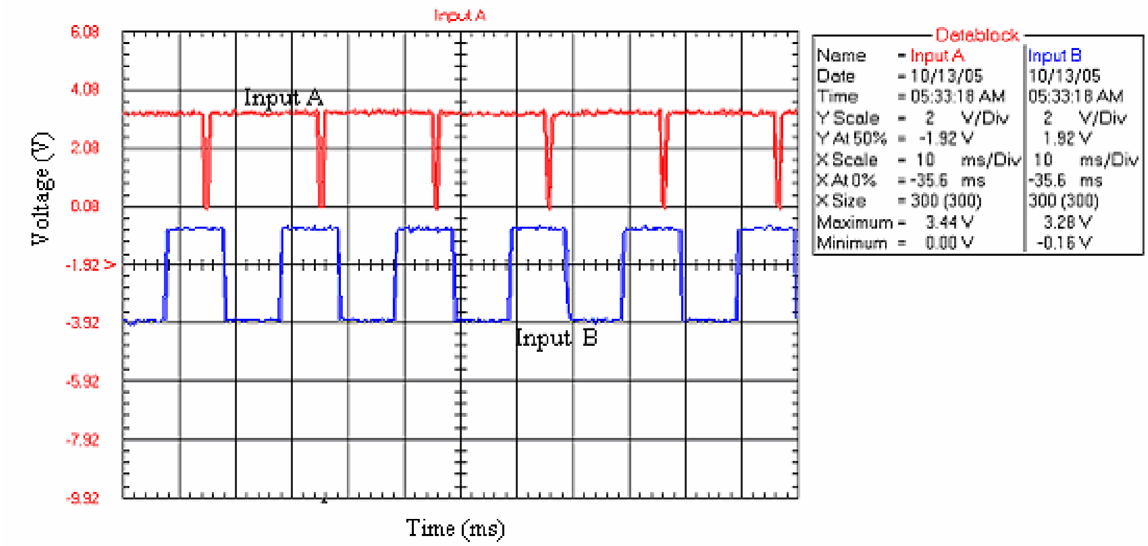

Fig.7.16 Waveform of ZCD of R-Phase (input B) and Firing Pulse of Thyristor - 1 (input A) at Vc = 1, Scale X - axis – 10 msec/Div. & Y - axis – 2 V/Div.

From the logic of inverse cosine firing scheme angle between R-phase and thyristor-1 at Vc=1 is equal to 120^0 and $\alpha = 90^0$.

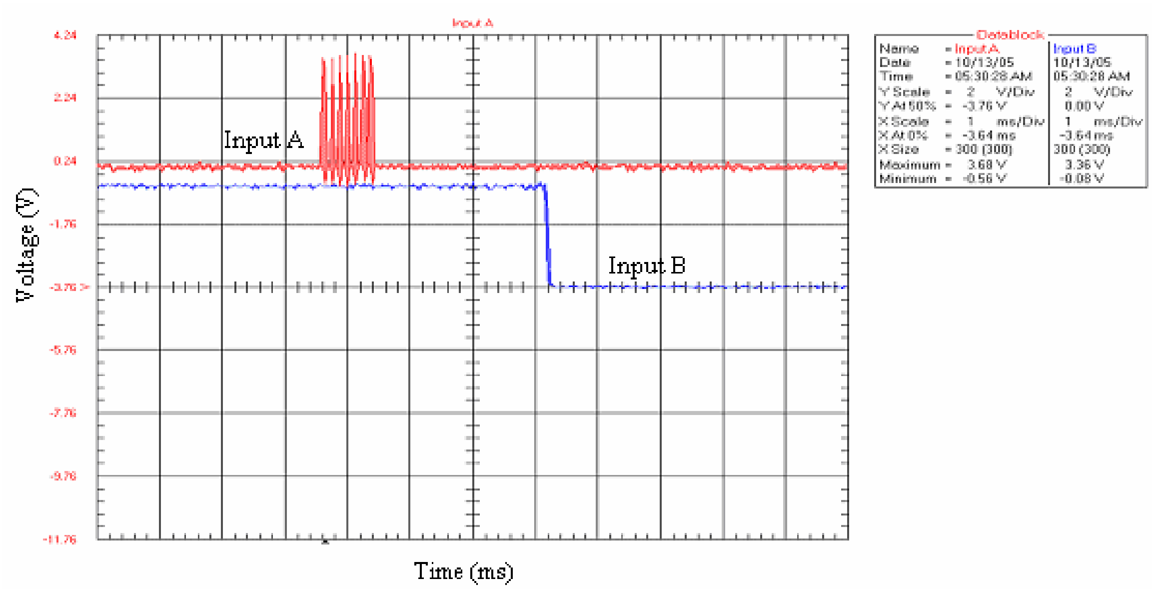

Fig. 7.17 Waveform of R-Phase (Input B) and Input to the Pulse Transformer for Thyristor – 1 (Input A), Scale X - axis – 1 msec/Div. & Y - axis – 2 V/Div.

From waveform it can be seen that number of pulses has been applied to the pulse transformer primary to avoid the heating of thyristor gate-cathode circuit.

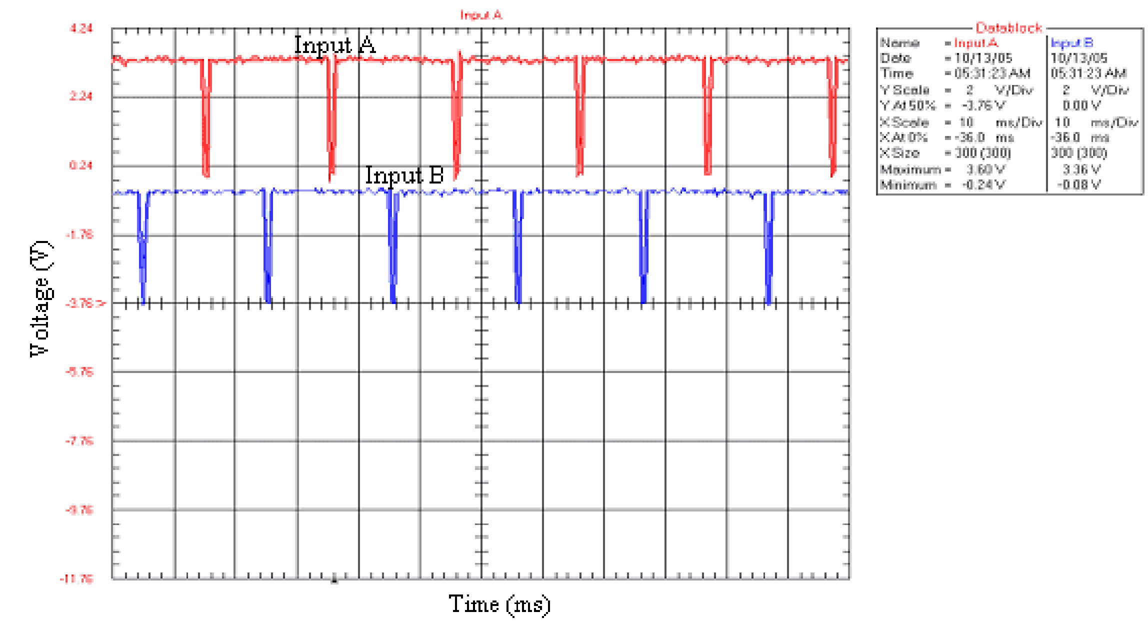

Fig. 7.18 Waveform of Firing Pulses for Thristor 1 (Input B) and Thyristor- 4 (Input A) at Vc = 1, Scale X - axis – 10 msec/Div. & Y - axis – 2 V/Div

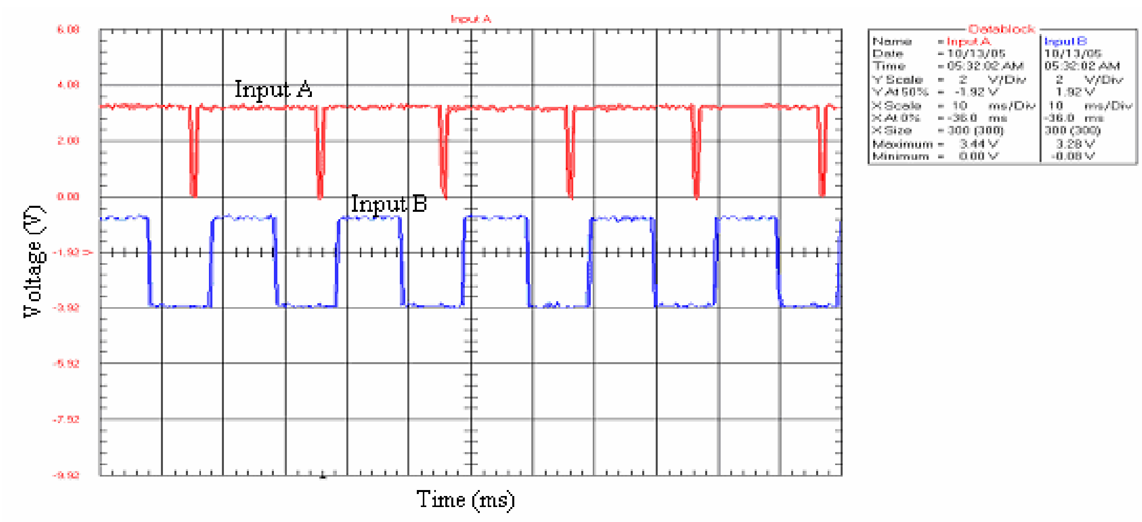

Fig 7.19 Waveform of ZCD of R-Phase (Input B) and Firing Pulse for Thyristor - 4 (Input A) at Vc = 1, Scale X - axis – 10 msec/Div. & Y - axis – 2 V/Div

From the waveform it can be seen that angle between R-phase and thyristor-4 = 300^0

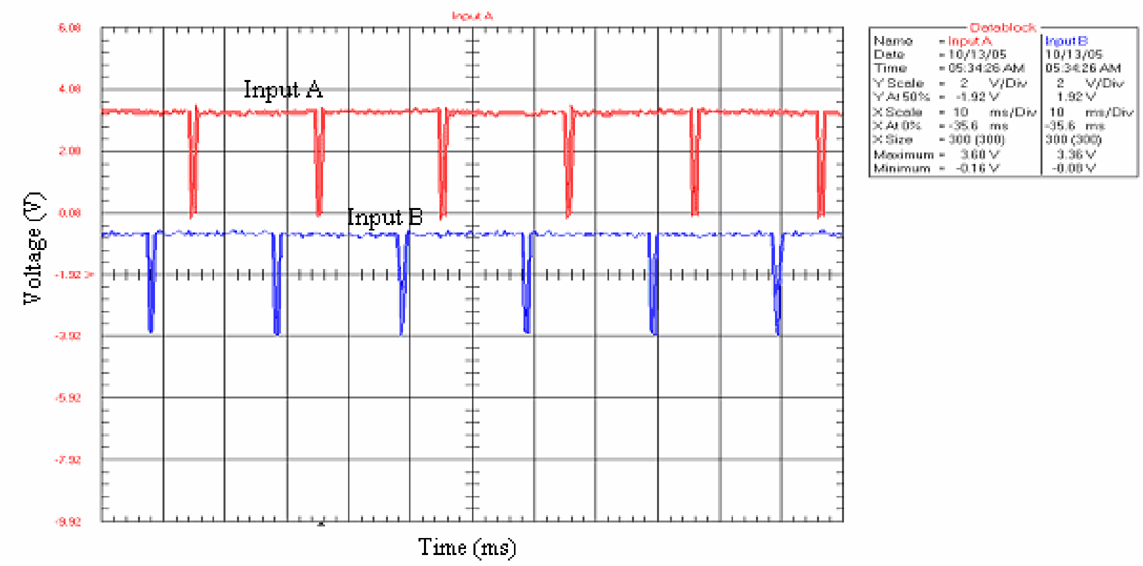

Fig. 7.20 Waveform of Firing Pulses for Thyristor - 1 (Input B) and Thyristor - 2 (Input A), Scale X-axis – 10 msec/Div. & Y-axis – 2 V/Div

From waveform it can be seen that there was an angle of 60^0 between thyristor -1 and thyristor -2 that normally occurs in bridge rectifier.

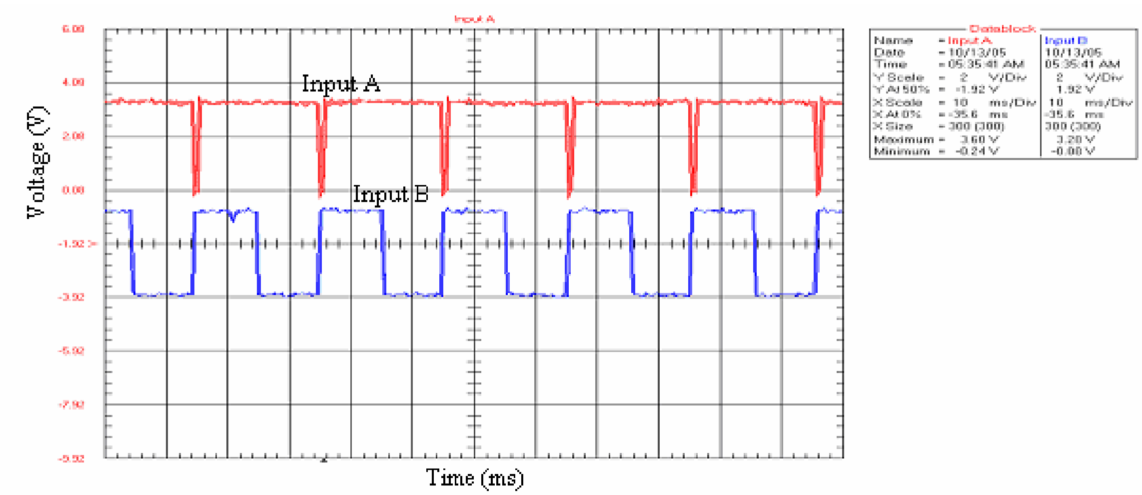

Fig. 7.21 Waveform of ZCD of R-Phase (Input B) and Firing Pulse for Thyristor - 2 (Input A), Scale X-axis – 10 msec/Div. & Y-axis – 2 V/Div

From waveform it can be seen that thyristor -2 will trigger after 180^0 of R-phase when Vc=1 so angle $\alpha = 90^0$.

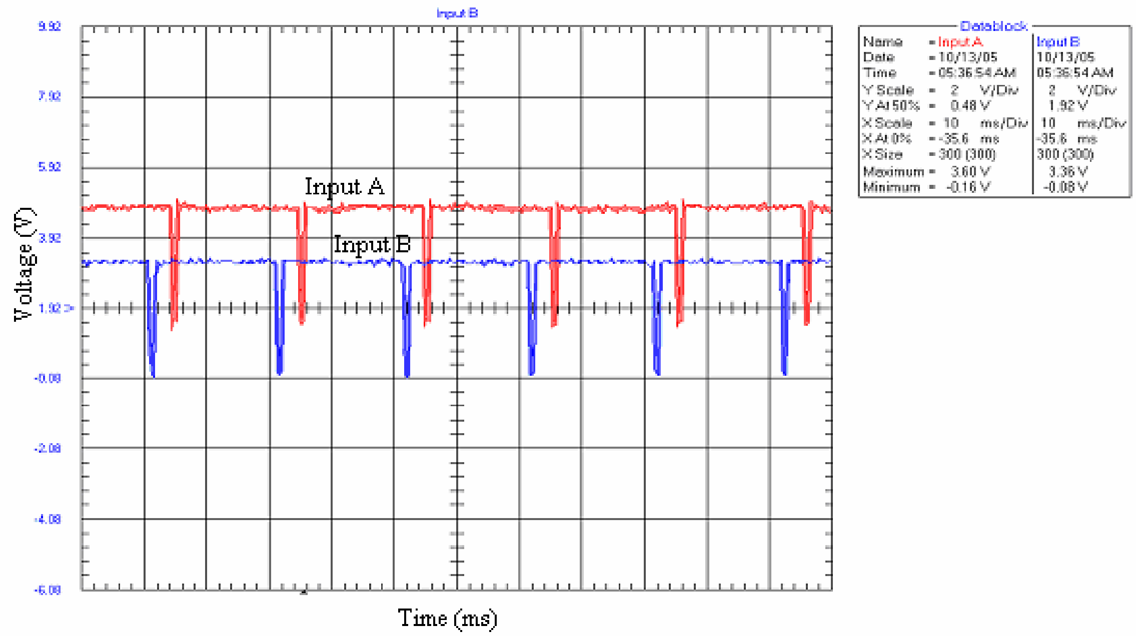

Fig. 7.22 Waveform of Firing Pulses for Thyristor -6 (Input A) and Thyristor -1 (Input B) at Vc = 1, Scale X - axis – 10 msec/Div. & Y - axis – 2 V/Div

From waveform it can be seen that in bridge rectifier the firing sequence of thyristor is 61,12,23,34,45,56 and again cycle repeats. In this case angle between thyristor -6 and thyristor -1 = 60^0.

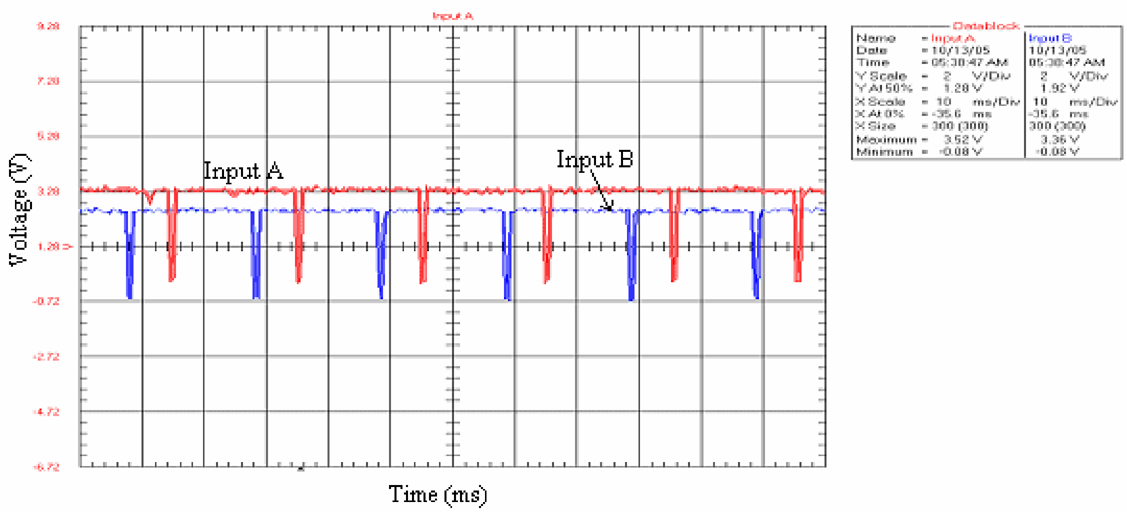

Fig. 7.23 Waveform of Firing Pulses for Thyristor - 4 (Input B) and Thyristor - 6 (Input A) at Vc = 1, Scale X - axis – 10 msec/Div. & Y - axis – 2 V/Div

7.2.2 Results of Controlled Rectifier

The output of the controlled rectifier is taken for the various firing angle. The firing angle is changed manually. Following Table 7.1 shows the firing angle, line voltage and DC output voltage at various firing angle.

Table 7.1
Output Voltage s with Different Firing Angle

Firing angle α	DC voltage V_{DC}	Line voltage V_{RY}
0^0	39.5 V	31.3 V
30^0	35.3 V	31.3 V
60^0	16.9 V	31.3 V
90^0	2.8 V	31.3 V

Following figure No.7.23 shows the output of the controlled rectifier at various firing angle.

Waveform at $\alpha = 0^0$:

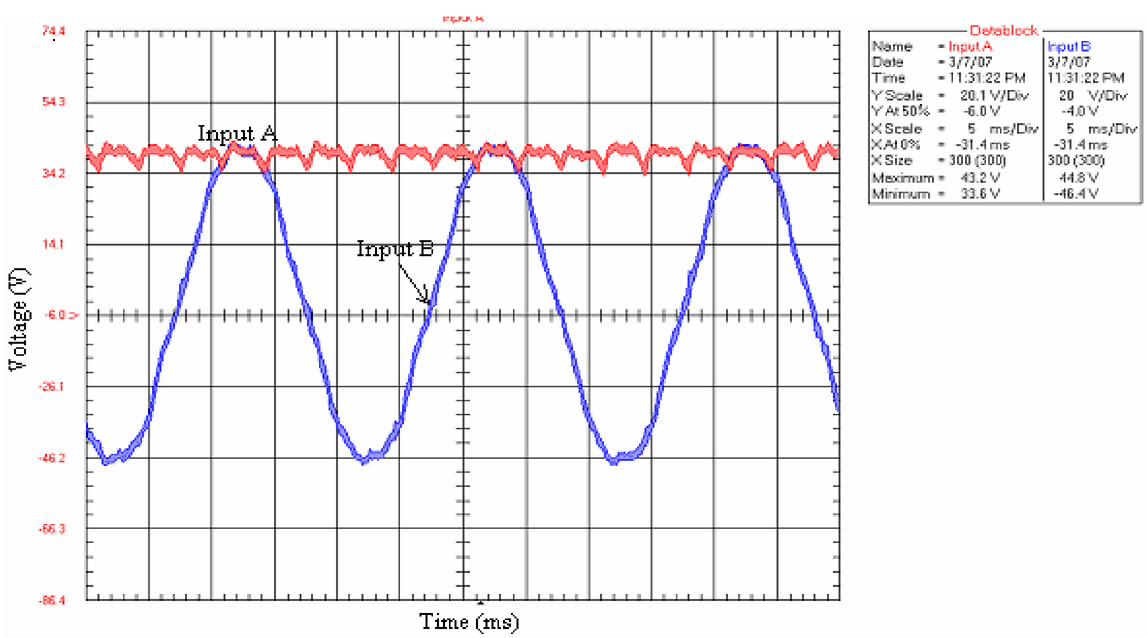

Fig. 7.24 Waveform of DC Voltage V_{DC} (input A),
Scale X - axis – 5 msec/Div. & Y - axis – 20.1 V/Div. and Line Voltage V_{RB} (input B) with RL Load and $\alpha = 0^0$, Scale X - axis – 5 msec/Div. & Y - axis – 20 V/Div.

Waveform at $\alpha = 30^0$;

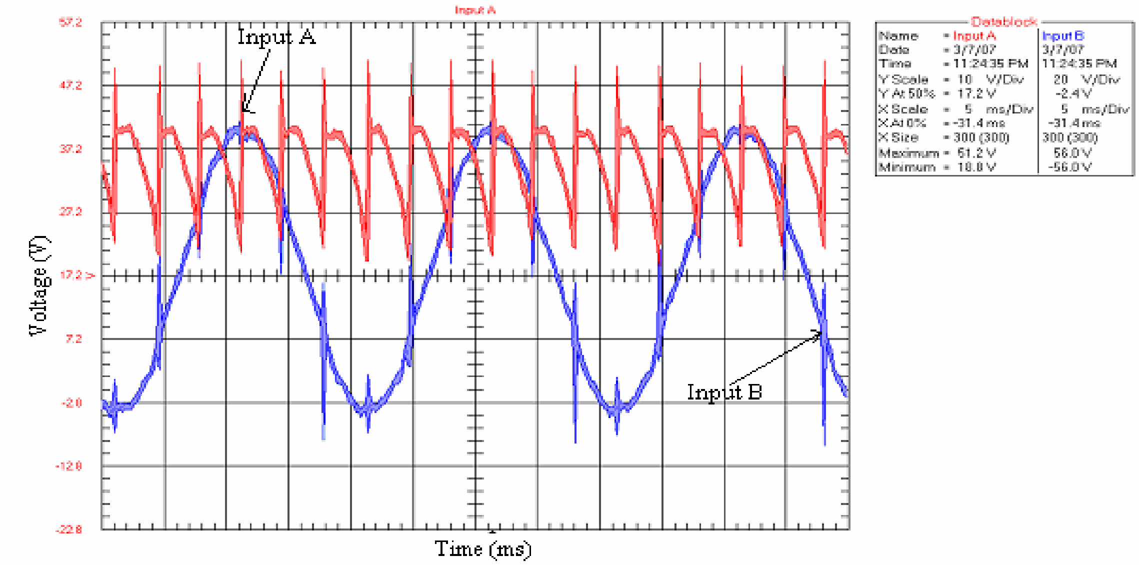

Fig. 7.25 Waveform of DC Voltage V_{DC} (input A),
Scale X - axis – 5 msec/Div. & Y - axis – 10 V/Div. and Line Voltage -V_{RB} (input B)
with RL Load and $\alpha = 30^0$, Scale X - axis – 5 msec/Div. & Y - axis – 20 V/Div.

Waveform at $\alpha = 60^0$;

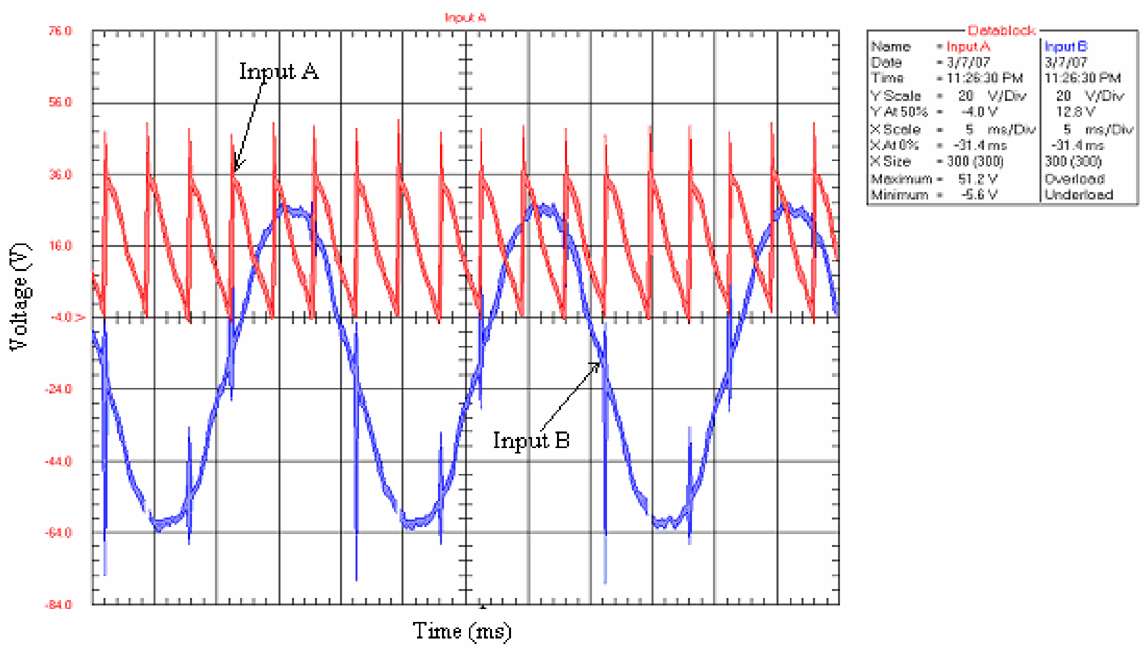

Fig. 7.26 Waveform of DC Voltage V_{DC} (input A),
Scale X - axis – 5 msec/Div. & Y - axis – 20 V/Div. and Line Voltage -V_{RB} (input B)
with RL Load and $\alpha = 60^0$, Scale X - axis – 5 msec/Div. & Y - axis – 20 V/Div.

Waveform at α = 90^0 ;

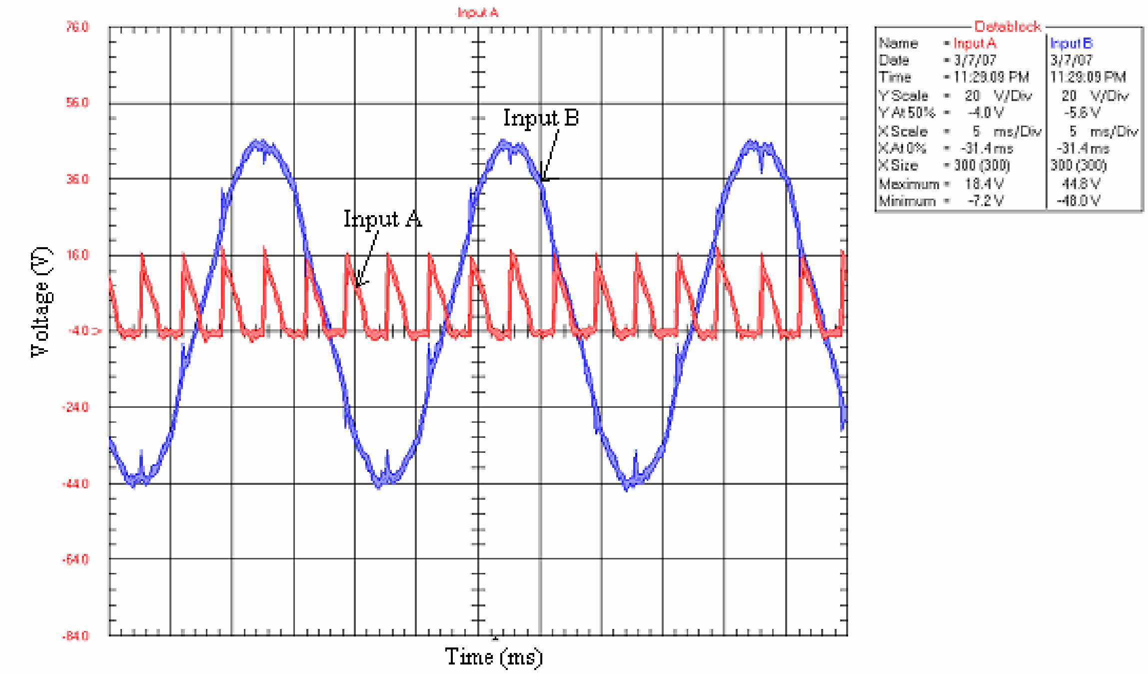

Fig. 7.27 26 Waveform of DC Voltage V_{DC} (input A),
Scale X - axis – 5 msec/Div. & Y - axis – 20 V/Div. and Line Voltage -V_{RB} (input B)
with RL Load and α = 90^0, Scale X - axis – 5 msec/Div. & Y - axis – 20 V/Div.

7.3 Current Control

The current control algorithm was checked with the RL load. The current was sense with the help of the Hall sensor. The Hall sensor gives the 4V at 200A. The inductor used has limitation that current must be below the 2A. The Digital scope available was not able to give proper result at this small value. The result of for the current controller was checked with analog Ampere meter and it was found that current controller work properly. The result for current controller is shown in Fig. 7.27. The current waveform was taken with the help of the Code Composer Studio.

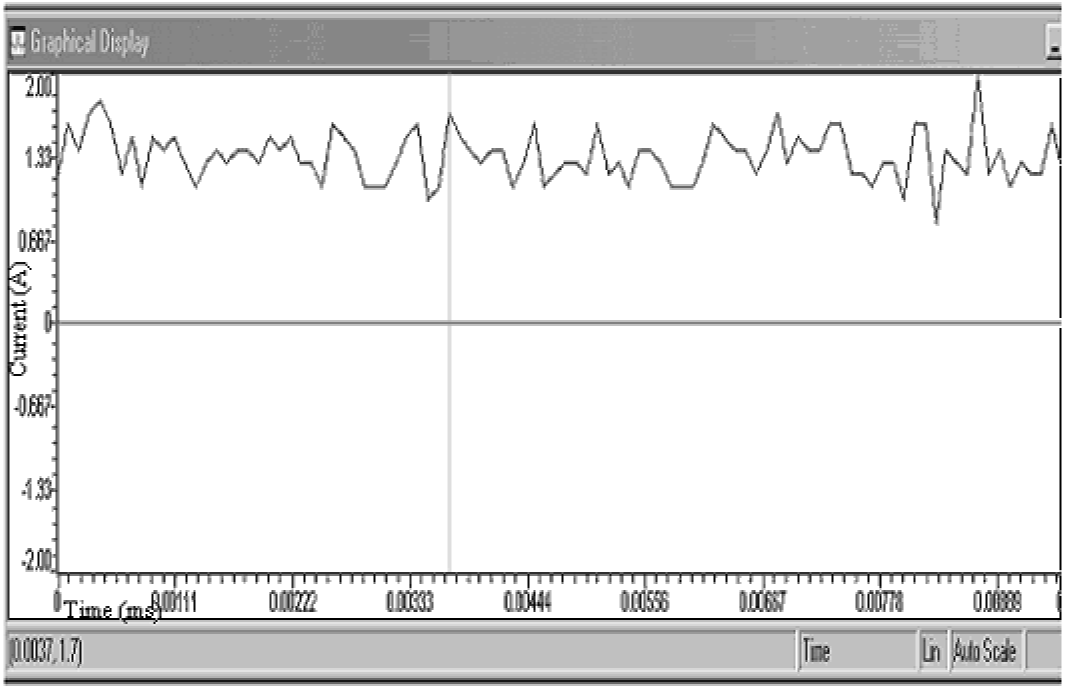

Fig. 7.28 Waveform of DC Current in Current Control Mode with RL Load, Current Reference I^* = 1.5 A, Scale X - axis – 0.00111 msec/Div. & Y - axis – 0.667 V/Div.

Chapter 8
Conclusions and Scope for Future Work

8.1 Conclusions

In this thesis, fundamental of DC motor drive and DC motor has been described. It also contains design of speed controller and current controller by taking some assumption. According to these method simulation studies have done and found that the gain and time constant of the speed controller and current controller required some fine-tuning to obtain good transient performance.

From the simulation of DC motor drive under different operating condition the following results have been obtained and found that reference speed has been achieved with some speed ripple under steady state and transient condition.

Condition in simulation		Reference Speed in rpm	Obtained Speed in rpm
Steady-state condition		1220	1220 (± 5)
Transient condition	Speed change from rated to 90% of rated	1159	1159 (± 8)
	M_L change from rated to 50% of rated	1159	1159 (± 7)

Experimental results of V_{DC} for different firing angle has been summarized below.

Firing angle α in degree	Theoretical V_{DC} in Volt	Experimental V_{DC} in Volt
0^0	42.25	39.5
30^0	36.59	35.3
60^0	21.12	16.9
90^0	0	2.8

Experimental result for constant current has been carried out with reference current of 1.5 A and achieved it.

8.2 Scope for Future work

The following works are to be done further.

- Testing of complete DC Drive.
- Extend this project for 4 Quadrant Drive
- Design of DC motor drive for various Ratings.

Chapter 9
Bibliography

[1] Dubey G. K., "Power semiconductor controlled drives", Prentice-Hall, New Jersey, 1989.

[2] W. Leonhard, "Control of Electric Drives",3rd edition, Springer-verlag.1985.

[3] Bose B. K., "Modern Power Electronics and AC Drives", Prentice-Hall,2002.

[4] www.powerdesigners.com\infoweb\freebooks\powerelectronics.htm

[5] Rashid M. H., "Power Electronics Circuits, Devices and Applications", 2nd edition, Prentice-Hall,India,2001.

[6] Krishnan R.," Electric motor drives: Modeling, Analysis and control",Prentice-Hall,2001.

[7] A. H. Ula, J.W. Steadman, J. M. Wu, "Design and Demonstration of microcomputer controller for an industrial sized DC motor", IEEE *Trans.on energy cons*., Vol. 3, No 1, pp. 102 –110, March 1988.

[8] Timothy D. Collings and William J. Wilson. "A Fast-Response Current Controller for Microprocessor-Based Thyristor DC Motor Drives", *IAS*, VOL. 21, NO. 5, pp-921 – 927, SEP-OCT, 1991

[9] Joos G. and Barton T. H., "Four-quadrant variable speed drive-design consideration", *IEEE proc.*, Vol. 63, No. 12, pp. 1660-1668,1975

[10] Chawla M. P. S., Mehta K. S., Abroal C. V. and Sarkar B., "Software Based Speed Control of Nonlinear DC Drive With Sliding Mode / Variable Structure Approch",1993

[11] Kuo B. C., "Automatic Control Systems",7th edition, John Wiley & sons,1995.

[12] Jun-Keun Ji and Seung-Ki Sul, "DSP-Based Self-Tuning IP Speed Controller with Load Torque Compensation for Rolling Mill DC Drive", *IEEE Trans.on Ind. Elect.*, Vol. 42, No. 4, Aug 1995.

APPENDIX-A: PHOTOGRAPH OF HARDWARE

Photograph of Control Card

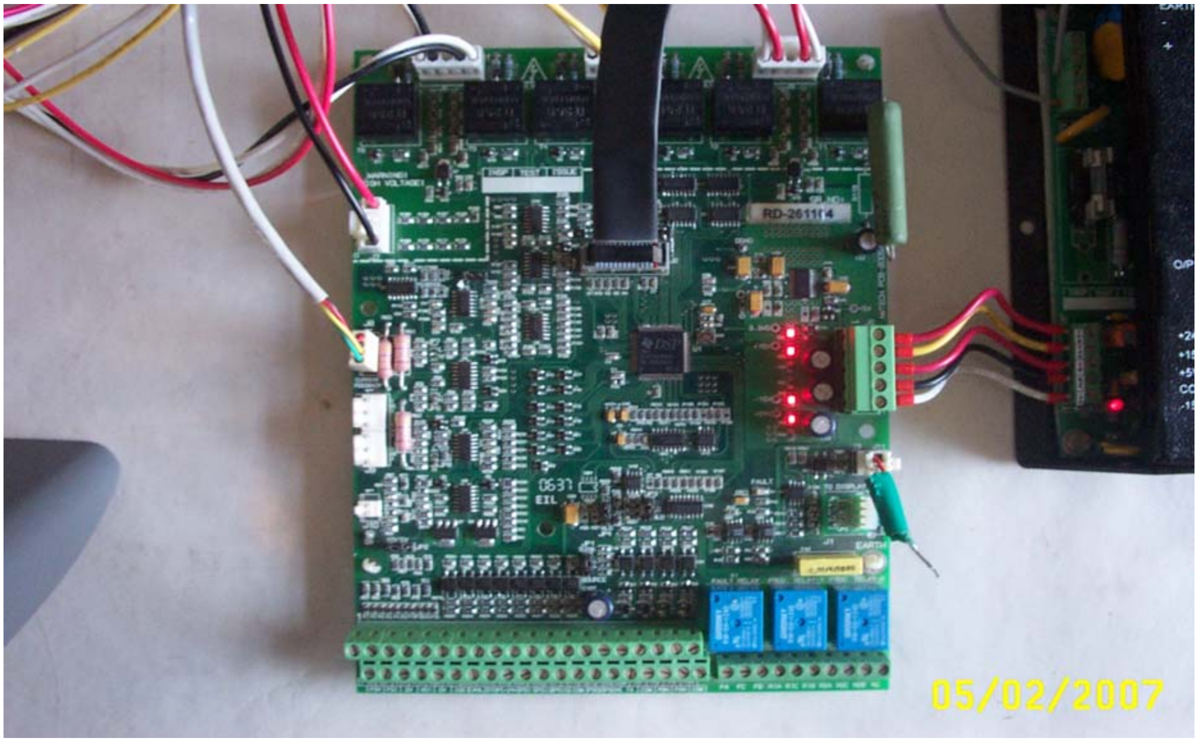

Photograph of Experimental Set Up

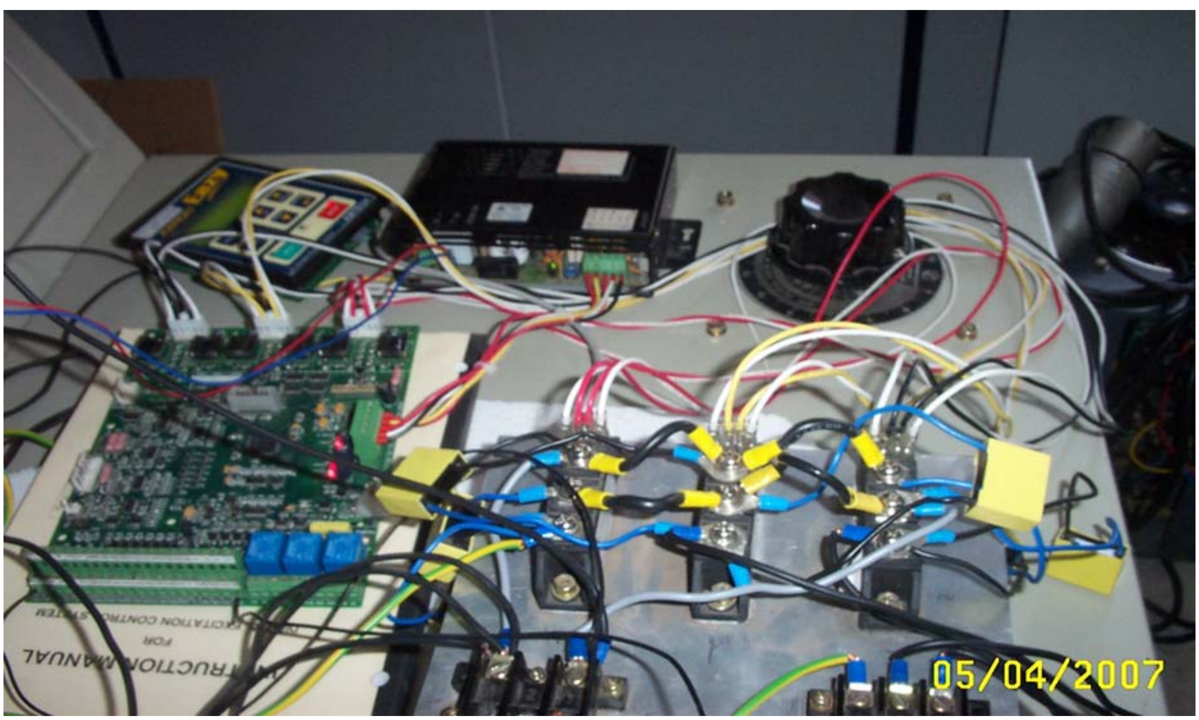

Photograph of Keypad and Display Unit

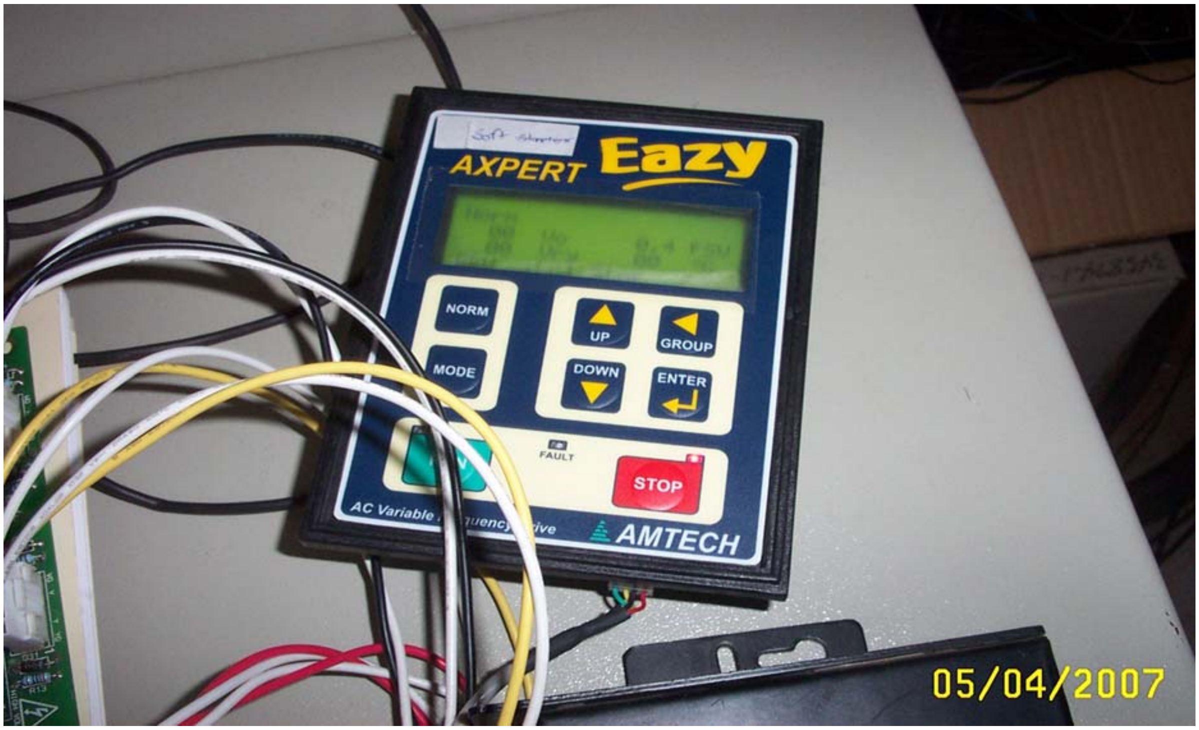

Photograph of Experimental Set up

APPENDIX-B: TMS320 FAMILY OVERVIEW

The TMS320 family consists of fixed point, floating point, multiprocessor digital signal processors and fixed point DSP controllers. TMS320 DSP's have architecture designed specifically for real time signal processing. The 'F28xx' series of DSP controllers combines this real time processing capability with controller peripherals to create an ideal solution for control system applications. The following characteristics make the TMS320 family the right choice for a wide range of applications.

- Very flexible instruction set
- Inherent operational flexibility
- High-speed performance
- Innovative parallel architecture
- Cost effectiveness

TMS320F28xx SERIES OF CONTROLLERS

Designers have recognized the opportunity to redesign the existing systems to use advanced algorithms that yield better performance and reduce system component count. DSP's enable:

- Design of robust controllers for a new generation of inexpensive motors
- Elimination or reduction of memory looks up tables through real time polynomial calculations, there by reducing system cost.
- Use of advanced algorithms that can reduce the number of sensors required in a system.
- Control of power switching inverters, along with control algorithm processing
- Single processor control of multi motor systems

FEATURES of TMS320F2811

High-Performance Static CMOS Technology

150 MHz (6.67-ns Cycle Time)

Low-Power (1.8-V Core @135 MHz, 1.9-V Core @150 MHz, 3.3-V I/O) Design

- High-Performance 32-Bit CPU (TMS320C28x)
  - 16 x 16 and 32 x 32 MAC Operations
  - 16 x 16 Dual MAC
  - Harvard Bus Architecture
  - Fast Interrupt Response and Processing
  - Unified Memory Programming Model
  - 4M Linear Program/Data Address Reach
  - Code-Efficient (in C/C++ and Assembly)
  - TMS320F24x/LF240x Processor Source Code Compatible
- On-Chip Memory
  - Flash Devices: Up to 128K x 16 Flash
  - ROM Devices: Up to 128K x 16 ROM
  - 1K x 16 OTP ROM
  - L0 and L1: 2 Blocks of 4K x 16 Each Single-Access RAM (SARAM)
  - H0: 1 Block of 8K x 16 SARAM
  - M0 and M1: 2 Blocks of 1K x 16 Each SARAM
- Boot ROM (4K x 16)
  - With Software Boot Modes
  - Standard Math Tables
- Clock and System Control
  - Dynamic PLL Ratio Changes Supported
  - On-Chip Oscillator
  - Watchdog Timer Module
- Three External Interrupts
- Peripheral Interrupt Expansion (PIE) Block That Supports 45 Peripheral Interrupts
- Three 32-Bit CPU-Timers
- 128-Bit Security Key/Lock
  - Protects Flash/ROM/OTP and L0/L1 SARAM
  - Prevents Firmware Reverse Engineering
- Motor Control Peripherals
  - Two Event Managers (EVA, EVB)
  - Compatible to 240xA Devices
- Serial Port Peripherals
  - Serial Peripheral Interface (SPI)
  - Two Serial Communications Interfaces (SCIs), Standard UART
  - Enhanced Controller Area Network (eCAN)
  - Multichannel Buffered Serial Port (McBSP)
- 12-Bit ADC, 16 Channels
  - 2 x 8 Channel Input Multiplexer
  - Two Sample-and-Hold
  - Single/Simultaneous Conversions
  - Fast Conversion Rate: 80 ns/12.5 MSPS
- Up to 56 General Purpose I/O (GPIO) Pins

- Advanced Emulation Features
  - Analysis and Breakpoint Functions
  - Real-Time Debug via Hardware
- Temperature Options:
  - A: -40°C to 85°C (GHH, ZHH, PGF, PBK)
  - S/Q: -40°C to 125°C (GHH, ZHH, PGF, PBK)

PIN DIAGRAM

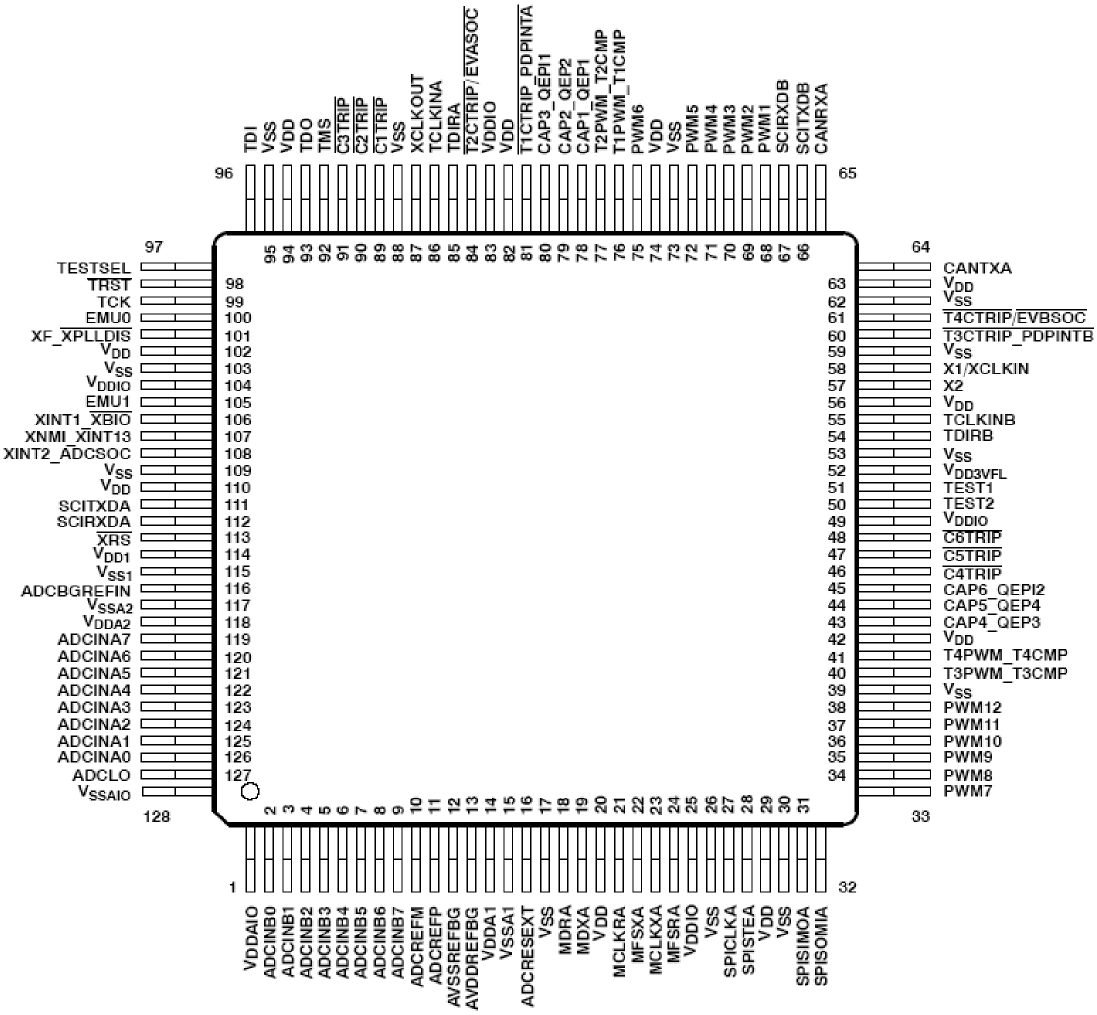

FUNCTIONAL OVERVIEW